R. & M. No. 2730
(13,039, 13,065)
A.R.C. Technical Report

MINISTRY OF SUPPLY

AERONAUTICAL RESEARCH COUNCIL
REPORTS AND MEMORANDA

Two-dimensional Control Characteristics

By

L. W. BRYANT, B.Sc., A.R.C.S.,
A. S. HALLIDAY, B.Sc., Ph.D.,
and
A. S. BATSON, B.Sc.,
of the Aerodynamics Division, N.P.L.

LONDON : HER MAJESTY'S STATIONERY OFFICE
1955
PRICE 12*s* 6*d* NET

Two-dimensional Control Characteristics

By

L. W. BRYANT, B.Sc., A.R.C.S.,
A. S. HALLIDAY, B.Sc., Ph.D.,
and
A. S. BATSON, B.Sc.,
of the Aerodynamics Division, N.P.L.

*Reports and Memoranda No. 2730**
April, 1950

Summary.—The design of lifting surfaces for aeroplanes depends fundamentally on two-dimensional data for the aerofoil sections, with flaps where necessary for control. Data of this kind are required for the use of designers, and for the development of methods of calculating control characteristics and stability derivatives for finite wings. Researches on the lift, pitching moments, and hinge moments of aerofoils with plain flaps have been carried out at the National Physical Laboratory at a Reynolds number of about 10^6. The results of the experiments have been presented in a generalised form, which shows promise of being applicable over a wide field. The generalised curves have been tested as far as possible from other sources, including some tests made on one of the National Physical Laboratory sections in a Royal Aircraft Establishment Tunnel at Reynolds numbers up to nearly 10^7. It appears that a suggestion due to Preston that the ratio of experimental lift slope ($dC_L/d\alpha = a_1$) to the theoretical value $(a_1)_T$, corresponding to the Joukowsky condition of flow past the trailing edge, provides a criterion giving the combined effects of Reynolds number, transition points, and aerofoil shape on $dC_L/d\alpha$, and is a very useful starting point for the estimation of control characteristics. The generalised charts in this report are intended for the estimation of hinge-moment and pitching-moment derivatives from the flap/chord ratio, E after $a_1/(a_1)_T$ has been determined from a special figure. The latter figure (Fig. 14) is a key to the whole process, and it would appear to be very desirable to improve its accuracy and usefulness by further experiments on two-dimensional lift slopes of thin wings at high Reynolds numbers.

1. *Introduction.*—1.1. In a series of papers[1,2,3] Preston originated a method of co-ordinating experimental results relating to plain hinged flaps which showed promise of considerable usefulness. The experimental values of a_1, a_2, b_1, b_2 are expressed as ratios of the corresponding theoretical values for potential flow, $(a_1)_T$, $(a_2)_T$, $(b_1)_T$, $(b_2)_T$, the circulation in the potential flow being that for which the Joukowsky condition at the trailing edge is fulfilled. It is argued that these theoretical values provide a suitable basis giving the major effects of variation of profile shape on the coefficients required for the determination of the characteristics of aerofoils with plain flaps. In R. & M. 1996[2] Preston points out that for steady viscous flow it is necessary to fulfil the Taylor condition† at the trailing edge instead of that of Joukowsky, and that this explains the sensitivity of the equilibrium circulation to the conditions of flow at the trailing edge. For a given incidence these conditions of flow largely depend on the transition point, the Reynolds number and the effective ' trailing-edge angle ' intended to represent the effective shape of the rearmost 5 per cent of the aerofoil profile. Thus the pressure distribution which determines a_1 and a_2 depends chiefly on the thickness/chord ratio, the flap/chord ratio, trailing-edge angle, position of transition, and Reynolds number ; and when these are given, experiment shows that a_1 and a_2 are both unique within a small margin.

* Published with the permission of the Director, National Physical Laboratory.

† The Taylor condition is that the ratio of discharge of vorticity into the wake from upper and lower surfaces of the aerofoil shall be equal in magnitude and opposite in sign, so that the total amount shed shall be always zero.

A

1.2. In R. & M. 2008[1] Preston at first found that a plotting of $b_1/(b_1)_T$ against $a_1/(a_1)_T$ gave an apparently unique curve for a given value of E, the flap-chord/aerofoil-chord ratio, but later[3] (1944) he recognised that this curve was actually only unique for a given aerofoil shape. There was still reason to believe that the curve was not dependent on Reynolds number or on the position of transition. To extend the range of experimental evidence it was decided to carry out a series of tests on new models, based on a low-drag design, so that transition could be delayed beyond the half-chord position. Further it was planned to modify the rear half of the model so that the trailing-edge angle of the section would be reduced in stages to zero. By this means it was hoped to obtain much thinner boundary layers as well as the thicker ones characteristic of large trailing-edge angles and of forward transition. This particular aim has not in fact been achieved to the extent that had been hoped and it is now realised that, apart from the possibilities of artificial reduction by suction, the boundary-layer thickness can be reduced drastically only by a very large increase in the Reynolds number of test. Nevertheless, the range of trailing-edge angles covered has revealed important facts about control coefficients, and has led to a possible framework for correlating a_1, a_2, b_1 and b_2 similar to that first suggested by Preston.

2. *Description of the Experiments.*—2.1. The aerofoil profiles tested for the purposes outlined in the preceding section are illustrated by Figs. 1 and 2; they are all of thickness/chord ratio 0·15, with maximum ordinate at 0·41c, and the series will be referred to as the 1541 series. The rear portion of the original aerofoil (called 1541, Fig. 1) has been systematically modified so as to give a range of trailing-edge angles from 0 to 19·2 deg. The trailing-edge angles (τ) were approximately :—

Section	1541a	1541 basic	1541b	1541c	1541d
τ deg	19·2	15	9·1	4·5	Cusp

The cusp was designed so that the derivatives dy/dx and d^2y/dx^2 were both zero, and in the manufacture a very thin boxwood trailing edge was fitted.

In the original programme, each modification was to be fitted with plain flaps with chord ratios ranging from 0·4 to 0·08, but there was time for only a portion of the programme to be completed. The transition point was varied in position from 0·1 to 0·7 of the chord from the leading edge by means of wires; in addition the transition was allowed to occur, without wires, between 0·65c and 0·7c. The gap at the hinge was either extremely small, approximately 0·03 in., or sealed with grease in all the experiments. The Reynolds number of the tests was $0{\cdot}96 \times 10^6$.

2.2. The models were 4-ft span and 30-in. chord and were suspended from a roof lift balance by means of a parallel motion linkage outside the tunnel; they were connected to the linkage by stout steel tubes, which were surrounded between the models and the tunnel walls by dummy aerofoils of the same section as the model under test. A plan of the model and dummies as set up in the 7-ft No. 2 Wind Tunnel is given in Fig. 3. The gaps between the aerofoil on the balance and the dummies at each end were of the order $\frac{1}{16}$ in.: an attempt to measure the effects of these gaps on lift and hinge moment led to the conclusion that the effects were almost within the limits of experimental error and could not be definitely determined. The effects of the gaps have therefore been treated as negligible. Hinge moments were measured by means of a wire attached to a short sting at one end of the flap and to a light balance on the roof of the tunnel. The hinges of the flap were small ball-bearings, kept well cleaned and lubricated, and were practically frictionless. Considerable care was taken to measure angles of incidence and flap angles accurately, because the ranges of these angles over which transition could be held fixed was small : the quantities required from the tests were slopes of lift and hinge moment with respect to these angles and could only be determined within 1 to 2 per cent if angles could be measured to about $\pm$ 0·05 deg, and it is believed that this was in the main achieved.

2.3. The work on the N.P.L. 1541 sections for the general investigation of two-dimensional characteristics of aerofoils with flaps was continued in the 7-ft No. 3 Wind Tunnel, in order to complete the research by measuring pitching moments, which had not been included in the experiments in the 7-ft No. 2 Wind Tunnel. Fig. 4 is a sketch of the method of mounting the models in the tunnel. The apparatus is substantially the same as was in use in the 7-ft No. 2 Wind Tunnel. Modifications were necessary before pitching moments could be satisfactorily measured. As before, the span of the portion on which the forces were measured was four feet, and dummy end-pieces of one foot six inches span were fixed to each of the tunnel walls ; the dummies were adjustable in angle so as to form a continuation of the working portion, except for a clearance gap of about $\frac{1}{16}$ in. The model was supported by two $1\frac{1}{4}$-in. diameter spindles attached to the ends of the model, twelve inches from the leading edge, passing through clearance holes in the dummy end-pieces and also in the tunnel walls. These spindles were connected to parallel linkages fixed to the outside walls of the tunnel. Vertical wires were fixed to the free ends of the linkages, and also to the outer ends of the split beam lift balance on the roof of the tunnel. The span of this balance was sufficient to overhang the tunnel walls. Ball-bearings were mounted in the linkages to carry the spindles thus enabling pitching moment to be measured on the model. This moment was transmitted, by a wire attached near the leading edge, to a small balance on the roof of the tunnel. Since the lift and pitching moment about a fixed axis were measured, the pitching moment about any other axis could be determined.

3. *The Variation of Lift Coefficient with Incidence.*—3.1. It will be appreciated that the lift-curve slope, a_1, is likely to be a fundamental measure of the conditions of flow round the section with boundary layers present : it is indeed taken as the basis for the procedure described in this report for the estimation of control characteristics. The experimental work at the National Physical Laboratory has on the whole established that the control derivatives can be determined with sufficient accuracy if a_1 is known. Unfortunately a_1 has proved an elusive quantity to measure with real precision. Two reasons account for the major difficulties :—

(*a*) the transition points cannot *both* be held fixed in a far back position over a range of incidence greater than $\pm$ 2 deg.

(*b*) the condition of the boundary layer, at any rate for this particular wing section, appears to be sensitive to a break in the wing surface, such as that at the flap hinge, even when transition occurs well in front of the flap, and even when the hinge gap is sealed.

The difficulties are more pronounced when the trailing-edge angle is large than when it is small.

It has been found possible to determine a_1 to $\pm$ $1\frac{1}{2}$ per cent when the wing is free from marked discontinuities in curvature, and free also from laminar and turbulent separation. Experiments conducted with the necessary precautions for finding a_1 to this degree of accuracy do not so far cover an adequate range of Reynolds number, or of section shape. The effect of Reynolds number in modifying the values for a_1 measured at the N.P.L. was computed by the method of R. & M. 1996[2], and these computations were shown to be roughly of the right order for one particular section by check tests done in a wind tunnel at the Royal Aircraft Establishment. But evidence from N.A.C.A.* sources suggests that the computations for wings with small trailing-edge angles are probably seriously in error. The results of a study of the evidence from both British and American sources are collected in Figs. 10 to 13 and are intended to provide the best available data for the estimation of a_1 as a basis for the further estimation of section characteristics with plain flaps.

3.2. *Theoretical Slope of the Lift-Incidence Curve* $(a_1)_T$.—The thickness/chord ratio is the principal parameter which determines $(a_1)_T$, whilst there are small variations depending upon the curvature of the leading edge and upon the trailing-edge angle or trailing-edge curvature.

* National Advisory Committee for Aeronautics, U.S.A.

An approximate formula due to H. C. Garner has been found accurate enough for use in control estimations, *viz.*:—

$$\frac{(a_1)_T}{2\pi} = e^{C_0}$$

where $$C_0 = \frac{8(y_{0\cdot25} + y_{0\cdot75}) + \sqrt{(6\varrho_L)} + \sqrt{(6\varrho_T)}}{6\sqrt{3}}$$

or alternatively

$$C_0 = \frac{8(y_{0\cdot25} + y_{0\cdot75}) + \sqrt{(6\varrho_L)} + 0\cdot1540 \tan \tau/2}{10\cdot392} \quad \ldots \quad (1)$$

Here $y_{0\cdot25}$ is the half-ordinate of the profile at the quarter-chord point
$y_{0\cdot75}$ is the half-ordinate of the profile at the three-quarter-chord point
ϱ_L is the radius of curvature at the leading edge
ϱ_T is the radius of curvature at the trailing edge
τ is the trailing-edge angle.

In Fig. 5 are plotted values of $(a_1)_T/2\pi$ as a function of t/c the thickness/chord ratio, for two families of related aerofoil sections. This may provide sufficient information for an estimate of $(a_1)_T$ in many cases.

3.3. *Experimental Results.*—3.3.1. The experimental results from the 7-ft Wind Tunnel are plotted as ratios $a_1/(a_1)_T$ in Fig. 14 for two positions of the transition (0·1 and 0·5) as fixed by suitable wires. The errors in the measured slopes appear to be of the order $\pm$ 1½ per cent. Included in the same figure are curves from data given in reports from the N.A.C.A. and from tests in the Compressed Air Tunnel at the N.P.L. These additional curves are commented on in section 4.

3.3.2. *Section* 1541a, *trailing-edge angle* 19·2 *deg, Fig.* 1.—All the measurements of a_1 are collected in Fig. 6 and plotted against position of transition. There appear to be two groups of results, and the upper, represented by the full line, are believed to correspond to the condition of unbroken surfaces and no trace of boundary-layer separation, either laminar or turbulent. Accordingly values from this curve are plotted on the curves of Fig. 9 which gives what are believed to be the best estimates of a_1 in terms of transition for Reynolds number 10^6. When the flap is 40 per cent chord (set at 0 deg and gap sealed) the values of a_1 corresponding to the dotted curve of Fig. 6 were almost invariably measured, and the reason for this had not been found when the investigation had to be discontinued. All later work with smooth surface up to at least 75 per cent of the chord from the leading edge confirmed the higher values which have been accepted.

3.3.3. *Section* 1541, *trailing-edge angle* 15 *deg, Fig.* 1.—The results for this section (*see* Fig. 7), are similar to those for 1541a with lower values when the surface was broken at the hinge of the 40 per cent flap, and the full line values for smaller flaps. The latter are used for plotting on Fig. 9.

3.3.4. *Sections with small trailing-edge angles,* 1541b.c.d., *Fig.* 2.—The results for these sections are plotted in Fig. 8, the full lines of Figs. 6 and 7 being reproduced as well in this figure. In the case of 1541b there is still the same tendency to low values with the 40 per cent flap, as indicated in Fig. 9 where the size of flap is given with most of the observation points plotted. In section 1541c the difference between 20 per cent and 40 per cent flap models is negligible, and apparently non-existent with the cusped aerofoil.

3.3.5. The curve A of Fig. 9 represents the value of the lift-curve slope as a function of trailing-edge angle when transition occurs at 0·1c on both surfaces, the surfaces are smooth up to well behind 60 per cent chord, and there is no separation of the boundary layer. Similarly curve B represents the lift-curve slope for transition at half-chord or beyond. Curve C gives the curve for a_1 taken from Ref. 4, which is said to be based mainly on tests at Reynolds numbers between 3 and 4 $\times$ 10^6. The slopes were taken over much larger angle ranges than those

determined for this report and they probably represent conditions of far forward transition on the upper surface, and considerably back on the lower. The accuracy claimed being only $\pm$ 5 per cent, curve C may be considered roughly to agree with the results of curves A and B even after making allowance for Reynolds number and for variations of aerofoil thickness.

3.4. *The Effect of Reynolds Number on the Slope of the Lift vs. Incidence Curve.*—3.4.1. One of the 1541 aerofoils, (1541a), has been tested in the R.A.E. No. 2, $11\frac{1}{2}$ by $8\frac{1}{2}$-ft Wind Tunnel over a range of Reynolds numbers, $2{\cdot}5$ to nearly 10×10^6. The values of $a_1/(a_1)_T$ derived from these tests for transition positions of $0{\cdot}1$ and $0{\cdot}5c$ are plotted against Reynolds number in Fig. 13. On the same figure are plotted the values of $a_1/(a_1)_T$ deduced from a number of N.A.C.A. tests of two-dimensional models, Ref. 5, which had trailing-edge angles of approximately 20 deg. In some cases it was stated in Ref. 5 that the tests were made with ' leading edge of standard roughness ' ; otherwise the position of the transition point was presumably some distance back from the leading edge. On Fig. 13 are plotted also a few points derived from tests of rectangular wings of aspect ratio 6 in the Compressed Air Tunnel at the National Physical Laboratory over a range of Reynolds numbers ; these experimental results were corrected for aspect ratio by using the empirical formula due to H. C. Garner :—

$$6/(a_1)_{\text{eff}} = 6/a_1 + 0{\cdot}064\sqrt{(a_1/6)} \quad .. \quad .. \quad .. \quad .. \quad .. \quad .. \quad (2)$$

where $(a_1)_{\text{eff}}$ is the measured lift slope. Each plotted point is labelled with a number specifying 100 times the thickness/chord ratio of the section, and those points for which transition is likely to be well forward are distinguished from the remainder for which transition is unknown.

3.4.2. Similar plottings of $a_1/(a_1)_T$ against Reynolds number are given in Figs. 10, 11 and 12 for aerofoils with trailing-edge angles in the neighbourhood of 5, 10 and 15 deg respectively. The data are taken from N.A.C.A. sources (Refs. 5, 6 and other reports), from Compressed Air Tunnel tests, as well as from the 1541 series tests in the National Physical Laboratory 7-ft Wind Tunnel. On each of the Figs. 10, 11, 12 and 13, full-line curves are drawn enclosing between them the majority of the plotted points. These curves were drawn so that cross-plotting against trailing-edge angle yielded smooth curves as in Fig. 14. In this figure the cross-plottings from the data of Figs. 10 to 13 are shown for the upper and lower limiting curves, for the lowest and highest Reynolds numbers of test, *viz.*, 10^6 and 10^7.

3.4.3. After Figs. 10 to 14 were drawn, further data from Ref. 6 were examined, and the upper and lower limiting curves for Reynolds number 6×10^6 plotted in Fig. 14. The agreement with the limiting curves of Figs. 10 to 13 is excellent.

3.4.4. The results for the 1541 series (Reynolds number 10^6) are included in Fig. 14 and are distinguished by the two dotted curves for the two transition positions $0{\cdot}1c$ and $0{\cdot}5c$. It will be noted that, when the trailing-edge angle τ is 20 deg, there is agreement between the upper limiting curve (Reynolds number = 10^6) and the 1541 tests with backward transition. When τ is small there is good agreement between the lower limiting curve and the 1541 data with forward transition. It is concluded that the lower limiting curves of Figs. 10 to 14 would correspond to far forward positions of the transition point, whilst the upper limiting curves apply to transitions well back. Where τ is small the upper limit applies to thinner sections ; it is probable that this limit should be lower for thick sections. Where transition is fairly definitely known it seems likely that $a_1/(a_1)_T$ can be estimated within $\pm$ 2 per cent but where transition is unknown the estimate may be in error by $\pm$ 5 per cent.

A further interesting feature of the 1541a tests in the Royal Aircraft Establishment Wind Tunnel (*see* Figs. 13 and 14) is the evidence that at the highest Reynolds number, about 10^7, the lift slope, corrected for compressibility effects, agrees with the lower limiting curve from the general data. The value from the Royal Aircraft Establishment Wind Tunnel definitely corresponds to a transition well forward on the upper surface in the neighbourhood of $0{\cdot}08c$.

3.4.5. Table 1 has been compiled with a view to suggesting a procedure for using Fig. 14 for determining $a_1/(a_1)_T$ in a given case, thickness/chord ratio, trailing-edge angle and Reynolds

number being known. The Table suggests likely values for Reynolds numbers 10^6, 6×10^6, and 10^7, trailing-edge angles 5, 10, 15 and 20 deg, and thickness/chord ratios 0·09 and 0·15, values being estimated for two extreme positions of the transition point. It is thought that Table 1 represents the available data sufficiently well for general use, although greater precision is highly desirable if the subsequent control estimations are to be as reliable as possible.

3.5. *Further Model Experiments Needed.*—In view of the basic importance of the quantity $a_1/(a_1)_T$, it is a matter of some urgency that further tests should be carried out with the specific purpose of determining lift slopes related to well-defined conditions, so that the chart, Fig. 14, may be better established. A range of Reynolds numbers should be covered, transition should be observed and controlled where necessary to give sufficient variation, and the sections chosen for test should be such as will supply the required number of key points on the chart. The main weakness lies in the region of small values of τ, and more data on thin sections in general is needed. In order that the conditions determining lift slope should be better understood, some attempt to measure displacement thicknesses of the boundary layers in the region of the trailing edge with greater accuracy than has hitherto been achieved is very much to be recommended. Accuracy is required in these measurements because it is a differential effect between the upper and lower boundary layers which is important in relation to the measured lift in any given case.

TABLE 1

Values of $a_1/(a_1)_T$

Trailing-edge angle (deg)	Transition forward						Transition back					
	$t/c \simeq 0{\cdot}09$			$t/c \simeq 0{\cdot}15$			$t/c \simeq 0{\cdot}09$			$t/c \simeq 0{\cdot}15$		
	$R=10^6$	6×10^5	10^7	$R=10^6$	6×10^6	10^7	$R=10^6$	6×10^6	10^7	$R=10^6$	6×10^6	10^7
0	0·825	0·90	0·92	0·825	0·88	0·90	0·92			0·86	0·95	0·97
5	0·80	0·865	0·885	0·79	0·845	0·865	0·885	0·97	0·99	0·84	0·925	0·945
10	0·78	0·83	0·85	0·76	0·815	0·835	0·85	0·925	0·95	0·82	0·90	0·92
15	0·76	0·80	0·82	0·73	0·79	0·815	0·82	0·89	0·915	0·805	0·875	0·90
20	0·74	0·77	0·79	0·70	0·765	0·79	0·79	0·86	0·89	0·79	0·85	0·88

4. *The Variation of Lift Coefficient with Flap Angle.*—4.1. *Theoretical Values of the Lift Derivative.* $\partial C_L/\partial\eta$ *or* a_2.—To a first approximation the ratio of the theoretical values of a_2 and a_1 is independent of thickness/chord ratio, so that the curve of a_2/a_1 against flap/chord ratio, E, for a thin flat plate, given in Fig. 18, may be used to determine $(a_2)_T$ from $(a_1)_T$.

4.2. *Experimental Results for the* 1541 *Series.*—The $a_2(a_2)_T$ ratio is plotted against trailing-edge angle in Fig. 15, for flap/chord ratios, $E = 0{\cdot}2$ and $0{\cdot}4$, and for two positions of transition. In Fig. 16, $a_2/(a_2)_T$ is plotted against $a_1/(a_1)_T$. It is clear from Fig. 16 that within the limits of experimental error (shown by the dotted lines for $E = 0{\cdot}2$) there is a definite relationship between these quantities for a given value of E. A few points for NACA 0015, from R. & M. 2314[11] and 2698[12] are shown in the figure and appear on the whole to be consistent with those of this report.

The experimental results at the remaining values of E are given in Fig. 17, where the ratio $a_2/(a_2)_T$ is plotted against E for a series of values of $a_1/(a_1)_T$. The experimental points have been modified slightly to make them correspond to the marked values of $a_1/(a_1)_T$ and are plotted to exhibit the degree of smoothing necessary to obtain a regular sequence of curves.

The curves of Figs. 16 and 17 are certainly independent of transition position and should be independent of Reynolds number.

4.3. *Chart for Finding a_2/a_1.*—When $a_1/(a_1)_T$ has been determined, from data such as those of Fig. 14, a_2/a_1 can be found from Fig. 18, where it is plotted against E in a family of curves with constant $a_1/(a_1)_T$.

In Ref. 4 Naylor and Lyons deduced two-dimensional values of a_2/a_1 from a large collection of data, mainly from American sources. Their two extreme curves for trailing-edge angles of $7\frac{1}{2}$ deg and 25 deg respectively are reproduced in Fig. 19, where they are shown dotted. The nearest corresponding curves from the data of this report are shown by the full lines for $a_1/(a_1)_T = 0{\cdot}85$ and $0{\cdot}70$ respectively. These two values of $a_1/(a_1)_T$ correspond to various combinations of the three parameters, Reynolds number, transition point, trailing-edge angle ; typical sets of these quantities are shown on the figure. It is clear that all the relevant parameters must be considered when estimating lift and that Fig. 3 of Ref. 4 is not generalised enough for correctly estimating a_2/a_1. But the data used by Naylor and Lyons would appear to confirm that the results of the investigation of the present report, expressed in terms of the ratio $a_1/(a_1)_T$, may be confidently used over a wide range of Reynolds numbers.

5. *Hinge Moments. Results of the Determination of b_1, $(\partial C_H/\partial\alpha)$.*—In Fig. 20 are given the results of special computations of $(b_1)_T$ divided by $(a_1)_T$, for the 1541 series and for Piercy sections of different t/c and τ. It will be noted that the theoretical value of b_1/a_1 is a function mainly of E and t/c and to a minor degree of trailing-edge angle, τ. To facilitate interpolation Fig. 21 is included, where $(b_1/a_1)_T$ is plotted against E for $\tau = 10$ deg, and for evenly spaced values of t/c. The curve for zero thickness is of course that for a thin plate (R. & M. 1095[8]). The inset figure in Fig. 21 provides for the correction necessary if τ is not 10 deg for the section under consideration. If the maximum thickness of the section occurs further forward than about $0{\cdot}35c$ it is preferable to use the method given by Thomas in Ref. 13 for the estimation of $(b_1)_T$.

The experimental values of b_1 are collected and exhibited in Figs. 22, 23 and 24. In Fig. 22 $b_1/(b_1)_T$ is plotted against E. It will be noted that the groups of curves for each trailing-edge angle are separated from one another. For medium values of τ there is little change in $b_1/(b_1)_T$ with E ; for larger values of τ, $b_1/(b_1)_T$ increases with E, whilst for smaller values of τ, $b_1(b_1)_T$ decreases with increase of E. It is remarkable that $b_1/(b_1)_T$ can actually exceed unity by a very large margin when $\tau = 0$. In Fig. 23, $b_1(b_1)_T$ is plotted against position of transition, and it will be clear that again for medium values of τ there is little change of $b_1/(b_1)_T$. It is curious that when transition is back at $0{\cdot}5c$ and $E = 0{\cdot}2$ the curves come closer together than when transition is either forward or very far back.

Thirdly, in Fig. 24, $b_1/(b_1)_T$ is plotted against τ and the relationship between these parameters is approximately linear.

6. *Hinge Moments. Results of the Determination of b_2, $(\partial C_H/\partial\eta)$.*—The theoretical values of b_2 are exhibited in Fig. 25 by plotting of $(b_1/b_2)_T$ against E. The thin-plate curve is taken from R. & M. 1095[8] and the values for $t/c = 0{\cdot}15$ were specially computed for the 1541 series of sections. To assist in interpolating for different values of t/c a family of curves, for $\tau = 10$ deg, was calculated by Thomas's method, Ref. 13, and is given in Fig. 26. Correction curves for use when τ is not 10 deg are inset in the figure.

In Figs. 27 and 28 $b_2/(b_2)_T$ is plotted against position of transition and trailing-edge angle respectively. Here again $b_2/(b_2)_T$ varies little with transition or with E when τ has a medium value. The relation between $b_2/(b_2)_T$ and τ is not quite linear ; the curves are considerably steeper for transition forward than for transition back.

7. *Hinge Moments. Relation between b_1 and a_1.*—7.1. The next two figures, 29 and 30, show the relationship between $b_1/(b_1)_T$ and $a_1/(a_1)_T$. On the assumption that b_1 will have its theoretical value when $a_1/(a_1)_T$ is unity, the quantity plotted is $b_1/(b_1)_T$ divided by $a_1/(a_1)_T$, which should tend to unity as $a_1/(a_1)_T$ tends to unity for all aerofoils. In each figure the graphs for the 1541 series are drawn for transitions $0{\cdot}1c$ and $0{\cdot}5c$, R being approximately 10^6. Curves for each trailing-edge angle are suggested which all meet in the neighbourhood of unity for both the plotted quantities.

7.2. Fig. 29 is drawn for $E = 0{\cdot}2$. From the results of the tests on the 1541a section ($\tau = 20$ deg) done in the R.A.E. No. 2, $11\frac{1}{2} \times 8\frac{1}{2}$-ft Wind Tunnel, the points for two transition positions are plotted along the lowest curve, to which they belong. The agreement is extraordinarily good for this class of measurement, and gives some grounds for confidence in the suggested method of generalising the resluts of this work.

7.3. Some further checks were sought among the numerous reports from the N.A.C.A. on this subject. Considerable difficulty was found in correlating the American work satisfactorily for this special purpose, and it was therefore concluded that a better check would be forthcoming by using curves which were recommended by American authors themselves as representative of their experimental results. Fig. 13 of Ref. 9 gives a family of such curves. Two values of τ, 12 and 20 deg, were selected and the corresponding values of the theoretical hinge-moment coefficient, $(b_1)_T$, estimated ; $(b_1)_T$ could be given values between fairly narrow limits. The quantity $a_1/(a_1)_T$ could be given a range of possible values according to t/c, etc. Finally, points were plotted for each trailing-edge angle which were means of the extremes of the estimated quantities. The result of this procedure in both Fig. 29 and Fig. 30 (which refers to $E = 0{\cdot}4$) is satisfactory as far as it goes, and proves that American data at least give rough agreement with the proposed generalised scheme. Until further experiments designed to yield all the necessary measurements, suitably co-ordinated, are undertaken, the checking over a wider range of variables is not possible.

8. *Hinge Moments. Relation between b_2 and a_1.*—In Figs. 31 and 32 the ratio b_2/a_1 divided by $(b_2/a_1)_T$ is given similar treatment to that given to b_1/a_1 divided by $(b_1/a_1)_T$ in Figs. 29 and 30. The graphs for two transitions $0{\cdot}1c$ and $0{\cdot}5c$ for the 1541 series are drawn and tentative curves drawn to meet near (1,1). Similar checks to those in Fig. 29 are shown by the plotted points in Fig. 28, which are derived from the tests in the R.A.E. No. 2, $11\frac{1}{2}$ by $8\frac{1}{2}$-ft Wind Tunnel. The agreement with the curve for the trailing-edge angle 20 deg is satisfactory for measurements of this character. The Royal Aircraft Establishment tunnel results for b_2 were more scattered than those for b_1.

Fig. 13 of Ref. 9 was used again to compare mean values of (b_2/a_1) divided by $(b_2/a_1)_T$ from American sources, and the points plotted for trailing-edge angles 12 and 20 deg are in very satisfactory agreement with the generalised scheme, in both Figs. 31 and 32.

One point for a trailing-edge angle of 30 deg derived from Fig. 13 of Ref. 9 is plotted in Fig. 31, and serves as a rough guide to extrapolation to large values of τ.

9. *Effect of Transition Movement on One Surface only.*—It is well known that in practice transition takes place on the upper surface of a wing a little to the rear of the point of maximum suction, apart from any local feature forward of this point which may cause premature transition. Assuming the surface to be perfectly smooth and the stream to be perfectly non-turbulent, transition on an aerofoil of 1541 type will occur at $0{\cdot}65c$ to $0{\cdot}7c$ on both surfaces at small angles of incidence and will travel forward very quickly on the upper surface with increasing incidence, beginning at $2\frac{1}{2}$ to 3 deg. On the lower surface transition will either remain at $0{\cdot}65c$ to $0{\cdot}7c$ or move slowly to the rear. It is important to know therefore what happens to the hinge moments on a flap when the positions of transition are not the same on upper and lower surfaces. Accordingly some experiments were made on the 1541 aerofoils in order to study the effect of asymmetry in transition. Fig. 33 shows the results of measurement of C_L made on all five of the aerofoils at 0 deg incidence with flaps set at 0 deg, and a transition wire placed at various positions on one surface only. The effect is to give a negative lift if the wire is considered to be

on the 'upper' surface of the symmetrical aerofoils. But this negative lift is much larger when the trailing-edge angle τ is large than when τ is small. Some light is thrown on the reason for this by Fig. 34, where C_H is plotted against position of wire. When $\tau = 19{\cdot}2$ deg, C_H is positive for forward transition on the upper surface, decreasing of course to zero as the transition moves back to a position near that of the lower surface ($0{\cdot}65c$ to $0{\cdot}7c$). However, when $\tau = 0$, C_H is negative for forward transition on the upper surface ; hence in this case there must be a positive lift on the flap which almost cancels the decreased lift on the forward part of the wing.

The ordinates of the curves Figs. 33 and 34 give a measure of the jumps in C_L and C_H which would occur if transition suddenly moved forward with change of incidence. As far as C_H is concerned it is apparent that for $E = 0{\cdot}20$ the most favourable trailing-edge angle is 9 or 10 deg, if the change of C_H with transition is to be a minimum ; this agrees with the conclusion above that b_1 is unaffected by transition change when $\tau = 9$ deg.

These considerations are further illustrated by Figs. 35 and 36. In Fig. 35, C_H is plotted against α for 1541 with 25 per cent flap in the upper figure, and for 1541a with 15 per cent flap in the lower. τ has the value 15 deg in the first case and 19·2 deg in the second. Curves are plotted for no wires, wires at $0{\cdot}1c$ on both surfaces and on one surface only. From $\alpha = 0$ deg to $\alpha =$ 2 deg the curve with no wires and that with upper wire only tend to be roughly parallel, and the two curves come together in the neighbourhood of $\alpha = 5$ deg when the transition occurs naturally on the upper surface at about $0{\cdot}1c$. It is difficult to understand the observations in the upper diagram at + 3 deg which do not agree with sufficient accuracy with those at — 3 deg to make the phenomena clear. It should be remarked that $\partial C_H/\partial\alpha$ with both wires is less negative than for no wires for the 1541 model.

Fig. 36 applies to the 1541d model, $\tau = 0$ deg. Here again from $\alpha = 0$ deg to $\alpha = 2$ deg the curve with no wires is approximately parallel to those with one wire. The curve for both wires is (in contrast to the case of $\tau = 19{\cdot}2$ deg, Fig. 35) steeper than that for no wires. Also, as explained in the comments on Fig. 34, the curve for upper wire only is below the no-wire curve at first ; the two curves come together at $\alpha = 5$ deg. The curve for lower wire only coalesces with the two-wire curve at $\alpha = 5$ deg, but at a point lying above the meeting point of the two former curves ; it appears that at 5 deg incidence the condition of the boundary layer on the lower surface is still appreciably affected by the presence of the wire at $0{\cdot}1c$ at 5 deg incidence so that the curves do not all coalesce at the same value of C_H.

It is clear that all tests of controls, when it is possible for transition to start far back at small incidence, should include cases where the transitions are asymmetrical (*see* R. & M. 2164[10]). It is not sufficient to confine the tests to the cases with natural transitions ; some knowledge of the effects on lift and hinge moments of movements of transition, both symmetrically and asymmetrically is required, because the conditions of transition on model and full-scale will in general be different.

10. *Values of C_H at Higher Incidence and Larger Flap Angles.*—So far only comparatively small changes of incidence and flap angle have been considered, and there has been no separation of the turbulent boundary layer on the upper surface at the trailing edge. Some data are available from tests up to 10 deg incidence and flap angle on the aerofoils 1541 and 1541a. These data are summarized in this section. Fig. 37 gives two examples of the measurements of C_H for the 1541 aerofoil with trailing-edge angle 15 deg. C_H is plotted against $\alpha + \eta$, so that it is easy to draw curves of (C_H, η) for constant α (full lines) and (C_H, α) for constant η (dotted lines). The former curves are linear over the range $\pm$ 5 deg at least so long as α lies between $\pm$ 2 deg, whilst the latter are linear over the range $\pm$ 2 deg, so long as $|\eta| \leqslant 5$ deg. These angle ranges define the limits for which the transition points on the two surfaces can be held fixed. Outside these ranges the movements of transition and the beginnings of turbulent boundary-layer separation at the trailing edge produce non-linear curves.

Fig. 38 gives examples of the effects of transition movements in the case of 1541a section with trailing-edge angle 19·2 deg. Linearity extends over the range $\pm$ 5 deg for the (C_H, η) curves so long as $|\alpha| \leqslant 1$ deg, and over the range $\pm$ 2 deg for the (C_H, α) curves so long as $|\eta| \leqslant 3$ deg. The waves nearest the origin in the (C_H, α) curves are due to the movement of transition forward in the neighbourhood of $|\alpha| = 2$ deg, the second turning point at about $|\alpha| = 6$ deg is due to the beginnings of turbulent separation.

In the experiments illustrated by Figs. 37 and 38 there were no wires to fix transition. A comparison of Fig. 38 with Fig. 39, where wires caused transition at $0 \cdot 1c$, shows that the waves in the (C_H, α) curves near the origin disappear when transition is held fixed at $0 \cdot 1c$ and does not change at $\alpha \simeq 2$ deg. Both $\partial C_H/\partial\alpha$ and $\partial C_H/\partial\eta$ are considerably reduced by the change to a forward position of transition, as has been recorded above in the discussion on b_1 and b_2. At the larger values of α and η the influence of the wires at first becomes small, because the natural transition, at any rate on the upper surface, is well forward. But the wires tend to cause an early turbulent separation on the upper surface, and wires on the lower surface are objectionable because in most cases on smooth wings the natural position for transition is well back where wires would produce complicated boundary-layer profiles not representative of practical conditions. Wires are therefore only suitable for controlling transition for experimental purposes over small ranges of α of the order $\pm$ 3 deg, and of η of $\pm$ 10 deg.

11. *Velocity Traverse at the Trailing Edge.*—Total-head and static-pressure tubes were employed with some of the models to measure velocity profiles at the trailing edge. The instruments were traversed along lines from the trailing edge at right-angles to the bisectors of each of the angles between the chord and the surface tangents ; this was taken to be an approximation to the normals to the streamlines. The results are illustrated by Figs, 40 to 42.

In Figs. 40 to 42, the ratio of local velocity q to stream velocity U_0 is plotted against distance from the trailing edge in terms of the aerofoil chord. The approximate location of the boundary-layer edges is also shown in every case.

Fig. 40 refers to the no-lift condition with $\alpha = \eta = 0$. The upper figure is for the condition ' wires at $0 \cdot 1c$', and the lower for ' no wires ', with transitions at $0 \cdot 65c$ to $0 \cdot 7c$. There is very little variation of δ/c, the boundary-layer thickness ratio, with section shape. It is also interesting to note the greater relative reduction of displacement thickness, readily seen from the profile shapes, due to the cusping of the section, when transition is back as compared with the forward transition.

Fig. 41 illustrates the velocity profiles for $\alpha = 2$ deg, $\eta = 0$ deg, C_L being in the neighbourhood of $0 \cdot 2$. There is again little effect on δ/c due to section shape in the upper figure (with wires) and in the lower figure (no wires) in the case of the lower surface. However, δ/c on the upper surface tends to become appreciably smaller as τ is reduced when transition is well back, and displacement thickness is considerably reduced on both surfaces by cusping the section.

Fig. 42 covers the case $\alpha = 0$ deg, $\eta \simeq 3$ deg, giving approximately the same C_L as in the case dealt with in Fig. 41. On the whole the behaviour suggests a similarity between the effects of setting over the flap and of increasing trailing-edge angle at constant incidence. The shapes of the upper-surface curves with wires at $0 \cdot 1c$ suggest a near approach to separation.

In Fig. 43, δ/c is plotted against trailing-edge angle for $\alpha = 2$ deg, $\eta = 0$, and also for $\alpha = \eta = 0$. The curves for ' no wires ' are drawn full ; those for ' wires at $0 \cdot 1c$ ' dotted. It will be noted that δ for no wires, lower surface, is almost unchanged by the change of incidence and by change of τ. On the other hand δ for the upper surface rises as τ increases. Trailing-edge angle has little effect on δ with transition forward, but the incidence effects are a decrease in δ, lower surface, and an increase on the upper surface.

Fig. 44 is similar to Fig. 43 with the plottings for $\alpha = 0$, $\eta \simeq 3$ deg, substituted for $\alpha = 2$ deg, $\eta = 0$. The remarks made above relating to Fig. 43 apply to Fig. 44 in the main. With no wires the rise of δ on the upper surface with τ is much more marked.

These data are recorded in this report because it is hoped later to explain the behaviour of control flaps in terms of the properties of the boundary layers. Preston's work (R. & M. 1996[2]) already gives some clue to the kind of correlation to be expected, but more research is required before reliable quantitative estimations become practicable.

12. *Outline of Procedure in Estimating a_1, a_2, b_1 and b_2.*—It is assumed that the geometrical shape of the section, flap chord ratio, transition points, Reynolds number, are known, and that an estimate of the effective trailing-edge angle, τ, can be made. The value of τ should be determined from the shape of the section from $0{\cdot}975c$ to $1c$. Then the procedure is as follows :—

(*a*) Find $(a_1)_T$ from Fig. 5, using known values of t/c and τ; or alternatively use the formula (1).

(*b*) Find $a_1/(a_1)_T$ from Fig. 14 or Table 1, using known values of Reynolds number, transition locations, and trailing-edge angle.

(*c*) Find a_2/a_1 from Fig. 18 from $a_1/(a_1)_T$ and E.

(*d*) Find $(b_1/a_1)_T$ and therefore $(b_1)_T$ from Fig. 21, using t/c and τ ; or alternatively use the method due to Thomas for estimating $(b_1)_T$ (Ref. 13).

(*e*) Find $(b_1/b_2)_T$ and therefore $(b_2)_T$ from Fig. 25 or 26 using t/c and τ ; or alternatively use Thomas's method for $(b_2)_T$ (Ref. 13).

(*f*) Find $b_1/(b_1)_T$ from Figs. 29 and 30, using $a_1/(a_1)_T$, E, and τ.

(*g*) Find $b_2/(b_2)_T$ from Figs. 31 and 32 using $a_1/(a_1)_T$, E, and τ.

(*h*) Some indication of the effect of movement of transition on one surface only is given by Figs. 33 and 34. But more data are needed, particularly with varied values of E.

13. *Variation of C_m with Incidence, m_1.*—The results of the experiments are plotted as C_m (uncorrected for tunnel interference) against α in Figs. 45 to 52 ; each figure applies to one of the four trailing-edge angles, and to a fixed value of E, $0{\cdot}4$ for Figs. 45 to 48, and $0{\cdot}2$ for Figs. 49 to 52. On each figure are plotted curves for the smooth wing surface, and also for the wing with transition wires on both surfaces at $0{\cdot}1c$. A few points in each figure give the results with one wire at $0{\cdot}1c$, at $0{\cdot}3c$ or at $0{\cdot}5c$ on the upper surface only. The curves for the smooth wing are linear only over a range of α between $\pm$ 2 deg, outside which the transition moves forward on the upper surface.

Fig. 53 is included to provide an indication of the general accuracy of the measurements. Any particular set of measurements appears to be reliable to within about $\pm 0{\cdot}0003$ in C_m, but when boundary layers are fairly thick as with the trailing-edge angles 15 and $19{\cdot}2$ deg, repeats tend to be less accurate, the limits being $\pm$ $0{\cdot}001$ in C_m.

The slopes of the curves (corrected for tunnel interference) are plotted as $m_1 = \partial C_m/\partial\alpha$ against trailing-edge angle, τ, in Fig. 56. Since the flaps are set at 0 deg in determining m_1, it might be expected that m_1 in Fig. 56 would be independent of E. The discrepancies are no doubt due to differences in boundary layers when the hinge gaps are located at different positions along the chord of the wing. As will be seen later the differences are partially explained when m_1 is related to the corresponding value of a_1.

The same results are plotted in an alternative manner in Fig. 57, in which the ordinates are the distances of the aerodynamic centre, measured as a fraction of the chord, from the leading-edge of the aerofoil and the abscissae are values of τ as in Fig. 56. The aerodynamic centre moves forward when the transition is moved forward ; it is also situated further forward for large than for small values of τ. The relation, $m_1/a_1 = 0{\cdot}25 - h$ is used to determine h, a_1 being the measured slope of the lift curve.

14. *Variation of C_m with Flap Angle, m_2.*—In Figs. 54 and 55, C_m is plotted against control angle, η, for the cases $E = 0{\cdot}4$ and $0{\cdot}2$ respectively. In each figure curves are shown for the four different trailing-edge angles, with the wing surfaces smooth and also with transition wires at $0{\cdot}1c$. The curves are linear over the range $\eta = \pm 5$ deg.

The slopes of the curves in Figs. 54 and 55 (corrected for tunnel interference) yield values of $m_2 = \partial C_m/\partial\eta$ for $\alpha = 0$. These are plotted in Fig. 58 against τ. In Fig. 59 values of the coefficient m are plotted against τ ; m is the quantity which is needed in the approximate formula for aileron reversal speed : $V_r^2 = (a_2 m_0)/(\frac{1}{2}a_1 m\rho c^2 s)$, where m_0 is the torsional stiffness parameter (*see* R. & M. 2186[19], equation (9).

m is determined by the equation :—

$$C_m = m_1\alpha + m_2\eta = (m_1/a_1 \times C_L) - m\eta$$

so that $$m = -m_2 + (a_2/a_1 \times m_1)$$

since $$C_L = a_1\alpha + a_2\eta.$$

Figs. 60 and 61 illustrate the effect of incidence on m_2. As would be expected from the observed movements of transition, little change is indicated in m_2 as α changes over the range ± 2 deg ; but it tends to decrease for larger angles of incidence as indicated by the results for $\alpha = 5$ deg.

15. *Observed Points of Transition.*—Transitions were observed by the paraffin evaporation method. The positions of transition appeared to be a little further forward on the models in the 7-ft No. 3 Wind Tunnel than in the 7-ft No. 2 Wind Tunnel, which is provided with a finer mesh honeycomb, and is therefore less turbulent. This is illustrated in Fig. 62 where position of transition on the wing without wires is plotted against α for $\eta = 0$. It will be seen that the movement of transition is small until α exceeds 2 deg ; this explains why the curves of Figs. 45 to 52 for the smooth wing are linear only over the range of $\alpha = \pm 2$ deg. Similarly as Fig. 62b shows that transition movement is small over the range $\eta = \pm 5$ deg ($\alpha = 0$ deg), the curves of C_m over this range of η in Figs. 54 and 55 are linear.

Figs. 62c and 62d illustrate the differences in transition for the two models with flaps of $E = 0{\cdot}4$ and $0{\cdot}2$. In the former case transition does not occur aft of the hinge line at $0{\cdot}6c$; in the latter case transition occurs as far back as $0{\cdot}7c$ up to just above one degree of incidence and over a wide range of η when $\alpha = 0$.

16. *Variation of C_m with Transition Movement at $\alpha = 0$.*—The points shown in Figs. 45 to 55 for the case with transition wires at various positions on the upper surface, α and η both being zero, were used to plot C_m against transition position in Fig. 63. The points actually plotted are the averages for the two values of E, since the values of C_m should be independent of E. C_m is a linear function of transition position within the limits of accuracy of measurement for all the models tested. For a given forward transition the boundary layers varied with the position of the hinge line so as to cause differences in C_m as much as $0{\cdot}003$; the mean lines drawn cannot therefore be expected to give C_m in some cases more nearly than $\pm 0{\cdot}001$. The curves give some indication of the increment of C_m arising from any rapid forward movement of transition such as occurs at about $1\frac{1}{2}$ to 2 deg from the no-lift incidence, or from the incidence of optimum lift. The increment depends on the trailing-edge angle of the section. If the position of the aerodynamic centre is determined from observations over a range of incidence of 4 deg, the error in position arising from uncertainty in transition movement, represented by an uncertainty in ΔC_m of $0{\cdot}001$ for $\Delta\alpha = 4$ deg, would be about $0{\cdot}0025c$.

Figs. 33 and 34 of section 9 are of interest in showing the changes in C_L and C_H with transition movement on the upper surface for $\alpha = \eta = 0$. It will be seen that the changes in C_L are smallest for the smallest value of τ, just as are corresponding changes of C_m.

17. *Relation between Aerodynamic Centre and Lift Slope.*—17.1. In a manner analogous to the treatment of hinge-moment coefficients in section 7 the measured values of h have been expressed as fractions of the corresponding potential flow values, *i.e.*, $(h)_T$, and plotted against $a_1/(a_1)_T$ in Fig. 64. It was found that the relation between $h/(h)_T$ and $a_1/(a_1)_T$ depended on τ, trailing-edge angle, just as was found in the case of hinge-moment coefficients, b_1 and b_2. Curves were drawn through the points from the N.P.L. tests to pass through the point (1,1). Some guidance in drawing these curves was obtained from points plotted from N.A.C.A. reports; theoretical values of h and a_1 were estimated for ten aerofoils. These aerofoils were tested by the N.A.C.A. authors at more than one Reynolds number in some cases, but most tests were done for $R = 6 \times 10^6$. In plotting the points from American sources, a small adjustment was made when the trailing edge angle of the tested aerofoil was not 5, 10, 15 or 20 deg although near one or other of these values. There is a negligible error in treating the τ's of the N.P.L. tests as 5, 10, 15 or 20 deg instead of the true values of 4·5, 9·1, 15 or 19·2 deg. The dotted curve in Fig. 64 shows the relation between Preston's generalised curve in Fig. 3 of Ref. 14 and the new family now presented.

Fig. 65 is drawn to facilitate estimations of aerodynamic centre. The two intermediate curves are slightly adjusted to give even spacing.

17.2 *Theoretical Values of h.*—Preston in Fig. 2 of Ref. 14 gives the results of his investigation of the potential flow values of h for a wide range of sections. Preston's figure is not satisfactory for dealing with some types of modern profiles. Thomas in Ref. 15 gives a formula for the approximate computation of $(h)_T$, which is very useful; but the possible error by its use is still notable. The question of estimating $(h)_T$ is under investigation at the N.P.L. It appears that for many purposes the collection of curves in Fig. 66 may be found sufficiently accurate. In this figure $(h)_T$ is plotted against t/c as in Fig. 2 of Ref. 14. The curves are drawn to represent aerofoils with positions of the maximum ordinate of the section x_m, ranging from $0{\cdot}3c$ to $0{\cdot}5c$. To give an idea of the degree of approximation attained when using this Fig. 66 for estimations, several points are plotted for typical aerofoils. The values of $(h)_T$ for the Piercy, Kármán-Trefftz, and Lighthill sections are exact; those for EQH were calculated by Goldstein's approximate method, Ref. 16, and are taken from Ref. 14. The points labelled Lighthill apply to a number of sections calculated by the Lighthill exact process, R. & M. 2112[17]; these it will be noticed tend to give lower values than the older sections. From the evidence of the plotted points in relation to the various curves, it is considered that, except for sections with x_m towards $0{\cdot}5c$, $(h)_T$ can be read off the curves of Fig. 66 with an error not exceeding 0·003. For the typical modern sections with x_m in the neighbourhood of 0·4 the error is likely to be quite small.

18. *Relation between m and Lift Slope.*—Finally the ratio $m/(m)_T$ is plotted against $a_1/(a_1)_T$ in Fig. 67. Fig. 67a refers to $E = 0{\cdot}4$ and Fig. 67b to $E = 0{\cdot}2$. Again a separate curve appears necessary for each value of τ. Scales of m for the 1541 models are given in each figure. $(m)_T$ was computed for the 1541 models using the Goldstein and Preston 'simple' method of Ref. 18. It appears, however, that $(m)_T$ is given with sufficient accuracy by the thin-plate value as given in the curve of Fig. 68, taken from R. & M. 1095. Two points computed for the 1541 models are plotted in Fig. 68, and the difference from the thin-plate value is negligible.

It seems that when $E = 0{\cdot}4$ in most cases, certainly for $a_1/(a_1)_T$ greater than 0·8, the theoretical value of m is near enough to use for practical purposes; on the other hand very few ailerons have chords as wide as $0{\cdot}4c$, and, as Fig. 67b shows, when E is 0·2 the theoretical value is not sufficiently representative of the actual value in most practical cases. However the reduction in the value of m below the theoretical value is seldom more than 10 per cent with modern sections, when E is 0·2.

In Fig. 67b are plotted all the measured points for tests of the 1541a section ($\tau = 19{\cdot}2$ deg.) in the R.A.E. No. 2, $11\frac{1}{2}$ by $8\frac{1}{2}$-ft Wind Tunnel. The general trend of the curve towards the extreme point (1,1) in the figure is fairly definitely indicated. The points from the R.A.E. tunnel include those for transition varying from $0{\cdot}15c$ to $0{\cdot}65c$, and Reynolds numbers varying from 2·5 to nearly 10 times 10^6.

19. *Acknowledgements.*—The authors wish to acknowledge the assistance of several of their colleagues who carried out a long and tedious sequence of experiments in connection with this work. In particular Miss D. K. Cox, Messrs. J. H. Warsap, W. C. Skelton and T. W. Brown contributed very largely to the work of observation and reduction.

The authors wish also to express their appreciation of the skill shown by Mr. F. J. Miles of the workshop staff in constructing the models, which had to be finished with very special care owing to the sensitivity of control forces to small inaccuracies in shape, particularly at the trailing edge.

LIST OF SYMBOLS

a_1	=	$\partial C_L/\partial\alpha$, rate of change of lift coefficient with incidence
a_2	=	$\partial C_L/\partial\eta$, rate of change of lift coefficient with flap setting
b_1	=	$\partial C_H/\partial\alpha$, rate of change of hinge-moment coefficient with incidence
b_2	=	$\partial C_H/\partial\eta$, rate of change of hinge-moment coefficient with flap setting
t		Maximum thickness of wing section
τ		Trailing-edge angle of the section
h		Height of tunnel cross-section ; also, position of aerodynamic centre
b		Breadth of tunnel cross-section
C_L'		Measured lift coefficient in tunnel
C_H'		Measured hinge-moment coefficient in tunnel
α'		Measured incidence
η		Measured flap deflection
s		Semi-span of model, excluding dummy ends
$\Delta\alpha$		Incidence correction due to tunnel-wall interference
ΔC_L		C_L correction due to tunnel-wall interference
ΔC_H		C_H correction due to tunnel-wall interference
l		Distance of centre of pressure from the leading edge
l_1		Value of l for lift due to incidence change
l_2		Value of l for lift due to flap angle
E		Ratio of flap chord to aerofoil chord
T		Suffix to denote theoretical values of the coefficients a_1, a_2, b_1, b_2 for potential flow with Joukowsky value of the circulation

APPENDIX

Tunnel Interference Correction.—The two-dimensional tunnel interference has been deduced from Ref. 7 (Bryant and Garner, 1950). The first correction to be applied to the measurements takes account of the increase in wind speed due to tunnel blockage. In the notation of Ref. 7, section 4.1,

$$\frac{(\Delta V)}{V} = 0{\cdot}62\frac{A'}{h^2} + 0{\cdot}50\frac{t^2}{ch}$$

where A', the sectional area of the wing, is approximately given by

$$\frac{A'}{ct} = 0{\cdot}67_5,$$

the tunnel height, $h = 7$ ft, $c = 30$ in., and $t/c = 0{\cdot}15$. Thus

$$\frac{(\Delta V)}{V} = 0{\cdot}0080 + 0{\cdot}0040 = 0{\cdot}0120 = 1{\cdot}2 \text{ per cent},$$

and the aerodynamic pressure $\frac{1}{2}\rho V^2$ is increased by 2·4 per cent. The measured coefficients are therefore corrected by a factor $0{\cdot}976_5$.

Denote by C_L' and C_H' the measured lift and hinge-moment coefficients corrected for tunnel blockage. Then, if α' is the measured incidence, in the range of linear slopes the tunnel derivatives are defined to be

$$(a_1)' = C_L'/\alpha',$$
$$(b_1)' = C_H'/\alpha'.$$

Similarly if α' is set to zero and the flap is given a measured deflection η for symmetrical sections

$$(a_2)' = C_L'/\eta,$$
$$(b_2)' = C_H'/\eta.$$

The interference in addition to tunnel blockage takes the form of an incidence correction $(\Delta\alpha)$, and of corrections applied to C_L' and C_H' on account of the induced curvature of flow.

$$(\Delta\alpha) = \frac{\pi}{48}\left(\frac{c}{h}\right)^2 C_L'(1 - 2l)$$

where l is the position of the centre of pressure measured as a fraction of the chord from the leading edge.

The respective corrections to C_L',C_H' are

$$(\Delta C_L) = -\frac{\pi}{192}\left(\frac{c}{h}\right)^2 C_L'\frac{\partial C_L}{\partial\gamma},$$

$$(\Delta C_H) = -\frac{\pi}{192}\left(\frac{c}{h}\right)^2 C_L'\frac{\partial C_H}{\partial\gamma},$$

where $$\frac{\partial C_L}{\partial\gamma} = 4\pi\frac{a_1}{(a_1)_T} = \text{approximately } \frac{2a_1}{1 + 0{\cdot}8t/c}$$

and $$\frac{\partial C_H}{\partial\gamma} = \left(\frac{\partial C_H/\partial\gamma}{b_1}\right)_T b_1$$

where for plain flaps the values of $\left(\frac{\partial C_H/\partial\gamma}{b_1}\right)_T$ in Ref. 7, Table 2, with $\lambda = 0$ may be used. γ denotes camber of the centre-line of the aerofoil.

It follows that the corrected experimental lift slope,

$$a_1 = \frac{C_L' + (\Delta C_L)}{\alpha' + (\Delta\alpha)} = \frac{1 - \frac{\pi}{192}\left(\frac{c}{\bar{h}}\right)^2 \frac{\partial C_L}{\partial \gamma}}{\frac{1}{(a_1)'} + \frac{\pi}{48}\left(\frac{c}{\bar{h}}\right)^2 (1 - 2l_1)},$$

and the corrected experimental hinge-moment slope,

$$b_1 = \frac{C_H' + (\Delta C_H)}{\alpha' + (\Delta\alpha)} = \frac{\frac{(b_1)'}{(a_1)'} - \frac{\pi}{192}\left(\frac{c}{\bar{h}}\right)^2 \frac{\partial C_H}{\partial \gamma}}{\frac{1}{(a_1)'} + \frac{\pi}{48}\left(\frac{c}{\bar{h}}\right)^2 (1 - 2l_1)},$$

where for a uniform incidence

$$l_1 = \tfrac{1}{4}.$$

If $\alpha' = 0$ and η is the measured flap deflection, the free-stream conditions corresponding to the tunnel test are a uniform incidence $(\Delta\alpha)$ with a flap deflection η

and $$C_L = C_L' + (\Delta C_L)$$
$$C_H = C_H' + (\Delta C_H).$$

It is now supposed that a_1 and b_1 are independent of η and the small incidence is represented by respective negative corrections $-a_1(\Delta\alpha)$, $-b_1(\Delta\alpha)$ to C_L, C_H. Then

$$a_2 = (a_2)'\left[1 - \frac{\pi}{192}\left(\frac{c}{\bar{h}}\right)^2 \frac{\partial C_L}{\partial \gamma} - a_1\left\{\frac{\pi}{48}\left(\frac{c}{\bar{h}}\right)^2 (1 - 2l_2)\right\}\right]$$

$$b_2 = (b_2)' - (a_2)'\left[\frac{\pi}{192}\left(\frac{c}{\bar{h}}\right)^2 \frac{\partial C_H}{\partial \gamma} + b_1\left\{\frac{\pi}{48}\left(\frac{c}{\bar{h}}\right)^2 (1 - 2l_2)\right\}\right]$$

where l_2 depends on the flap/chord ratio E and is given in Ref. 7, Table 1.

The corrections are finally expressed in the convenient form

$$a_1 = \frac{(a_1)'}{1 + (F + G)(a_1)'},$$

$$b_1 = \frac{(b_1)'}{1 + (G + H)(a_1)'}$$

$$a_2 = (a_2)' - (a_2)'a_1(F + G - J),$$

$$b_2 = (b_2)' - (a_2)'b_1(G + H - J),$$

where $$F = \frac{\pi}{192}\left(\frac{c}{\bar{h}}\right)^2 \times \frac{2}{1 + 0{\cdot}8t/c} = 0{\cdot}00373,$$

$$G = \frac{\pi}{48}\left(\frac{c}{\bar{h}}\right)^2 \times \frac{1}{2} = 0{\cdot}004175,$$

$$H = \frac{\pi}{192}\left(\frac{c}{\bar{h}}\right)^2 \left(\frac{\partial C_H/\partial\gamma}{b_1}\right)_T = 0{\cdot}002087\left(\frac{\partial C_H/\partial\gamma}{b_1}\right)_T$$

where $\left(\frac{\partial C_H/\partial\gamma}{b_1}\right)_T$ is given in Ref. 7, Table 2,

$$J = \frac{\pi}{24}\left(\frac{c}{\bar{h}}\right)^2 (l_2 - \tfrac{1}{4}) = 0{\cdot}01670\,(l_2 - \tfrac{1}{4}),$$

where l_2 is given in Ref. 7, Table 1.

REFERENCES

No.	*Author*	*Title, etc.*
1	A. S. Batson and J. H. Preston ..	The Effect of Boundary-Layer Thickness on the Normal Force Distribution of Aerofoils, with Particular Reference to Control Problems. R. & M. 2008. April 1942.
2	J. H. Preston	The Approximate Calculation of the Lift of Symmetrical Aerofoils taking account of the Boundary Layer, with Application to Control Problems. R. & M. 1996. May, 1943.
3	J. H. Preston and J. H. Warsap ..	Investigation of the Relations between Experimental and Theoretical Two-dimensional Characteristics for Two Wing–Plain-Flap Combinations involving Different Flap Convexities. A.R.C. Report 8184. November, 1944. (Unpublished.)
4	C. H. Naylor and D. J. Lyons	An Analysis of the Lifting Characteristics of Aerofoils and Controls with Special Reference to Methods of Estimation for Design Use. A.R.C. Report 7149. July, 1943.
5	K. L. Loftin (Jnr.) and H. A. Smith ..	Aerodynamic Characteristics of 15 N.A.C.A. Airfoil Sections at Seven Reynolds Numbers. N.A.C.A. Technical Note 1945. October, 1949.
6	K. L. Loftin (Jnr.) and H. A. Smith ..	Two-dimensional Aerodynamic Characteristics of 34 Miscellaneous Airfoil Sections. N.A.C.A. Research Memorandum, RM No. L8L08. (N.A.C.A./T.I.B./1920). January, 1949.
7	L. W. Bryant and H. C. Garner ..	Control Testing in Wind Tunnels. A.R.C. Report 13,465. (To be published.)
8	H. Glauert	Theoretical Relationships for an Aerofoil with Hinged Flaps. R. & M. 1095. April, 1927.
9	Thos. A. Toll	Summary of Lateral Control Research. N.A.C.A. Technical Note 1245. March, 1947.
10	L. W. Bryant and A. S. Batson ..	Experiments on the Effect of Transition on Control Characteristics, with a Note on the Use of Transition Wires. R. & M. 2164. November, 1944.
11	A. S. Batson, J. H. Warsap and T. W. Brown	Experiments on a 20 per cent Control with Tab fitted to NACA 0015 Aerofoil, with Especial Reference to Effect of its Section on Hinge Moment and Lift. R. & M. 2314. August, 1943.
12	A. S. Batson, J. H. Preston and J. H. Warsap	Experiments Giving Hinge Moments and Lift on a NACA 0015 Aerofoil Fitted with a 40 per cent Control, with Especial Reference to Effect of Curvature of Control Surface. R. & M. 2698. April, 1943.
13	H. H. B. M. Thomas	Correlation of Experimental and Theoretical Hinge Moment for Plain Controls. A.R.C. Report 11,401. March, 1948.
14	J. H. Preston	Correlation of the Position of the Aerodynamic Centre with Lift Slope for a Variety of Aerofoils in Various Wind Tunnels. A.R.C. Report 6809. June, 1943. (Unpublished.)
15	H. H. B. M. Thomas	Correlation of the Position of the Aerodynamic Centre of an Aerofoil with the Rate of Change of the Lift Coefficient with Incidence. A.R.C. Report 12,965. November, 1949. (Unpublished.)
16	S. Goldstein	A Theory of Aerofoils of Small Thickness. Part I. Velocity Distribution for Symmetrical Aerofoils. A.R.C. Report 5804. 1942.
17	M. J. Lighthill	A New Method of Two-Dimensional Aerodynamic Design. R. & M. 2112. April, 1945.
18	S. Goldstein and J. H. Preston ..	Approximate Two-Dimensional Aerofoil Theory. Part VI. Aerfoils with Hinged Flaps. A.R.C. Report 8877. August, 1945.
19	A. R. Collar and E. G. Broadbent ..	The Rolling Power of an Elastic Wing. R. & M. 2186. October, 1945.

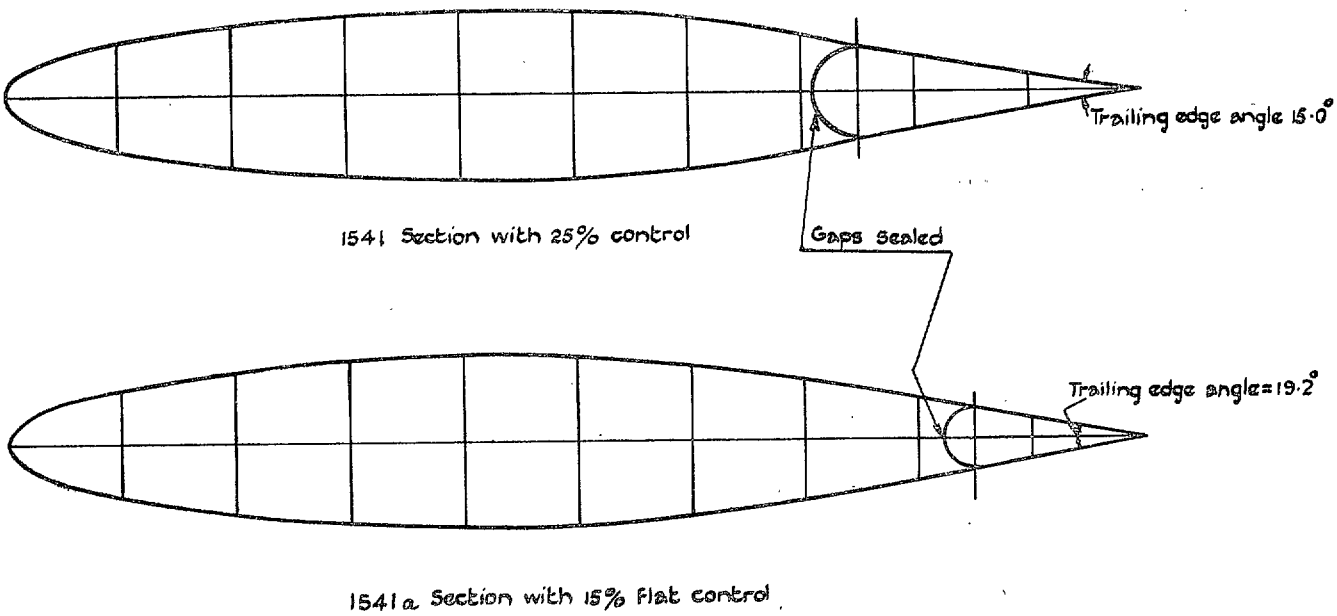
Trailing edge angle 15·0°
1541 Section with 25% control
Gaps sealed
Trailing edge angle=19·2°
1541a Section with 15% flat control

FIG. 1.

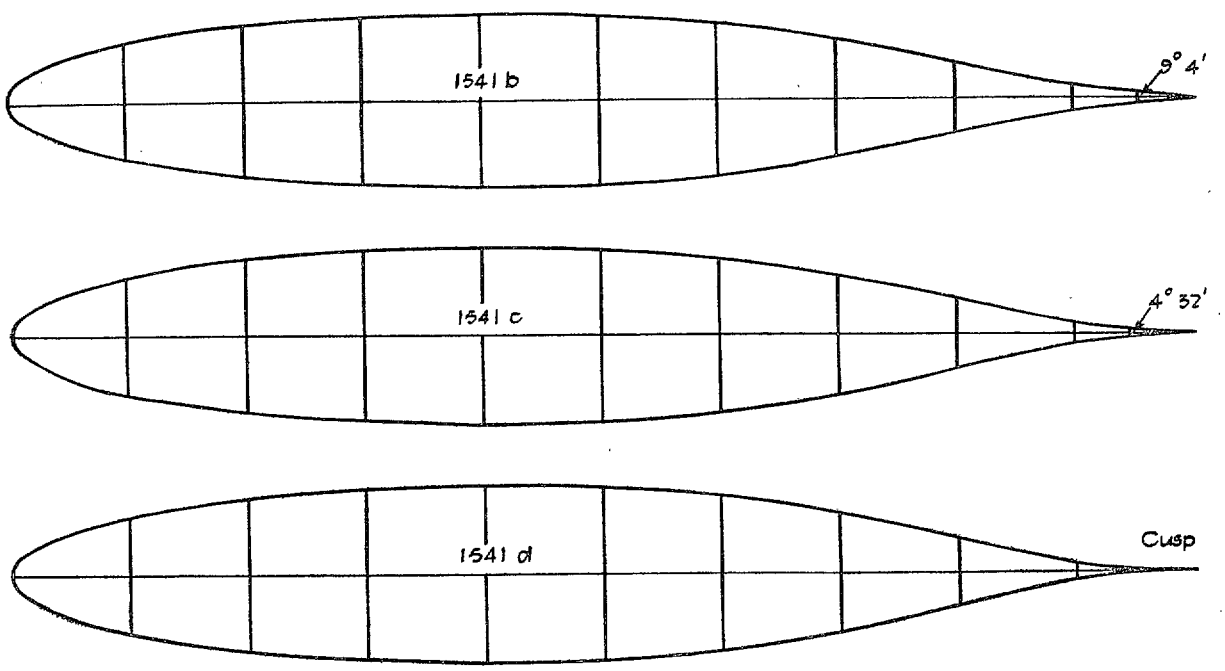
1541 b
9° 4'
1541 c
4° 32'
1541 d
Cusp

FIG. 2.

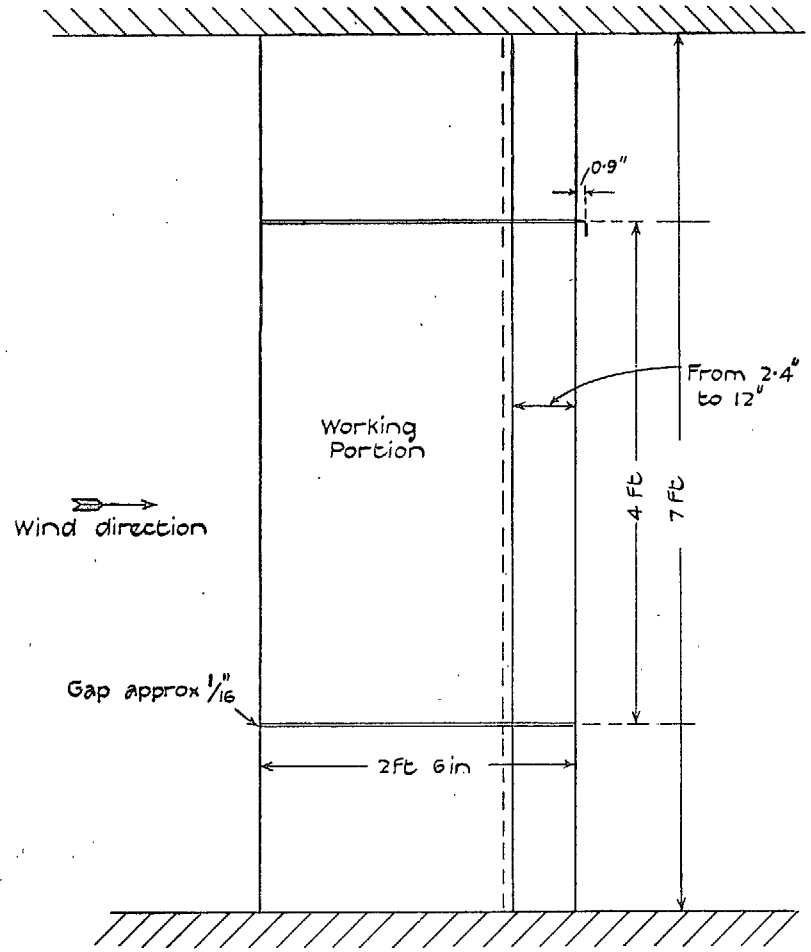

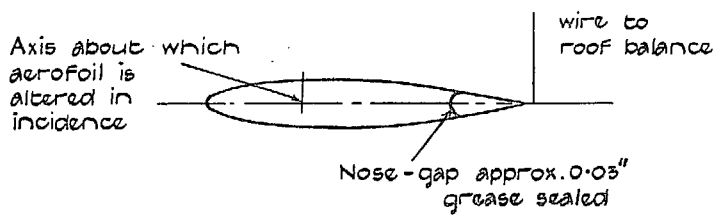

FIG. 3.

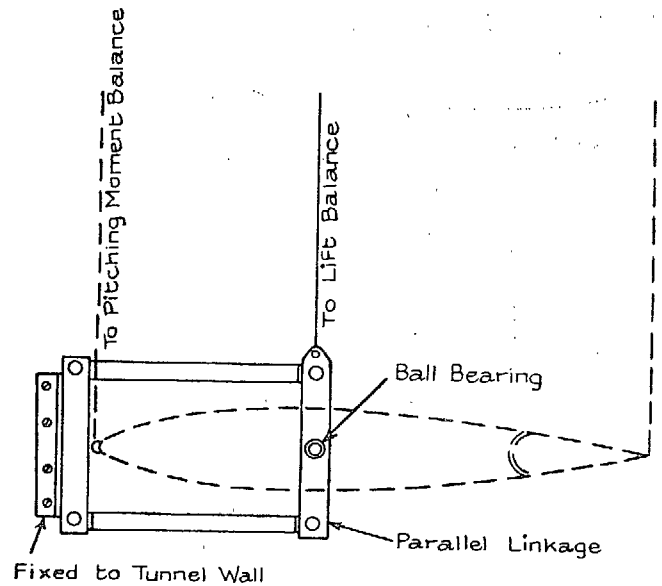

FIG. 4. Method of mounting the model.

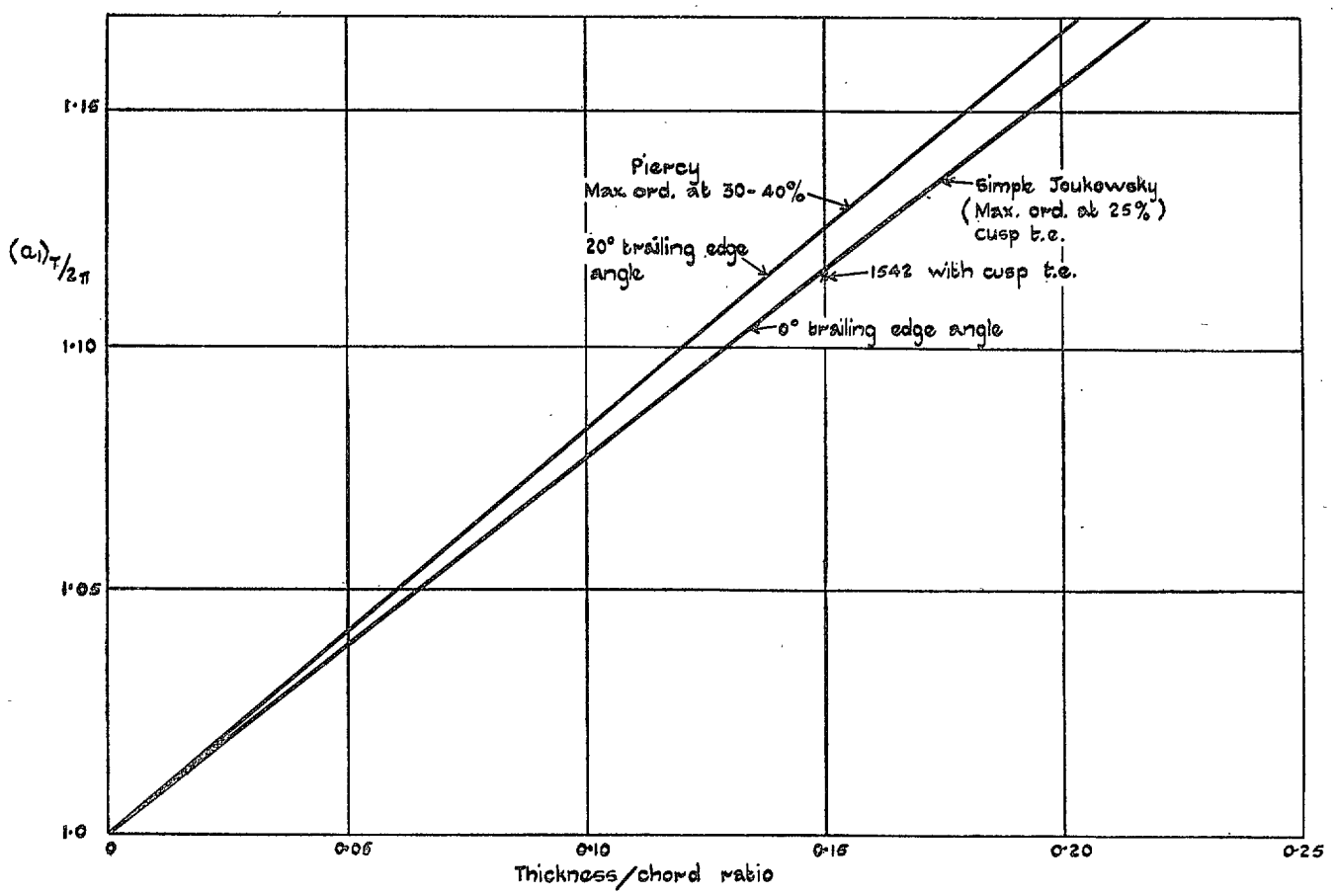

FIG. 5. Variation of $(a_1)_T$ with thickness/chord ratio.

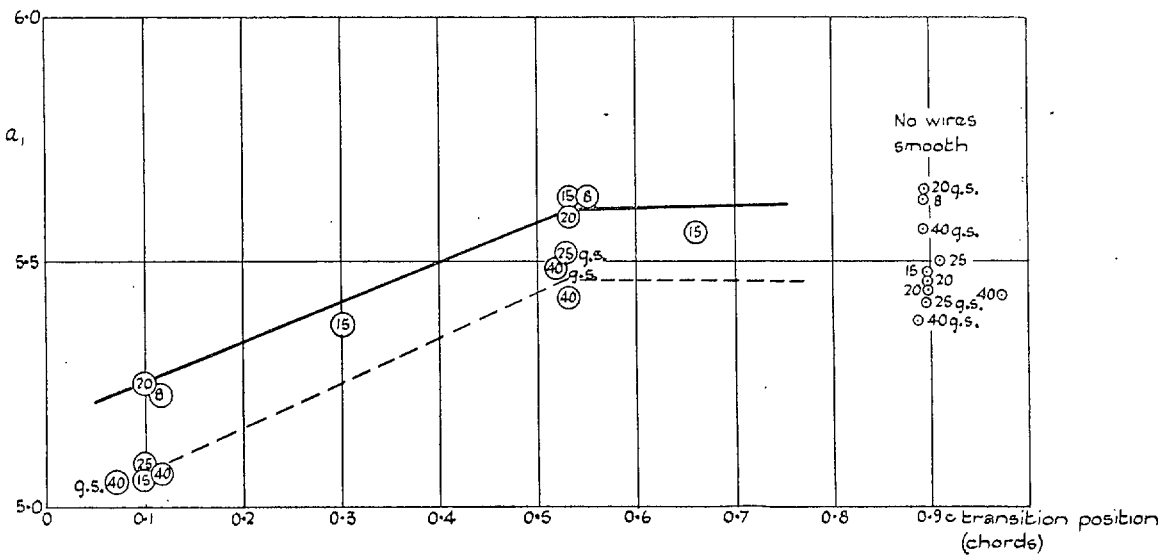

(20) means model with 20% flap set at 0°
g.s. = hinge gap grease - sealed

The full line gives the estimated a_1 for the surfaces free from boundary layer separation. Results for no wires are plotted to the scale of a_1 but not on the scale of transition.

FIG. 6. Lift slope of 1541a section from different models,

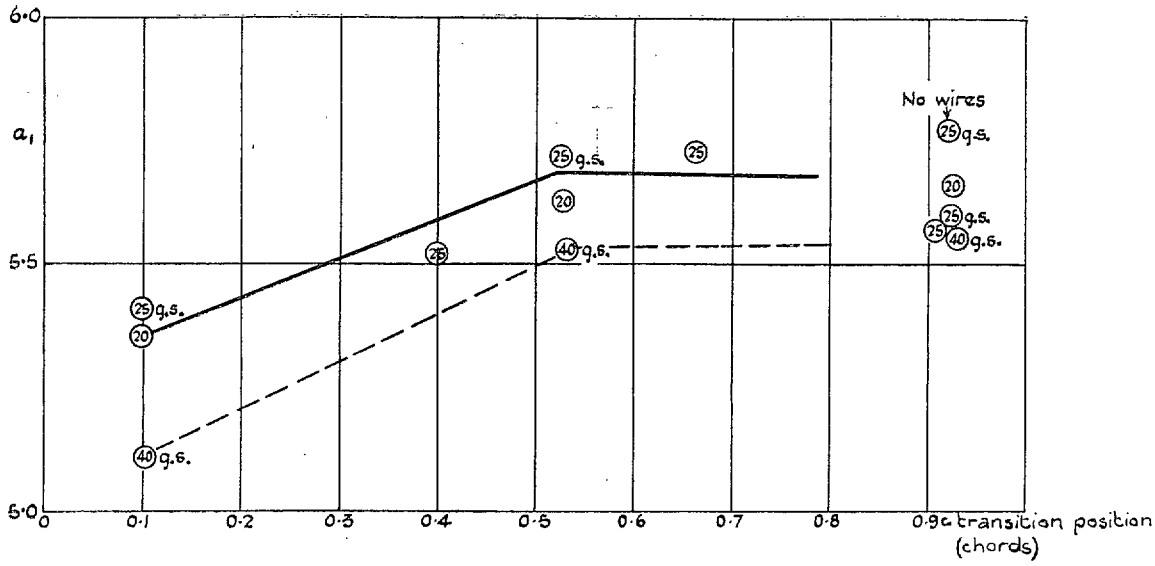

(20) means model with 20% flap set at 0°
g.s. = hinge gap grease sealed

The full line gives the estimated a_1 for the surfaces free from boundary layer separation. Results for no wires are plotted to the scale of a_1 but not on the scale of transition.

FIG. 7. Lift slope of 1541 section from different models.

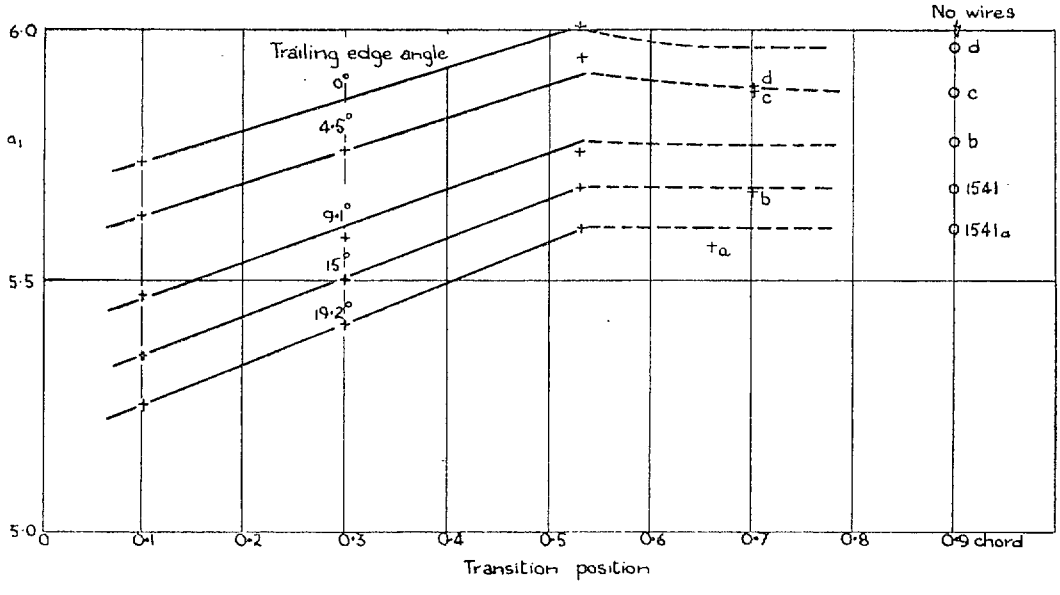

FIG. 8. Lift slope and position of transition.

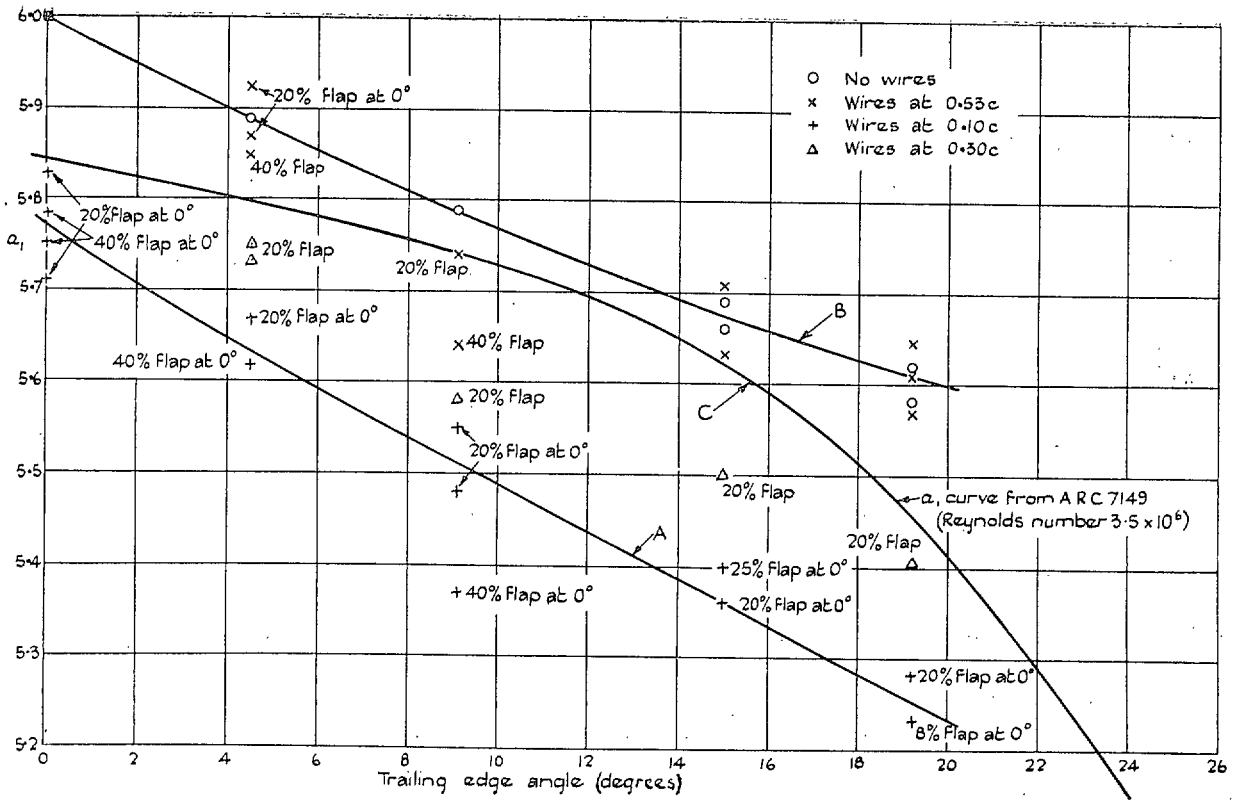

FIG. 9. Slope of the lift curve and trailing-edge angle. Reynolds number 10^6 approx.

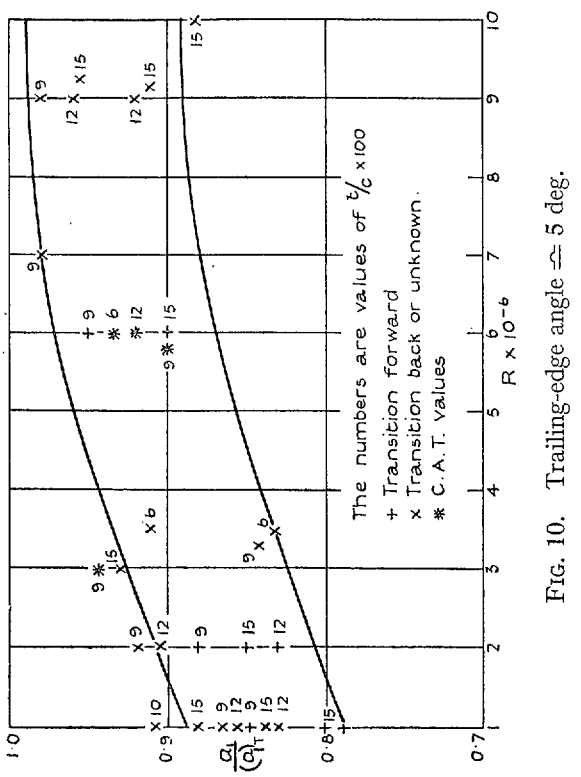

FIG. 10. Trailing-edge angle $\simeq 5$ deg.

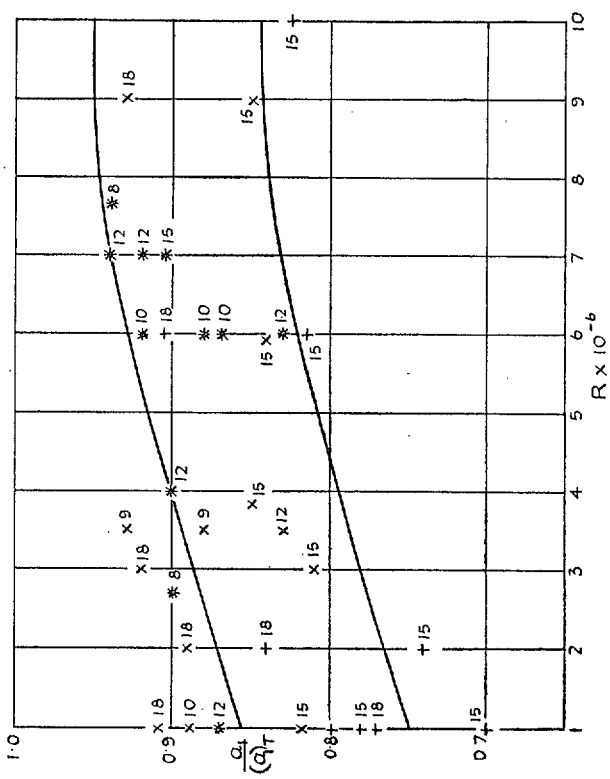

FIG. 11. Trailing-edge angle $\simeq 10$ deg.

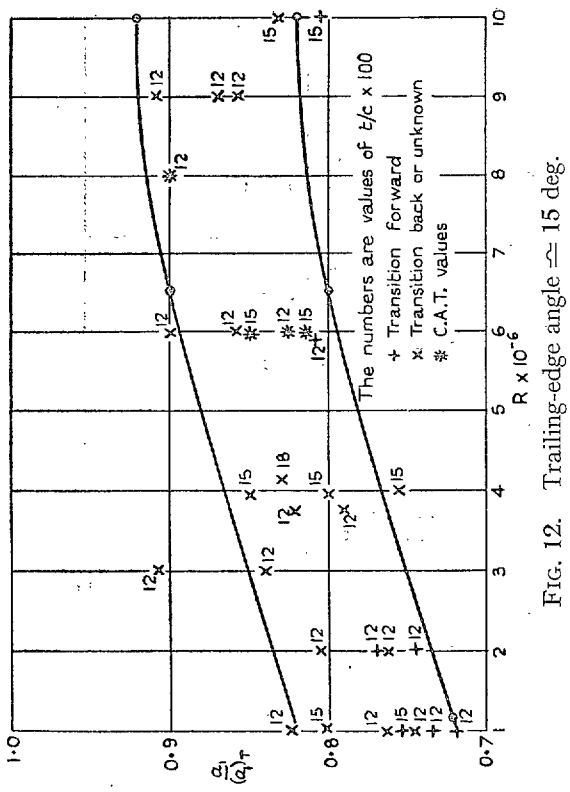

FIG. 12. Trailing-edge angle ≃ 15 deg.

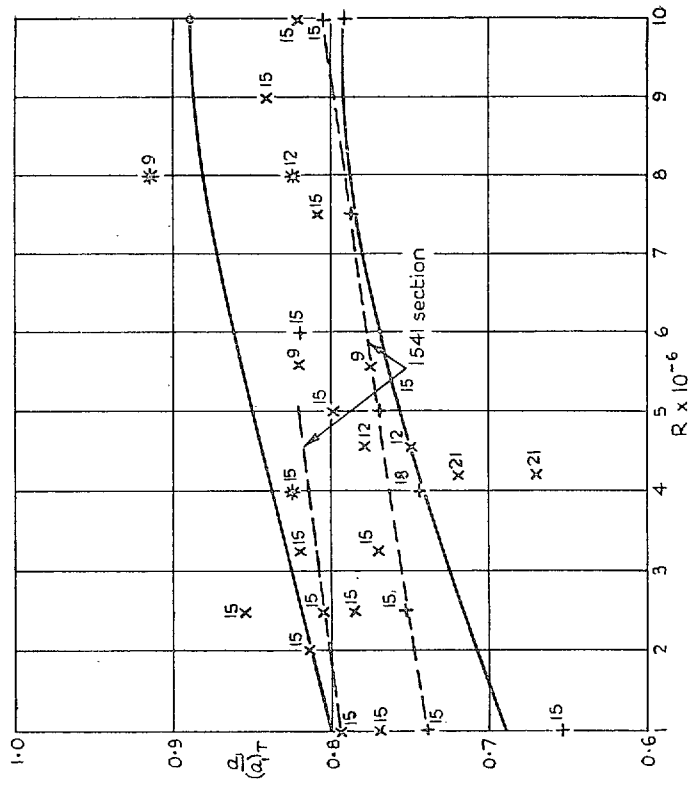

FIG. 13. Trailing-edge angle ≃ 20 deg.

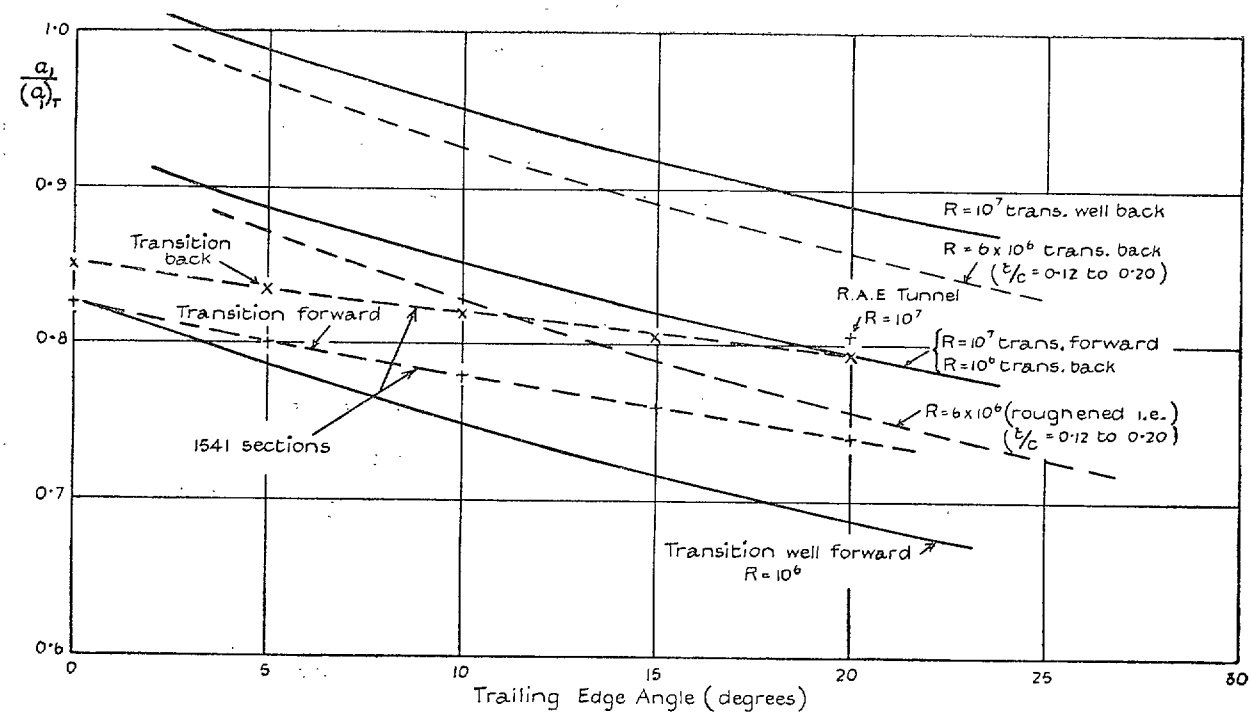

FIG. 14. Variation of $a_1/(a_1)_T$ with trailing-edge angle.

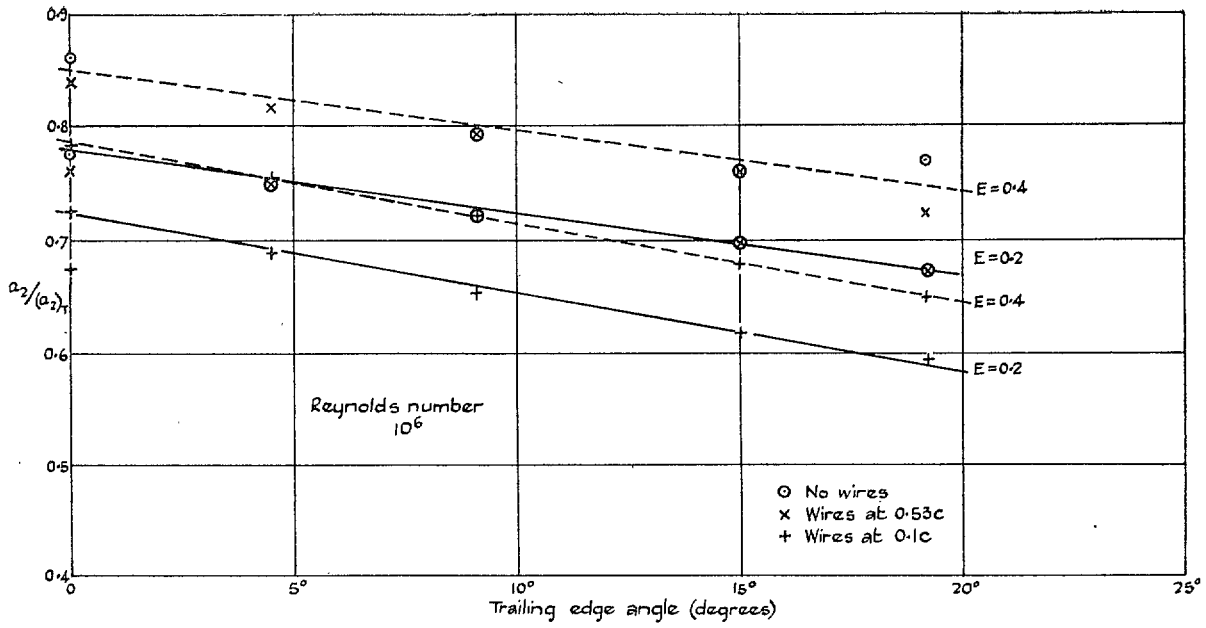

FIG. 15. Variation of $a_2/(a_2)_T$ with trailing-edge angle.

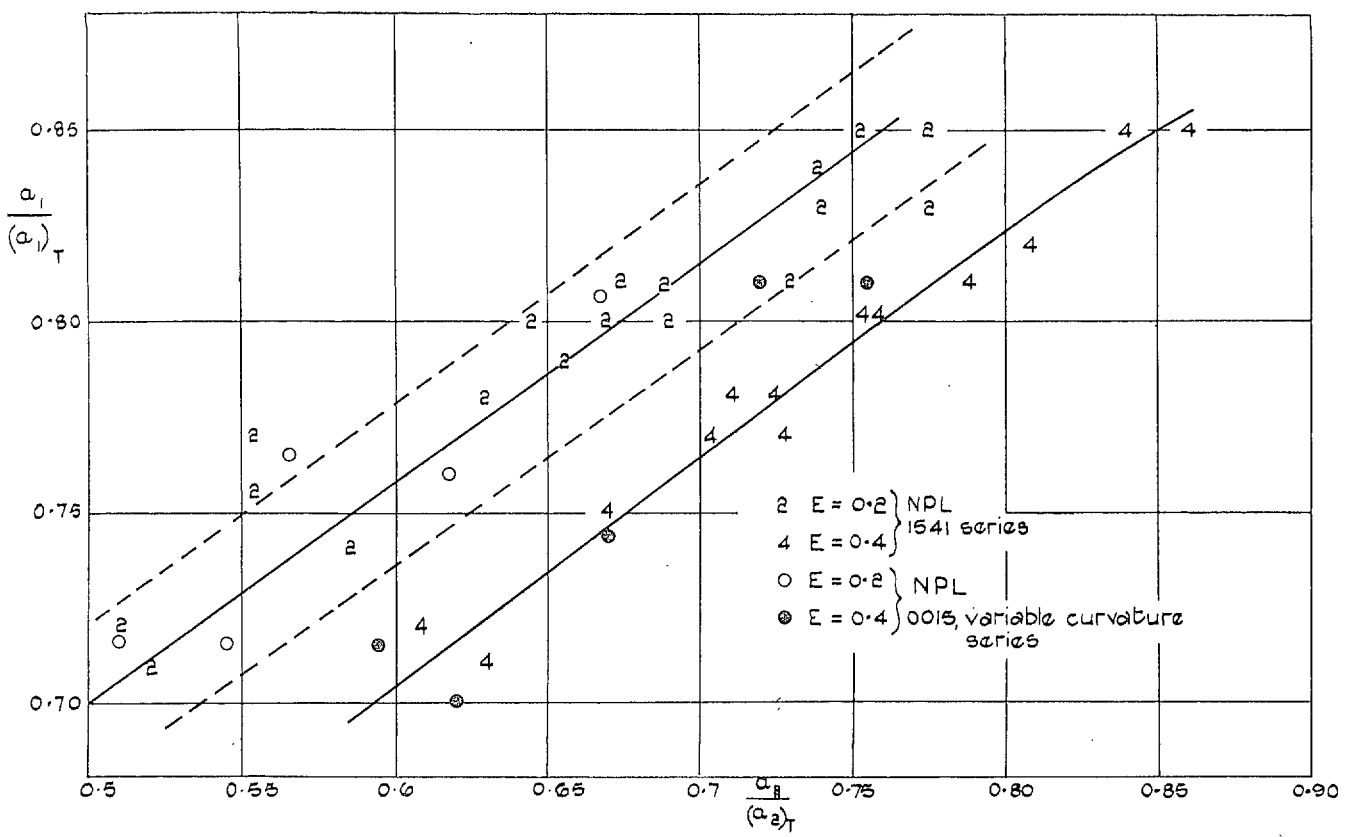

FIG. 16.

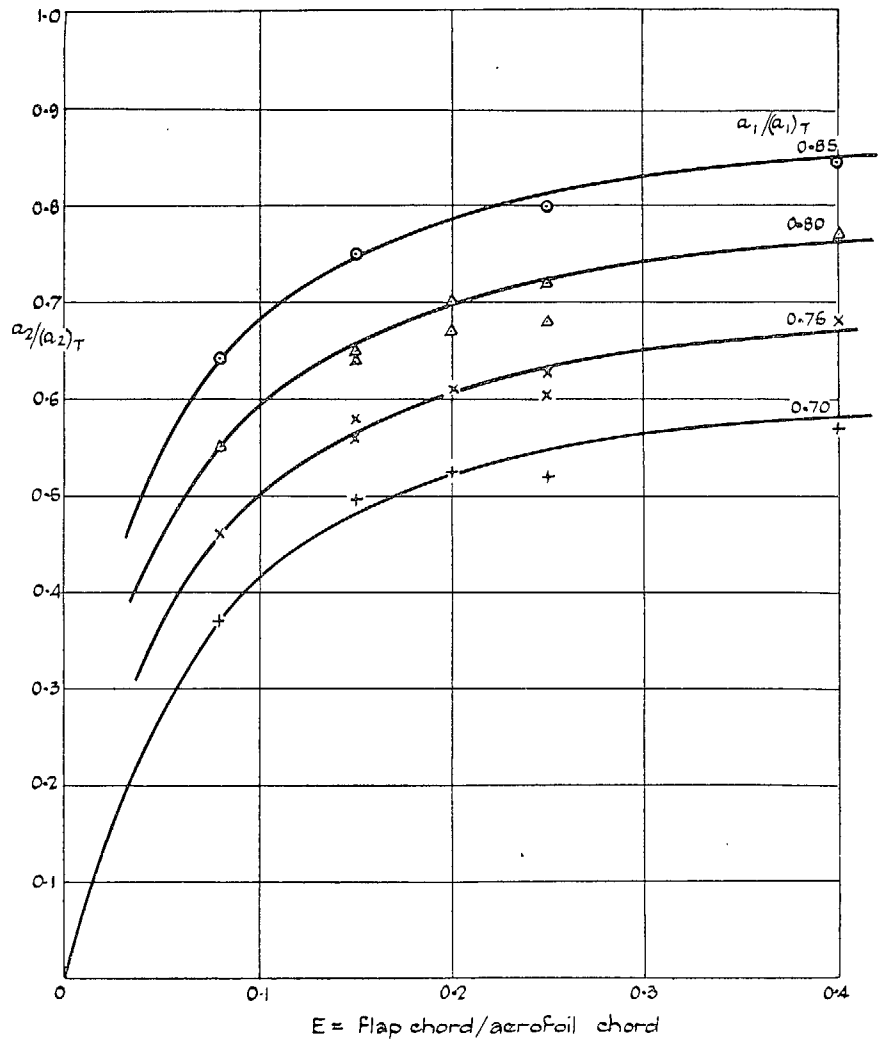

FIG. 17. Two-dimensional control characteristics. Lift due to flap and flap/chord ratio.

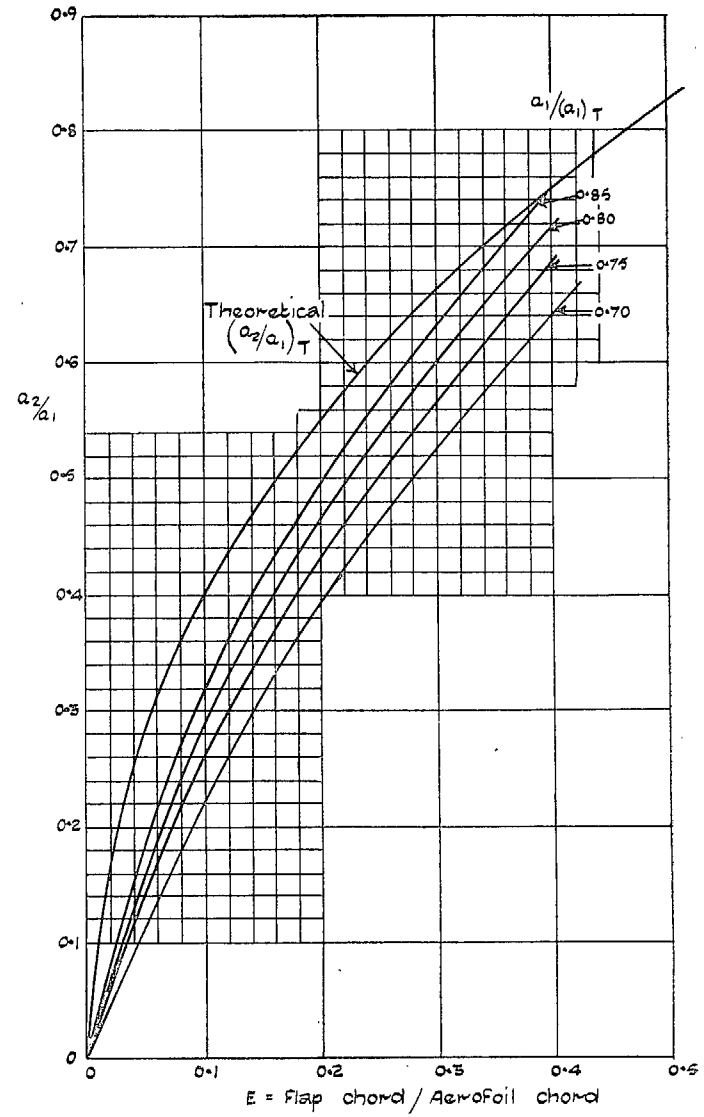

FIG. 18. a_2/a_1 and flap/chord ratio.

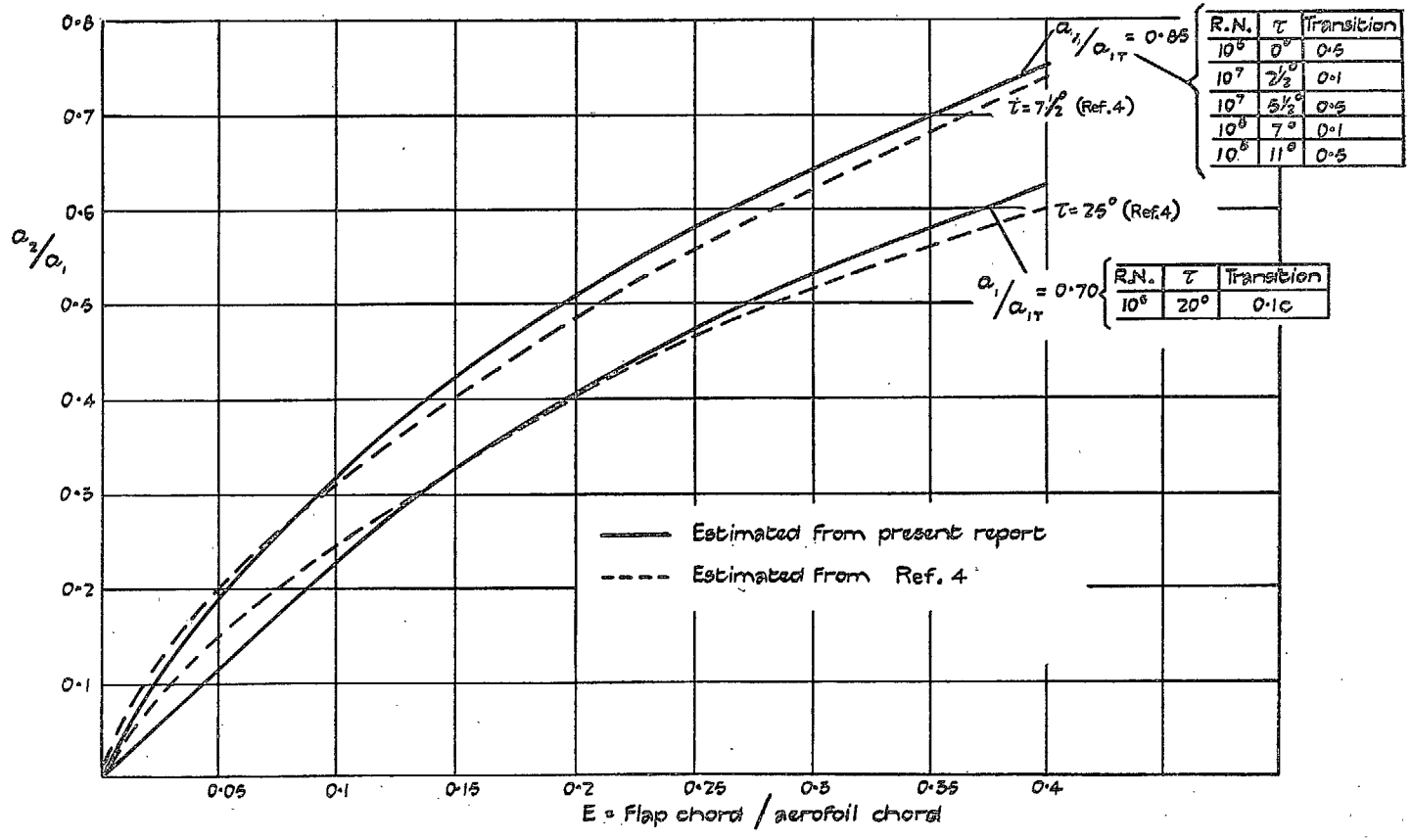
0·8
0·7
0·6
0·5
0·4
0·3
0·2
0·1
a_2/a_1
a_1/a_{1T} = 0·85
τ = 7½° (Ref. 4)
τ = 25° (Ref. 4)
a_1/a_{1T} = 0·70
R.N. | τ | Transition
10^6 | 0° | 0·5
10^7 | 2½° | 0·1
10^7 | 5½° | 0·5
10^6 | 7° | 0·1
10^6 | 11° | 0·5
R.N. | τ | Transition
10^6 | 20° | 0·1c
Estimated from present report
Estimated from Ref. 4
0·05
0·1
0·15
0·2
0·25
0·3
0·35
0·4
E = Flap chord / aerofoil chord

FIG. 19.

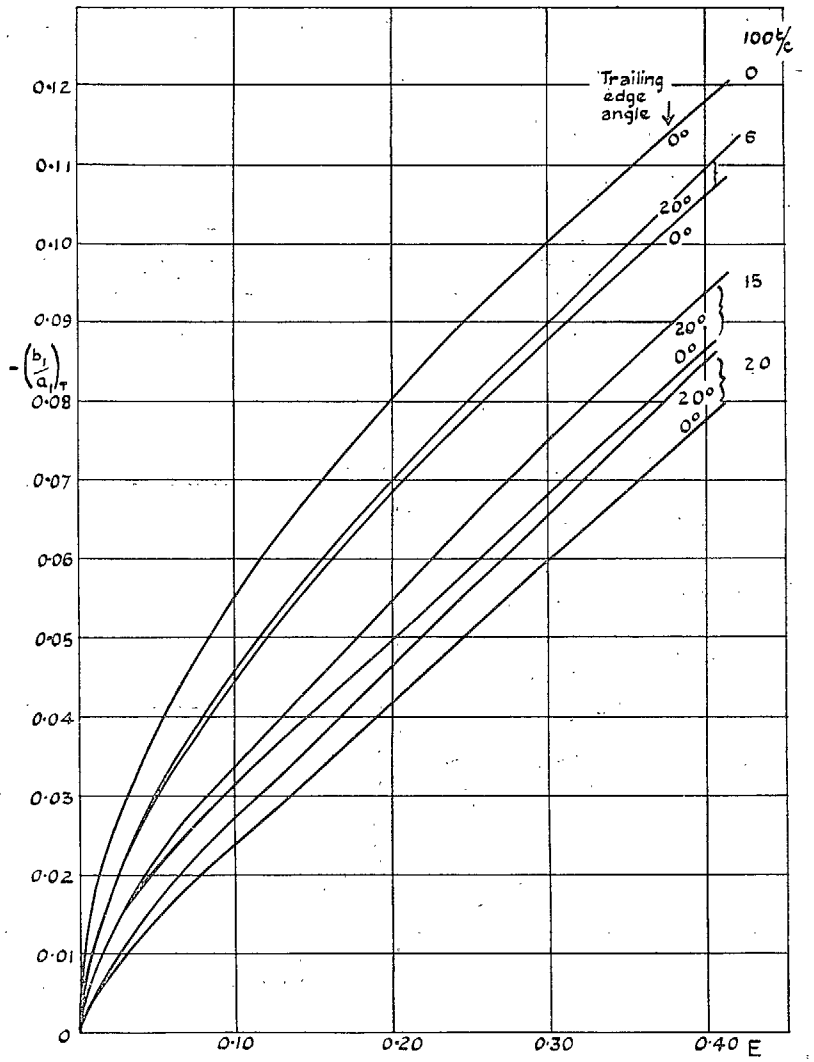

FIG. 20. Theoretical values of b_1/a_1.

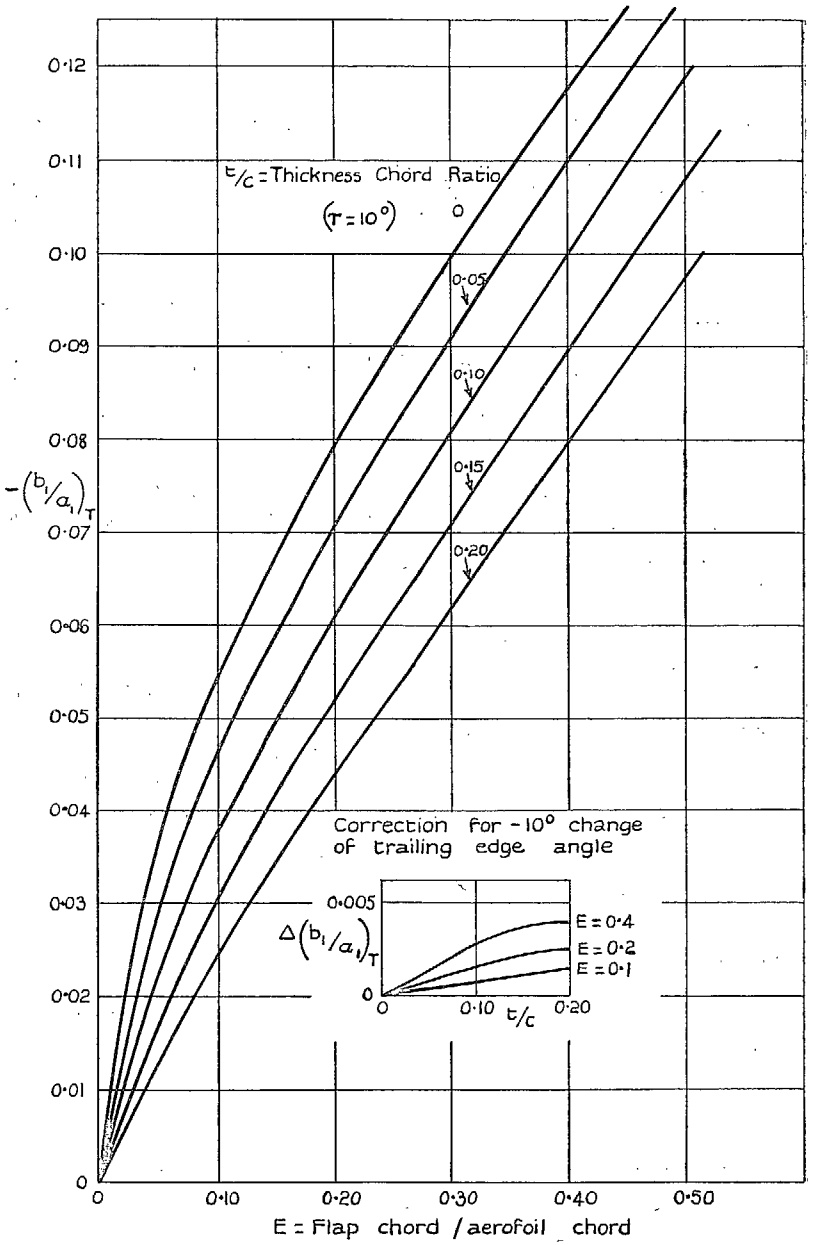

FIG. 21. Theoretical values of b_1/a_1.

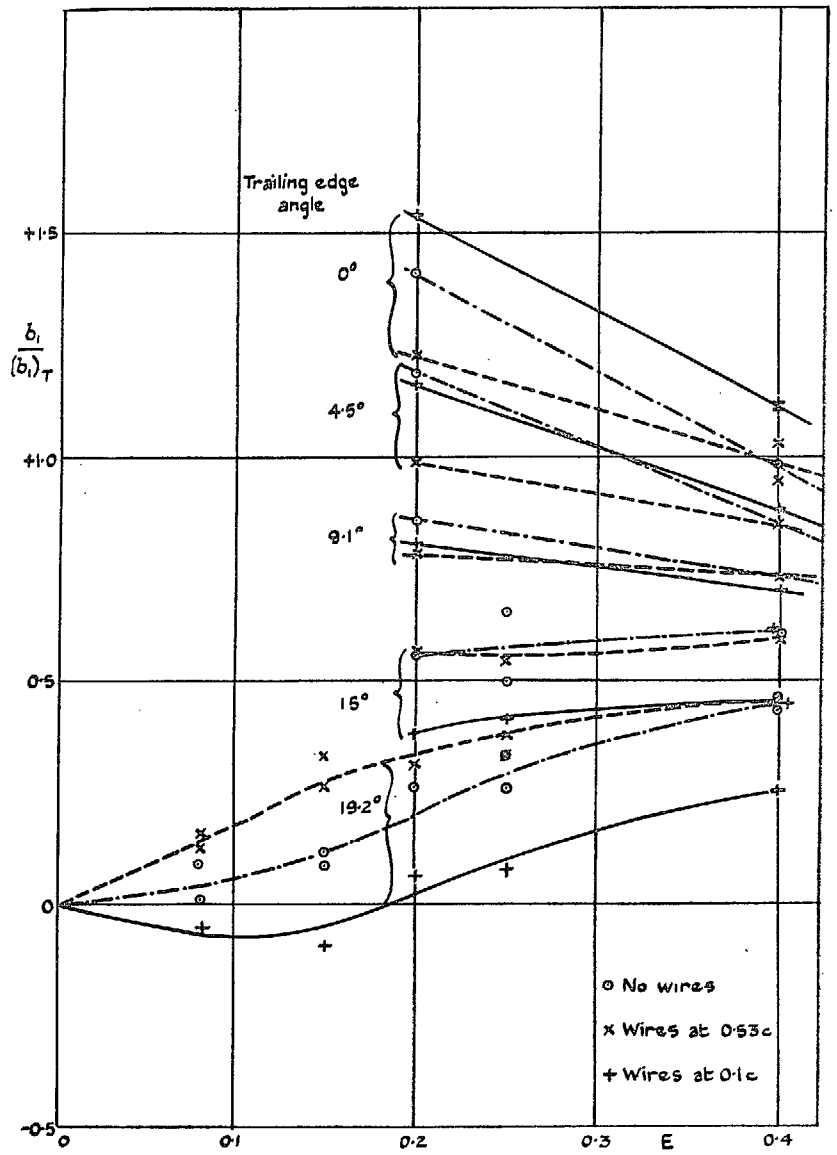

FIG. 22. Change of hinge moment with incidence. Effect of flap/chord ratio. Reynolds number 10^6.

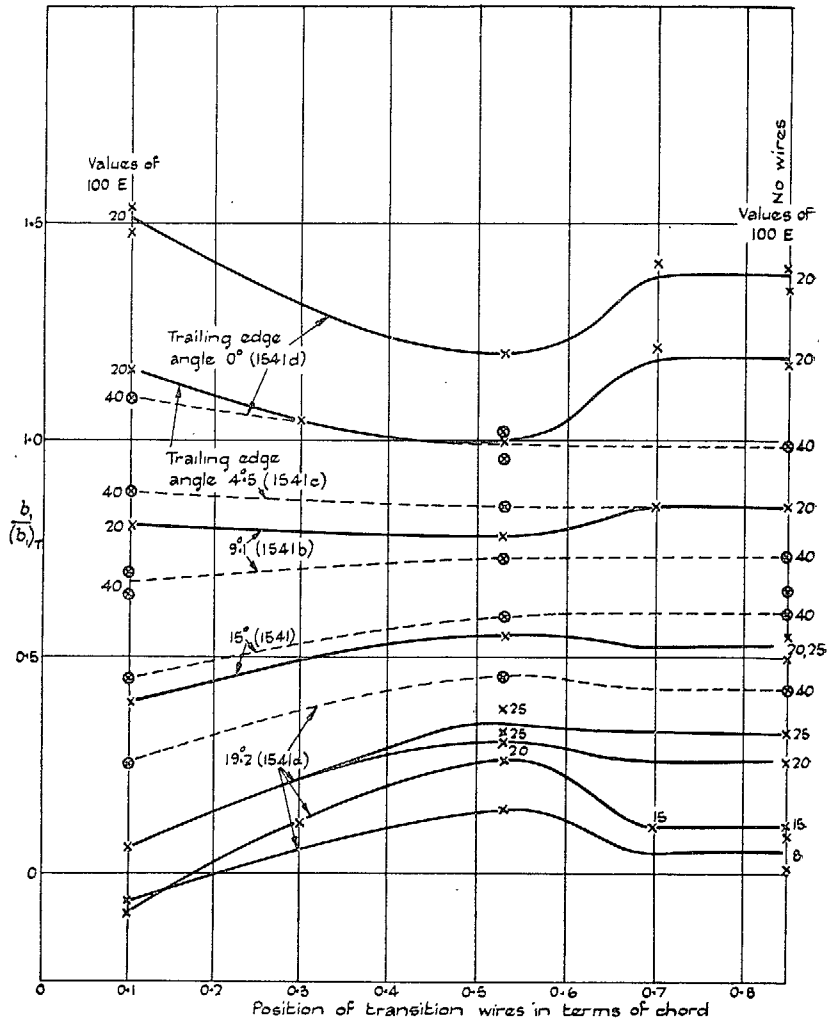

FIG. 23. Change of hinge moment with incidence. Effect of position of transition. Reynolds number 10^6.

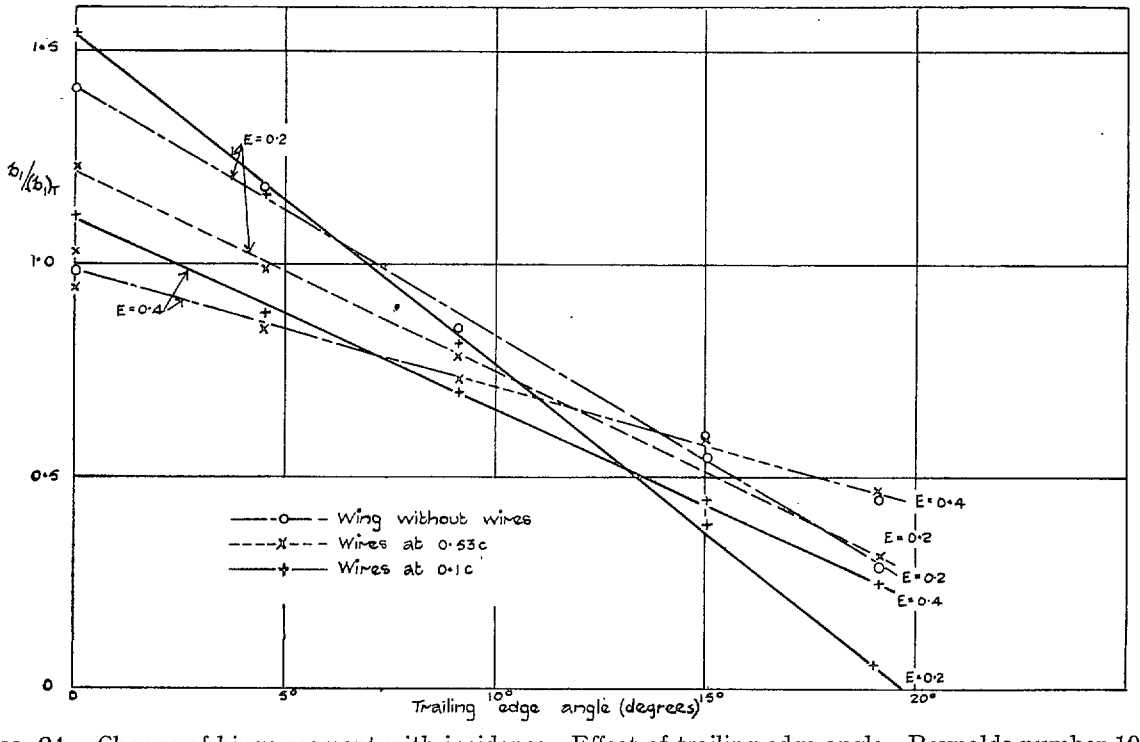

FIG. 24. Change of hinge moment with incidence. Effect of trailing-edge angle. Reynolds number 10^6.

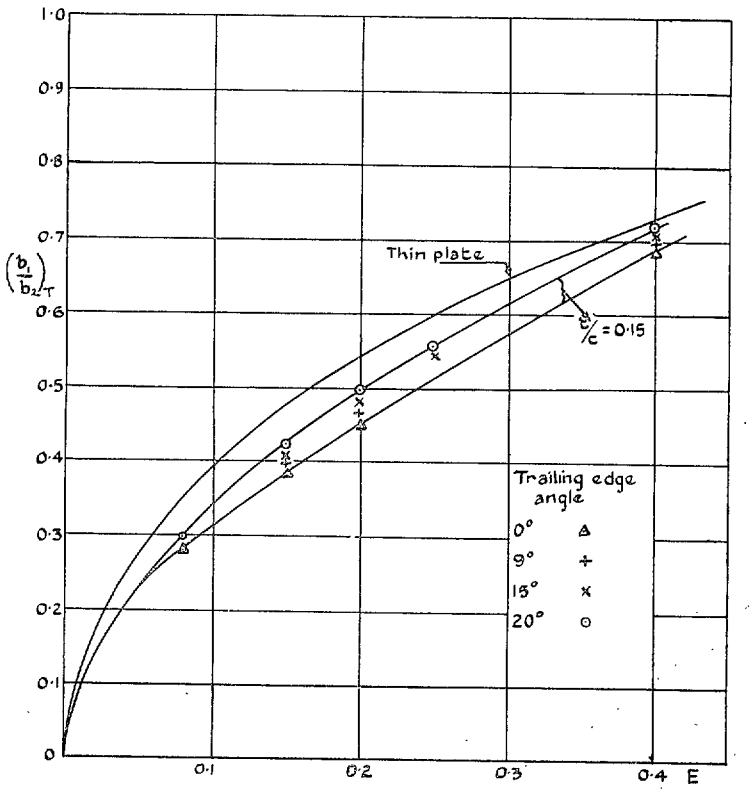

FIG. 25. Theoretical values of b_1/b_2.

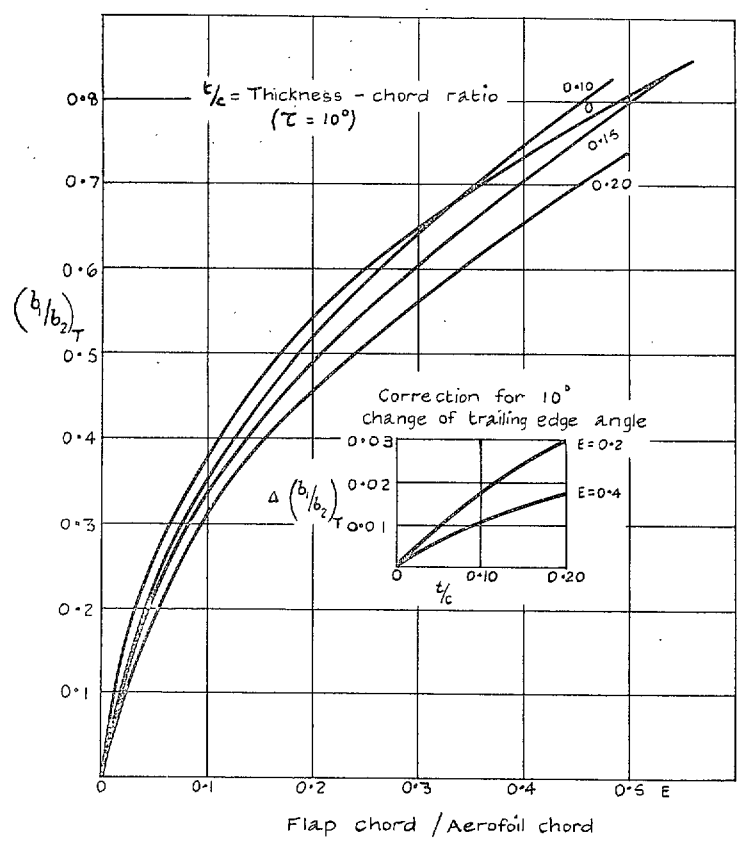

FIG. 26. Theoretical values of b_1/b_2.

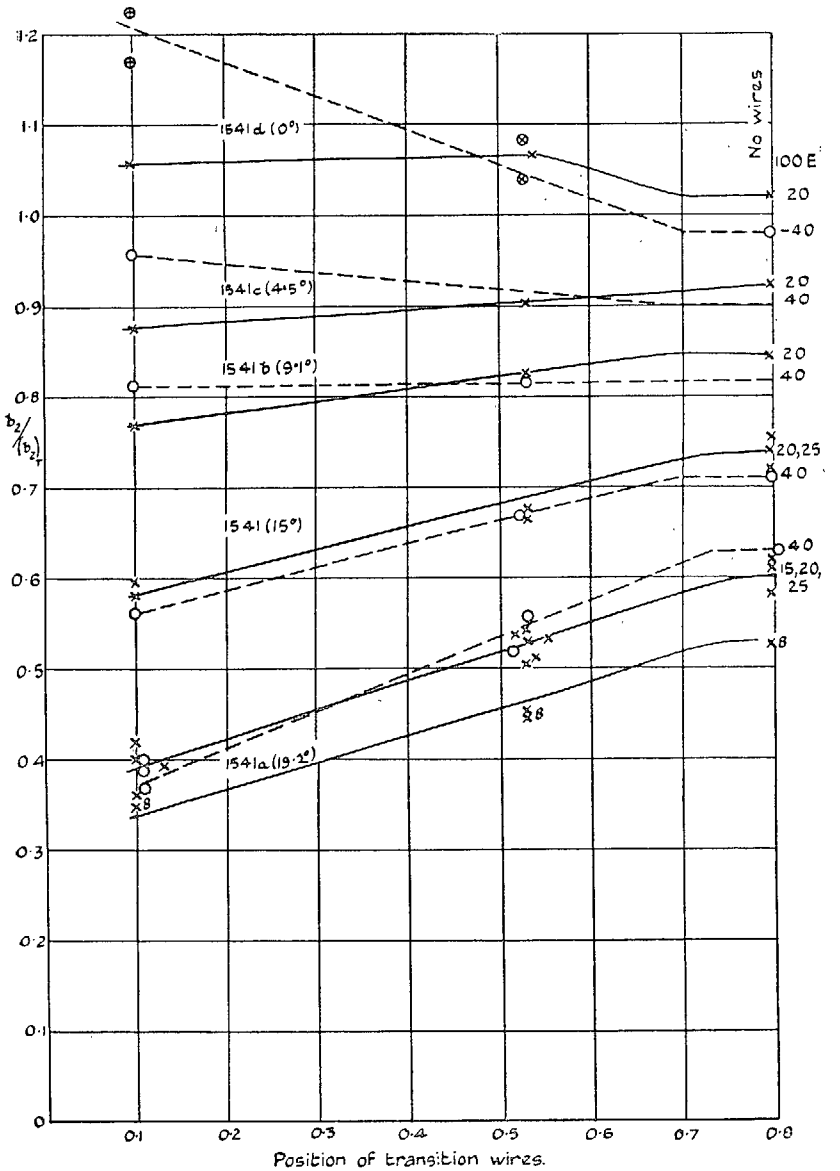

FIG. 27. Change of hinge moment with flap angle. Effect of position of transition. Reynolds number 10^6.

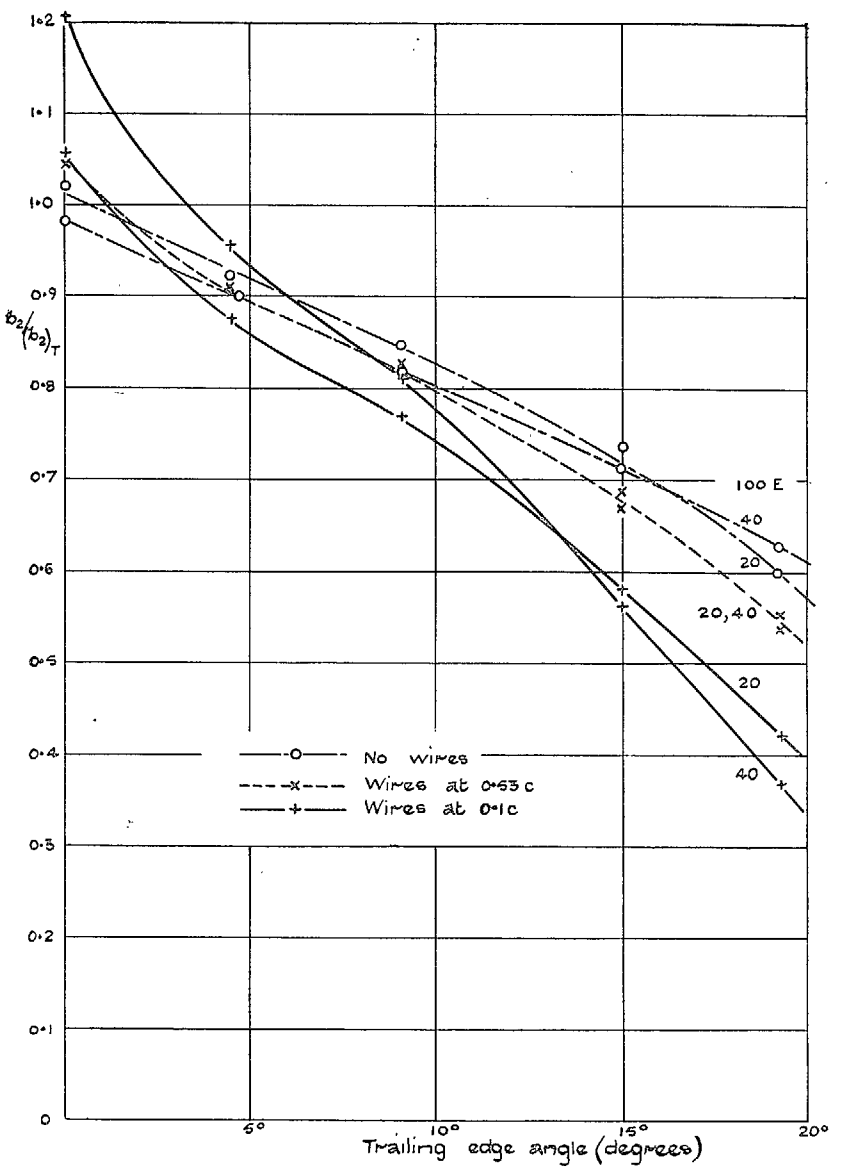

FIG. 28. Change of hinge moment with flap angle. Effect of trailing-edge angle. Reynolds number 10^6.

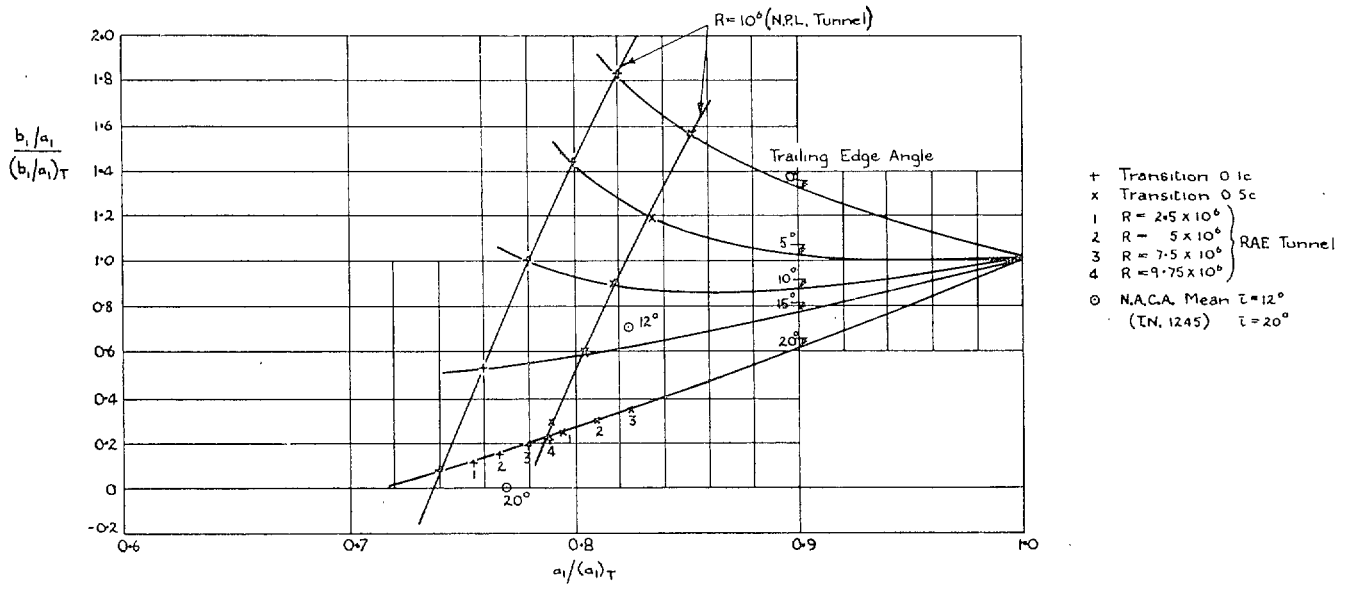

FIG. 29. Two-dimensional flap hinge moments. $E = 0{\cdot}2$. Chart for b_1/a_1.

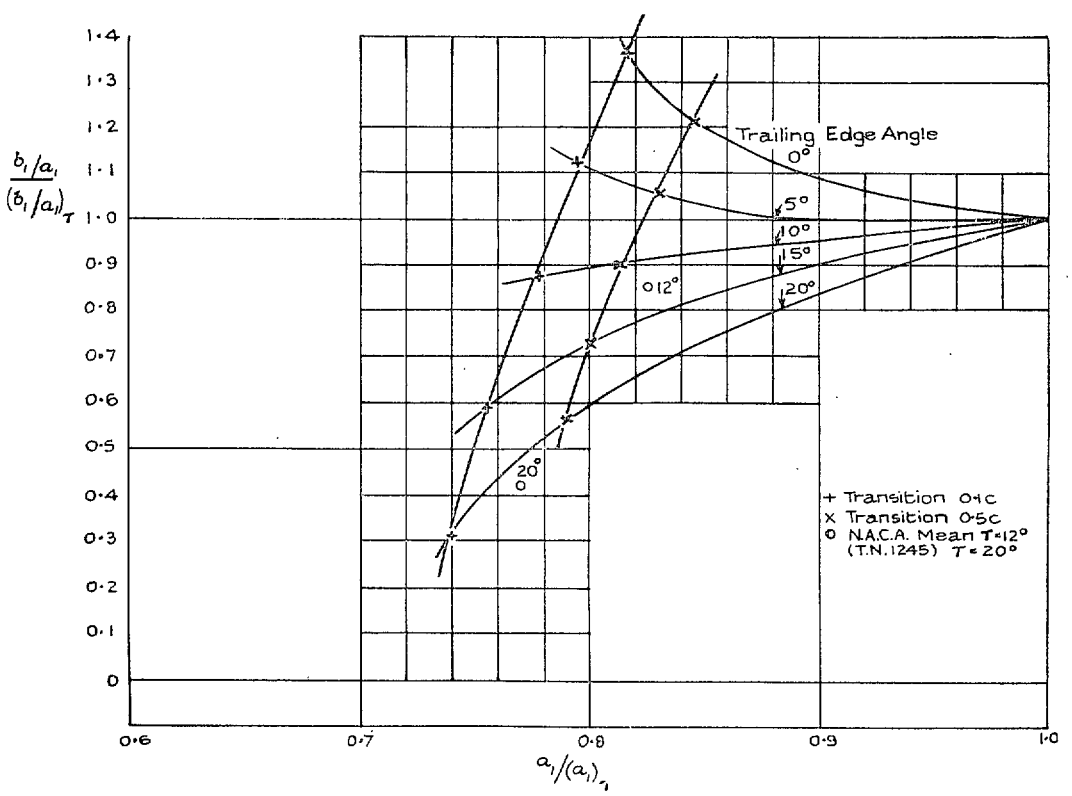

FIG. 30. Two-dimensional flap hinge moments. $E = 0{\cdot}4$. Chart for b_1/a_1.

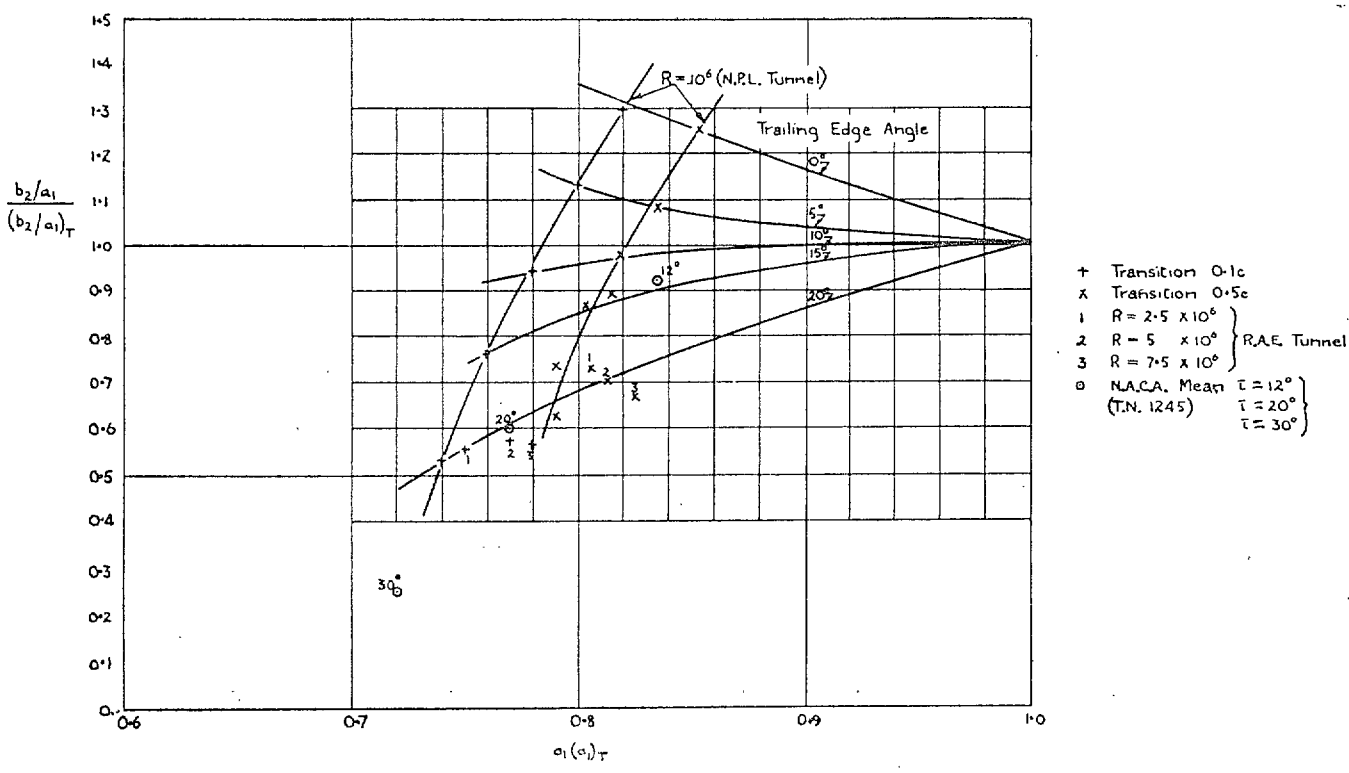

FIG. 31. Two-dimensional flap hinge moments. $E = 0{\cdot}2$. Chart for b_2/a_1.

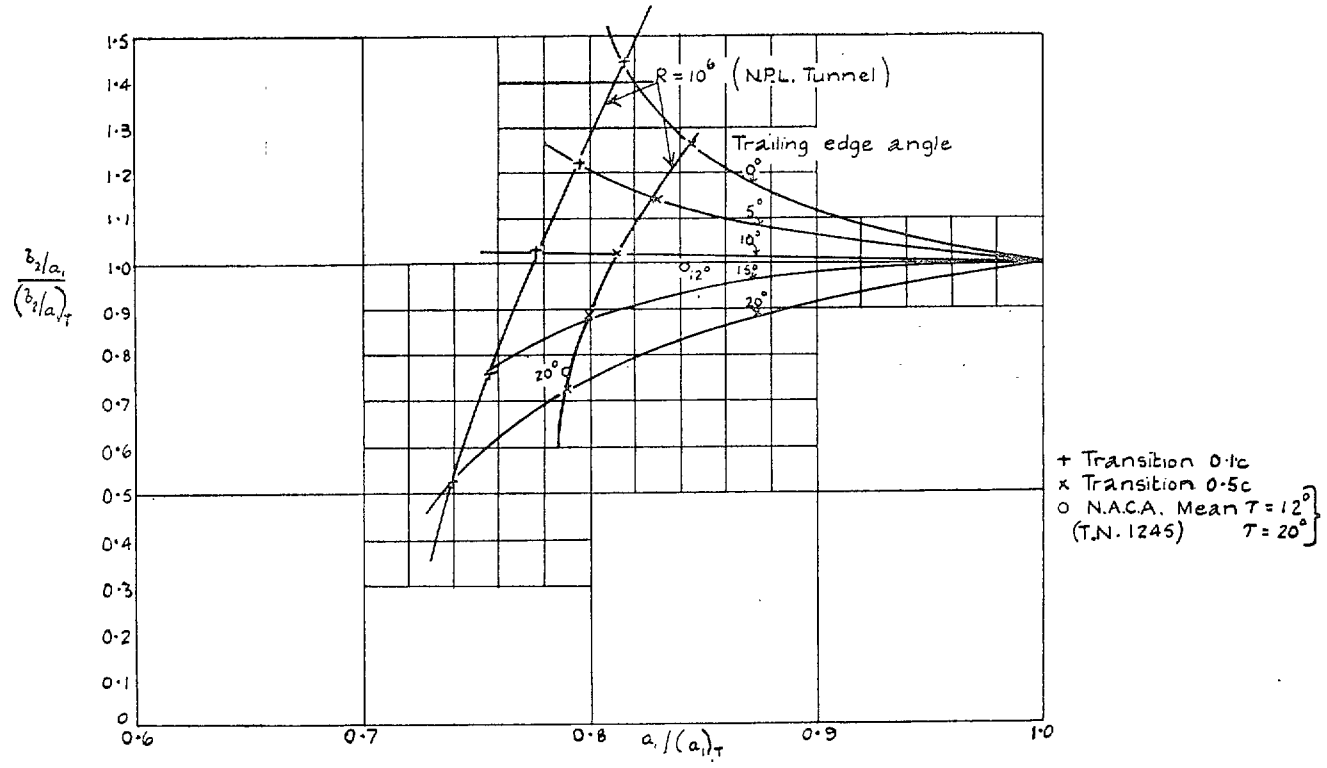

FIG. 32. Two-dimensional flap hinge moments. $E = 0{\cdot}4$. Chart for b_2/a_1.

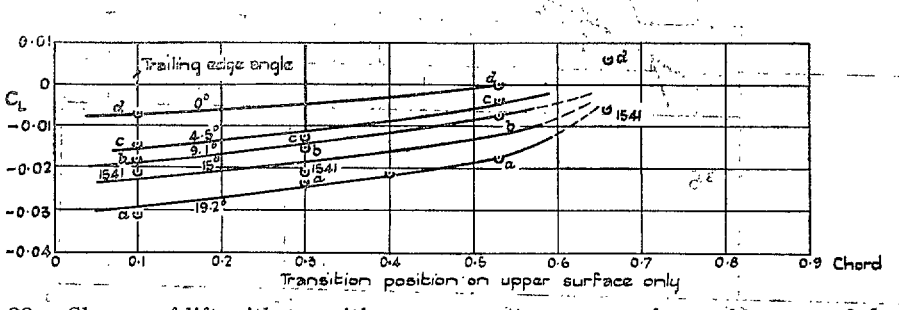

FIG 33. Change of lift with transition movement on one surface only. $\alpha = 0$ deg.

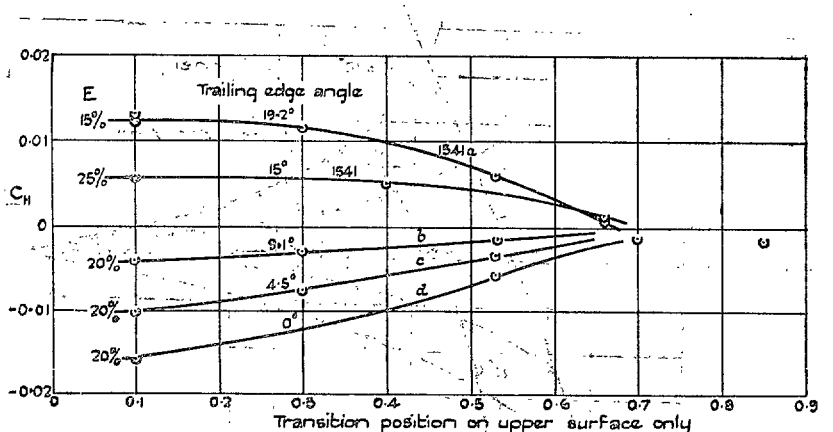

FIG. 34. Hinge-moment variation with transition movement on one surface only. $\alpha = 0$ deg.

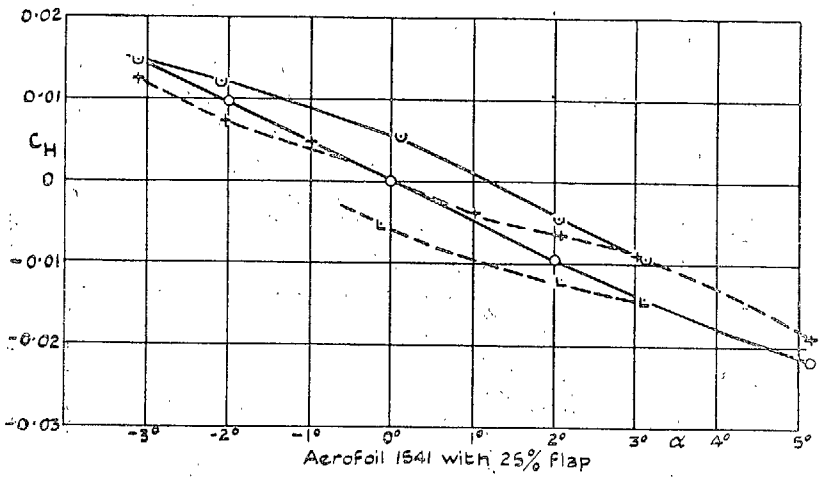

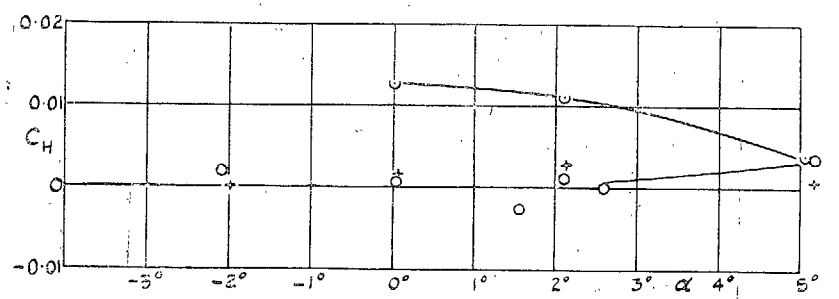

Aerofoil 1541a with 15% Flap

FIG. 35. Hinge-moment variation with incidence.

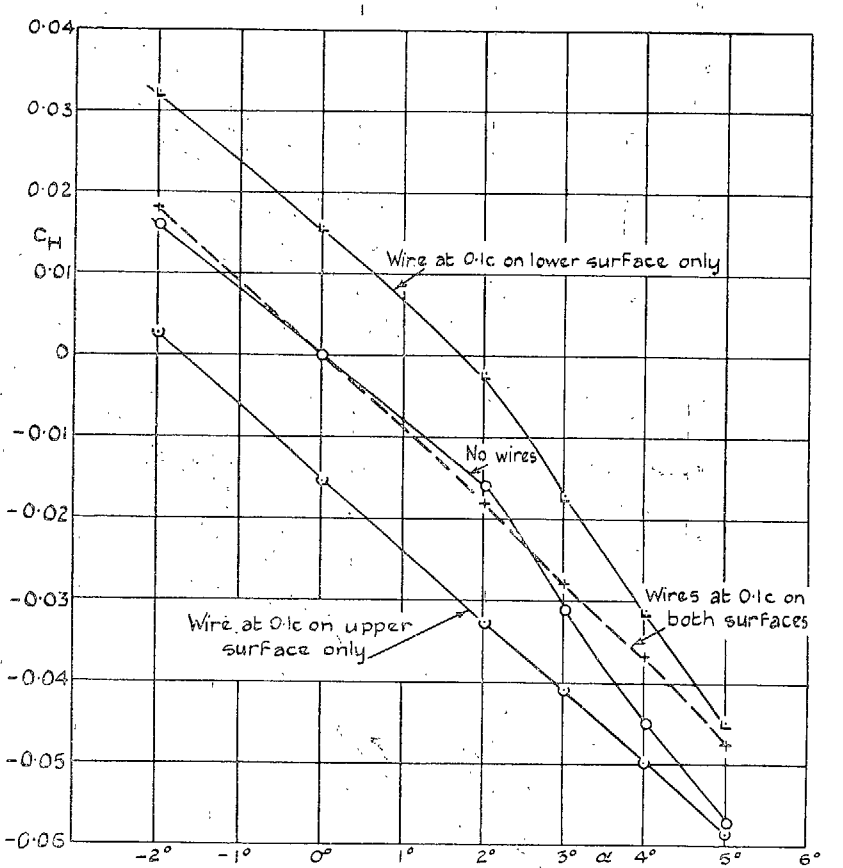

Aerofoil 1541d with 20% Flap

FIG. 36. Hinge-moment variation with incidence.

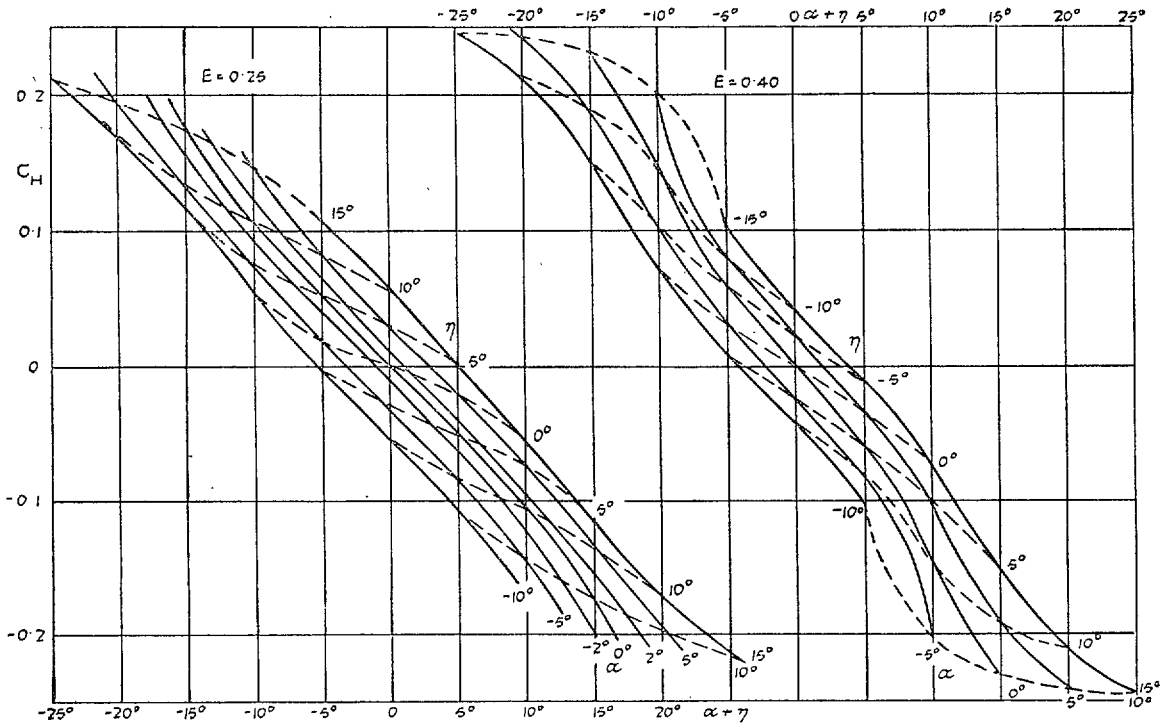

FIG. 37. 1541 Aerofoil. $\tau = 15$ deg. No wires.

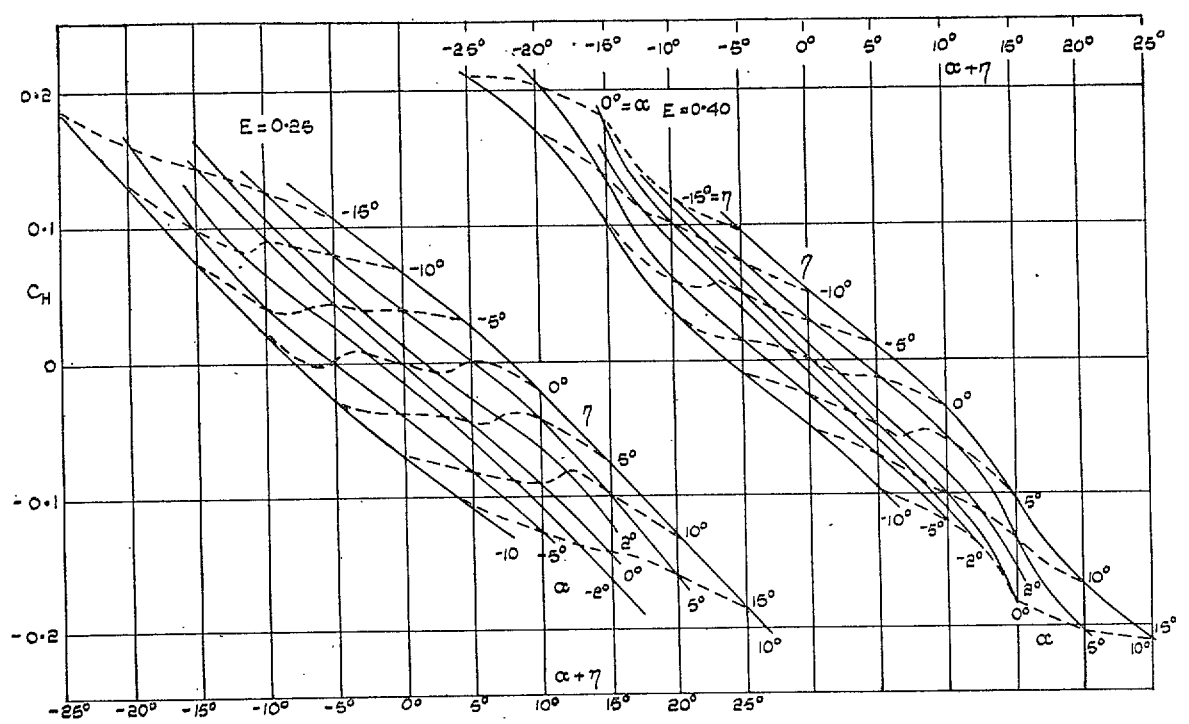

FIG. 38. 1541a Aerofoil. $\tau = 19{\cdot}2$ deg. No wires.

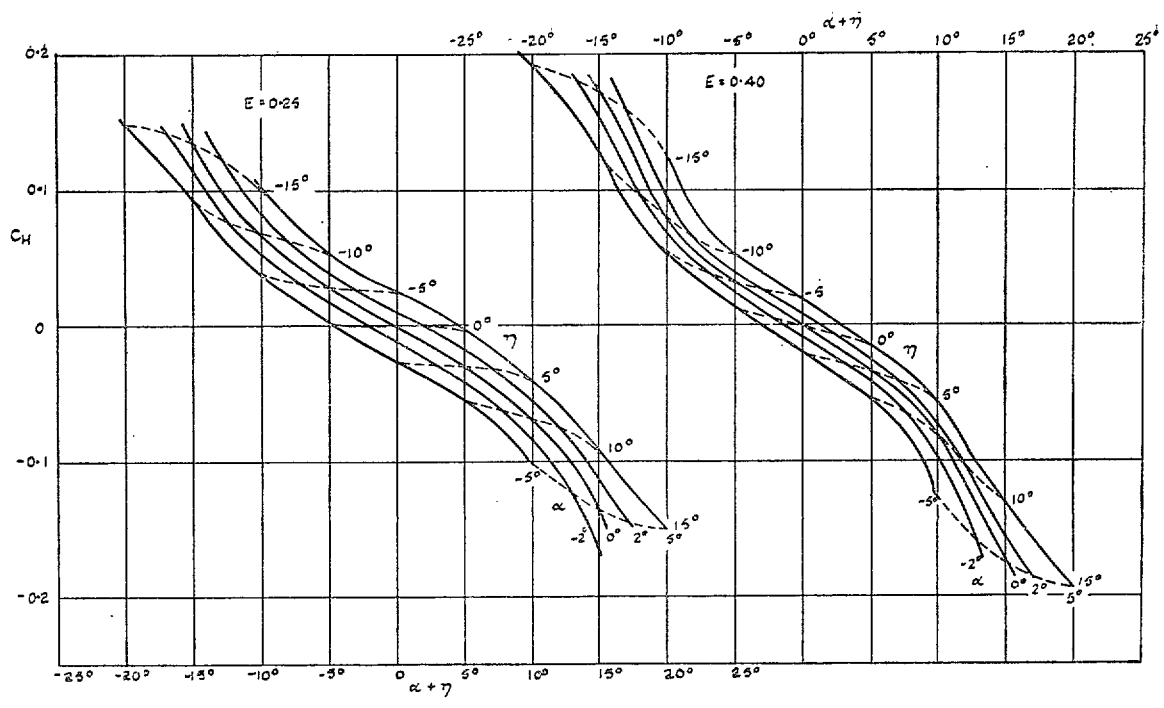

FIG. 39. 1541a Aerofoil. $\tau = 19{\cdot}2$ deg. With wires at $0{\cdot}1c$.

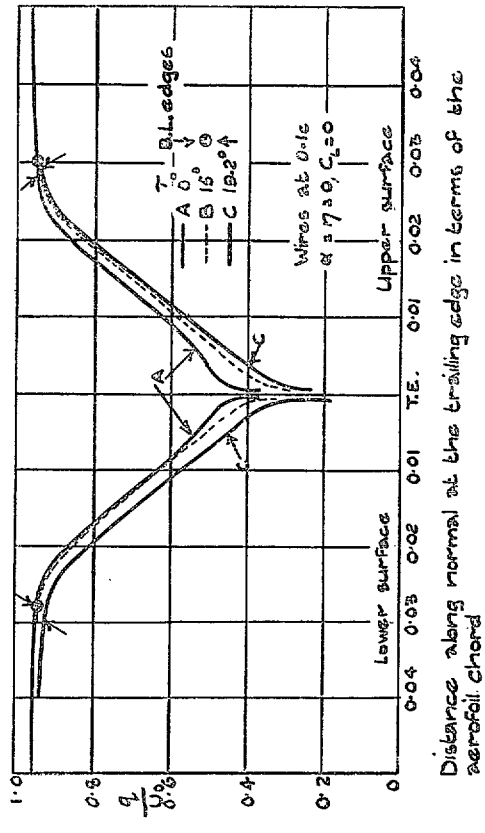

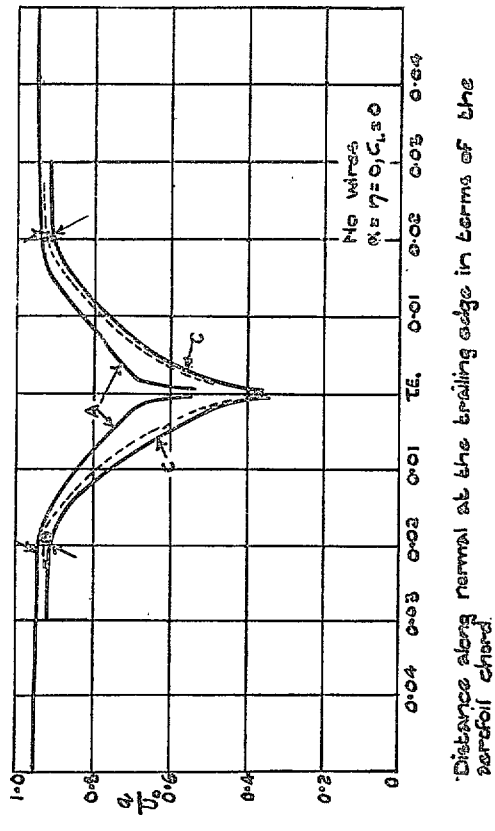

FIG. 40. Velocities at the trailing edge.

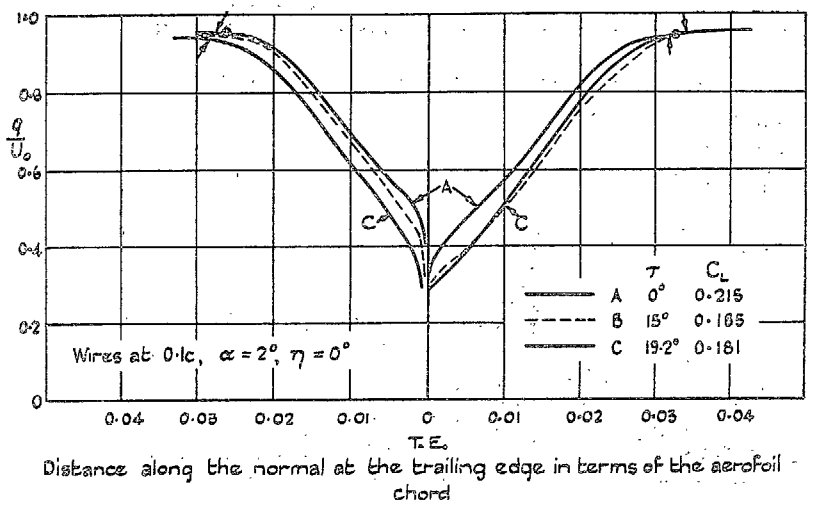

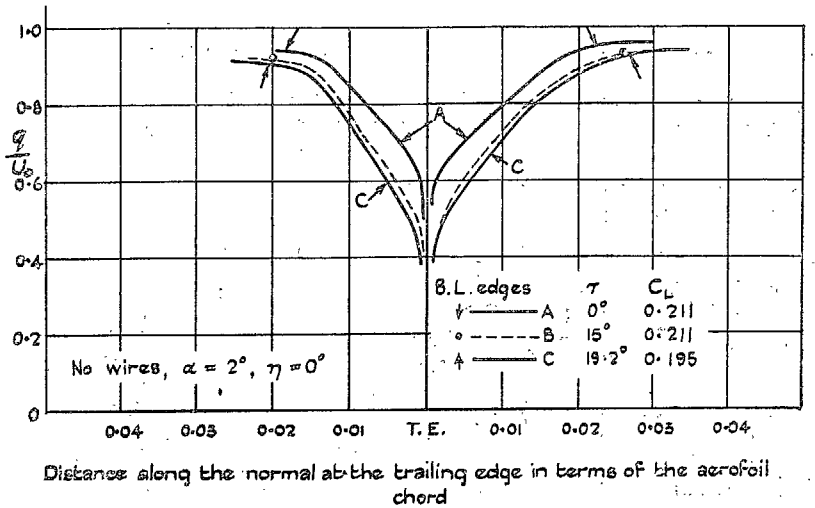

FIG. 41. Velocities at the trailing edge.

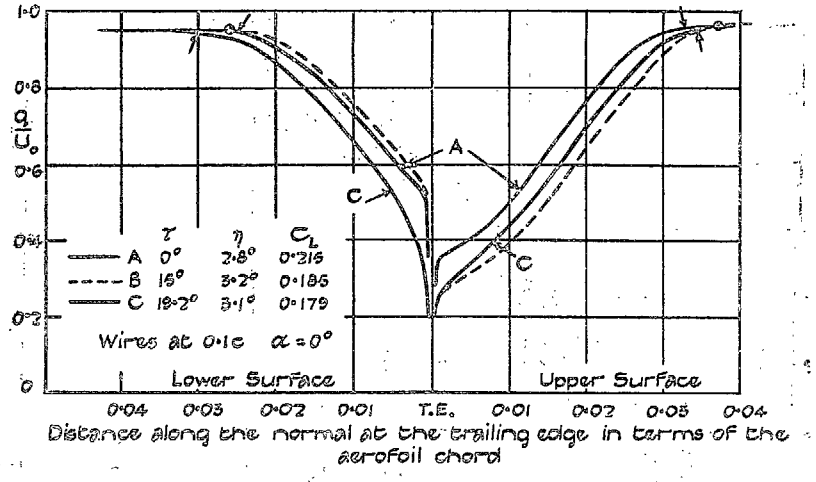

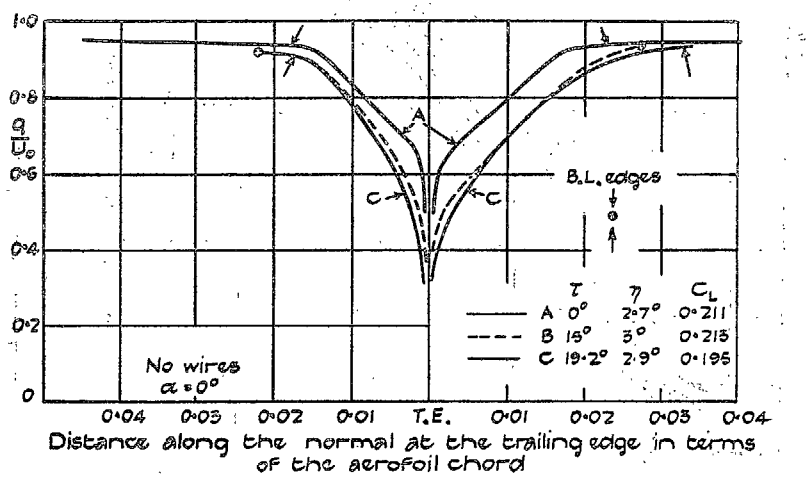

FIG. 42. Velocities at the trailing edge. 40 per cent flaps.

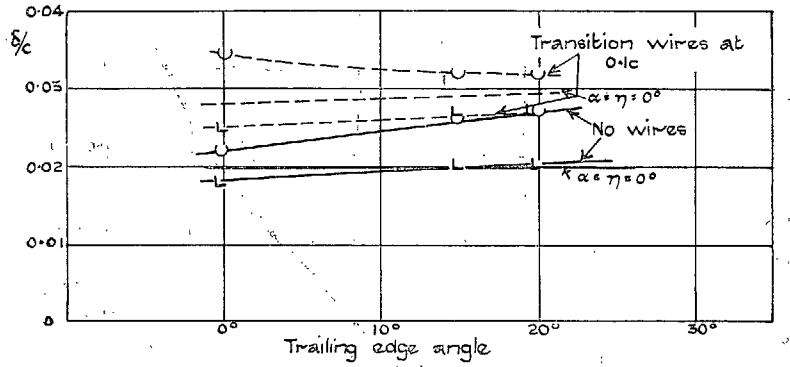

FIG. 43.

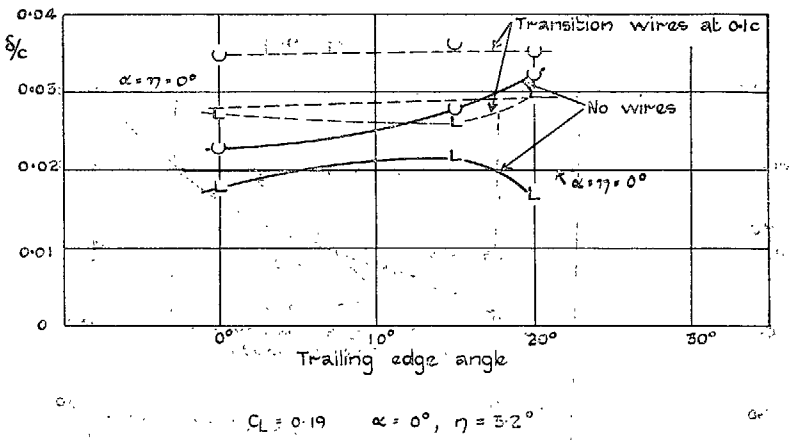

FIG. 44.

FIGS. 43 and 44. Boundary-layer thickness at the trailing edge.

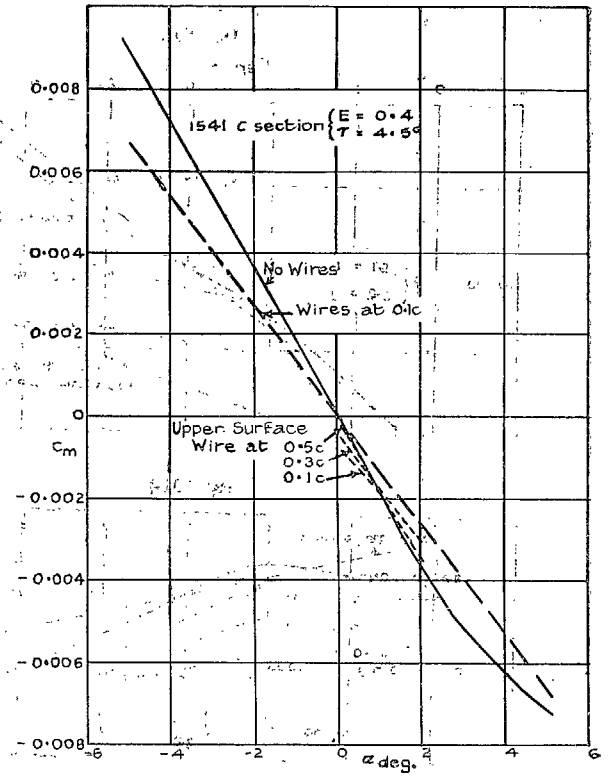

FIG. 45.

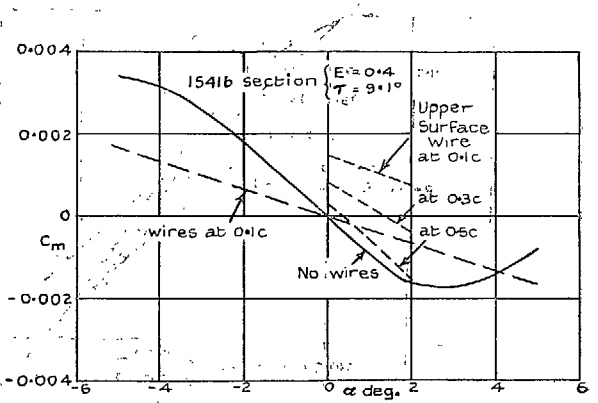

FIG. 46.

FIGS. 45 and 46. Relation between C_m and α.

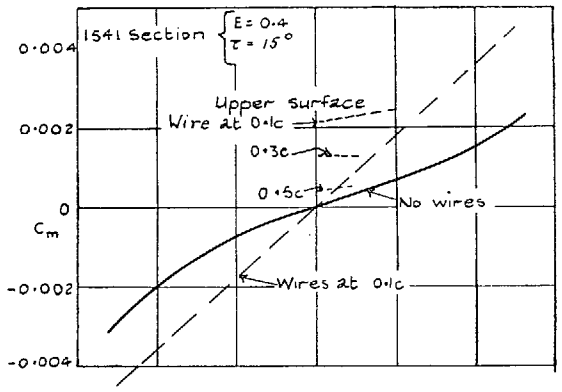

FIG. 47.

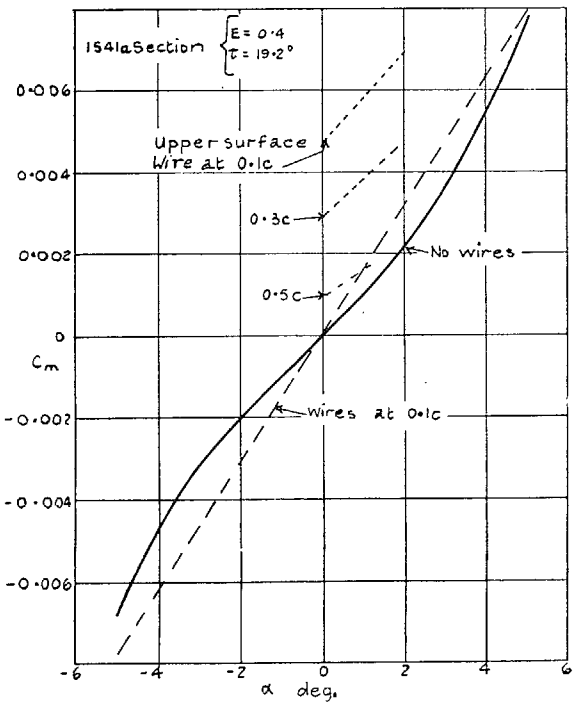

FIG. 48.

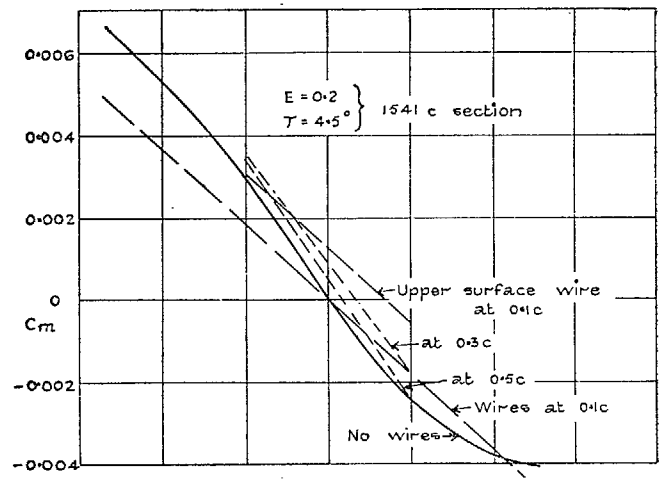

FIG. 49.

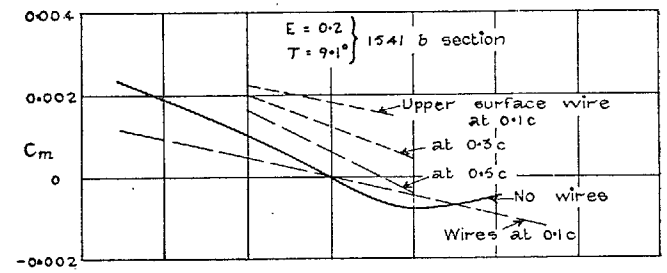

FIG. 50.

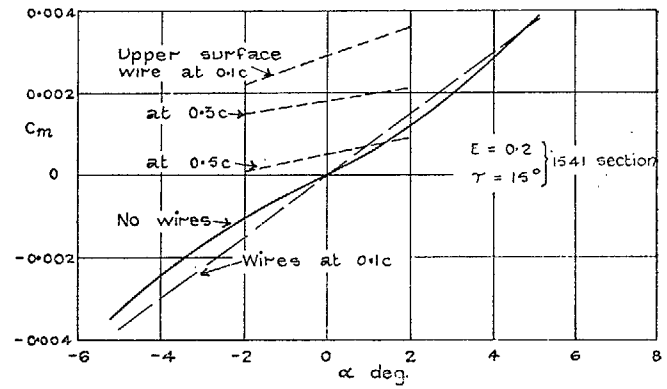

FIG. 51.

FIGS. 47, 48, 49, 50 and 51. Relation between C_m and α.

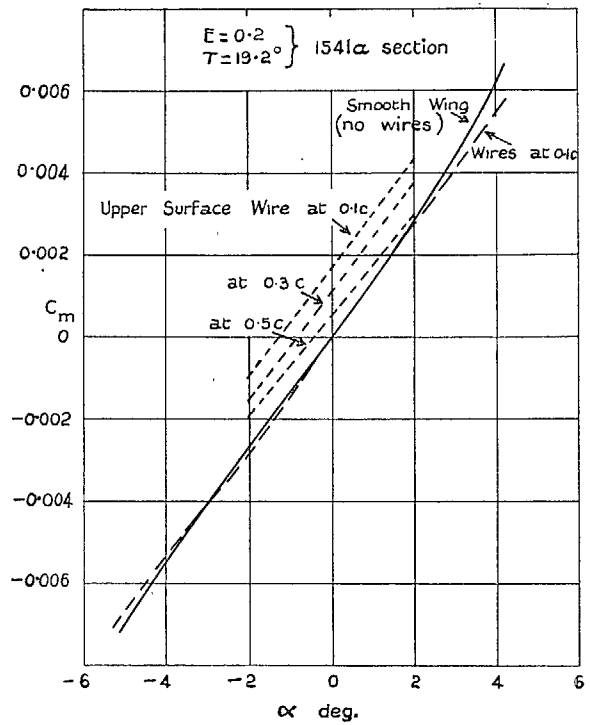

FIG. 52. Relation between C_m and α.

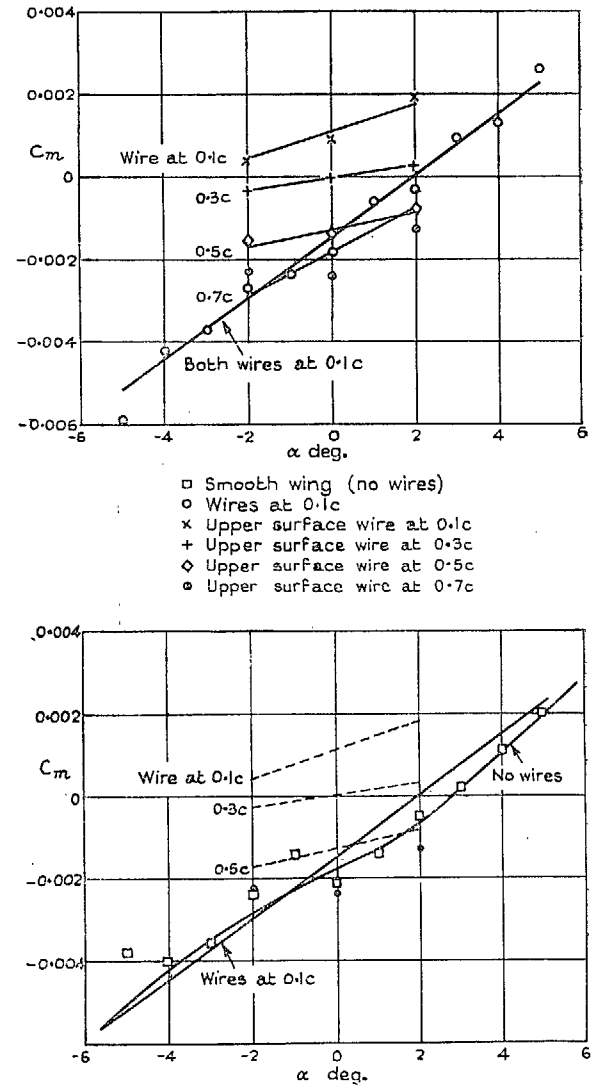

FIG. 53. Relation between C_m and α. (Illustrative of experimental accuracy.)

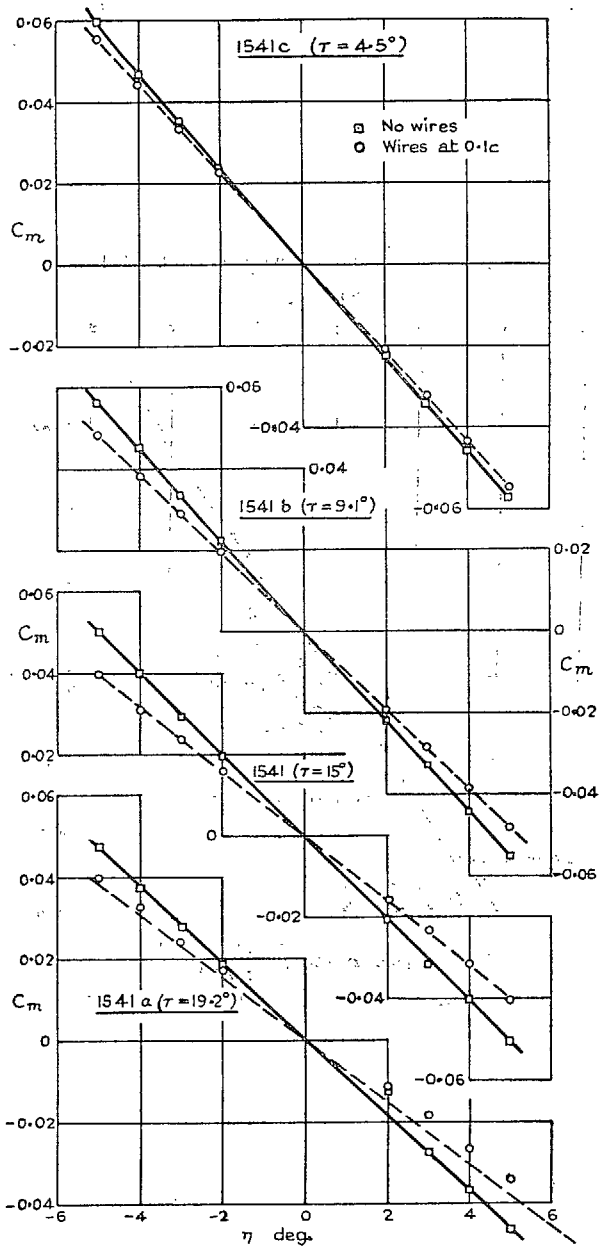

FIG. 54. Relation between C_m and flap angle η.
$E = 0{\cdot}4$.

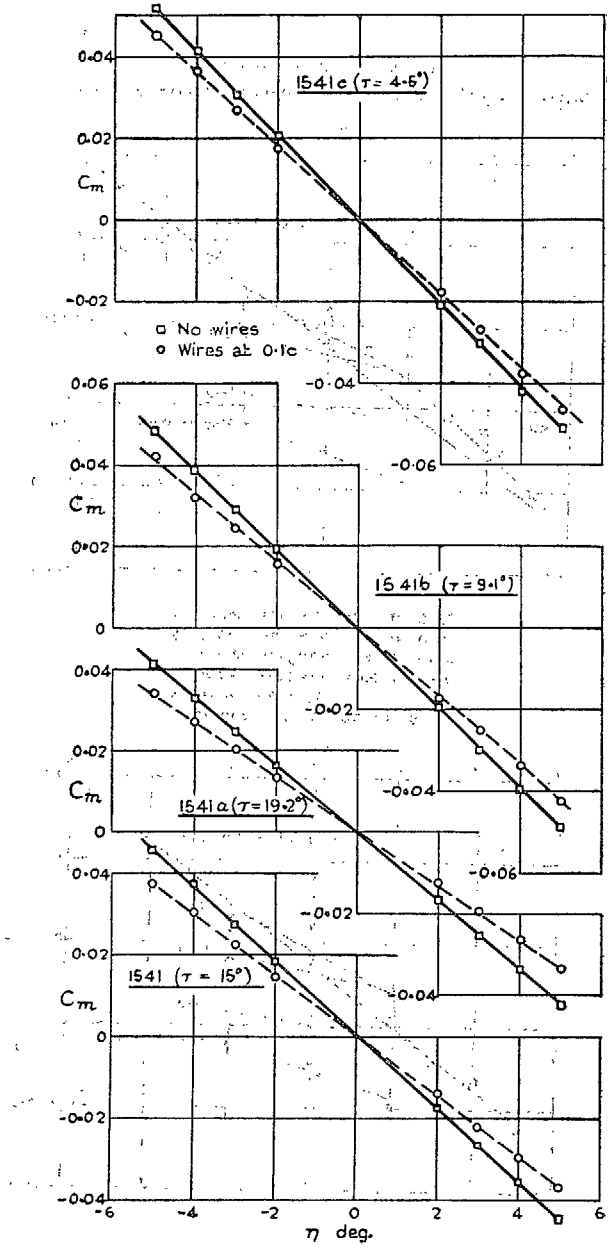

FIG. 55. Relation between C_m and flap angle η.
$E = 0{\cdot}2$.

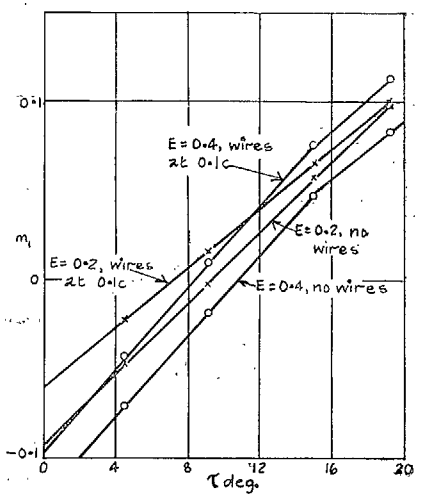

FIG. 56. Effect of trailing-edge angle on m_1.

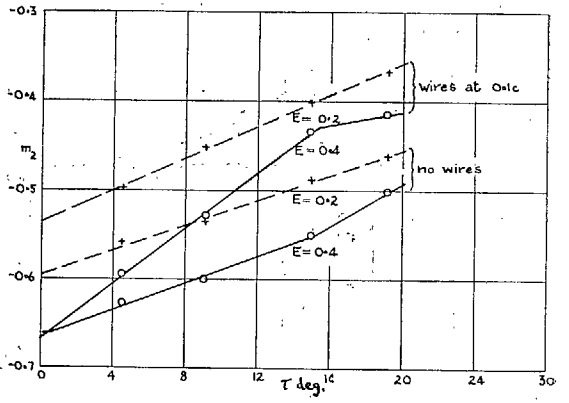

FIG. 58. Effect of trailing-edge angle on m_2.

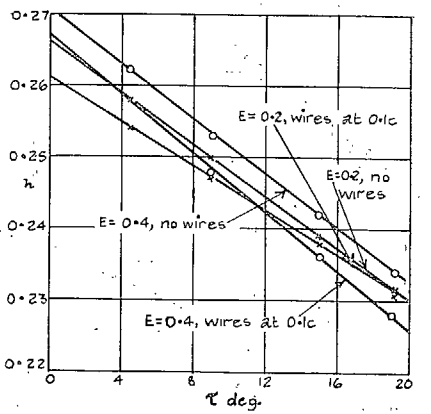

FIG. 57. Effect of trailing edge on aerodynamic centre.

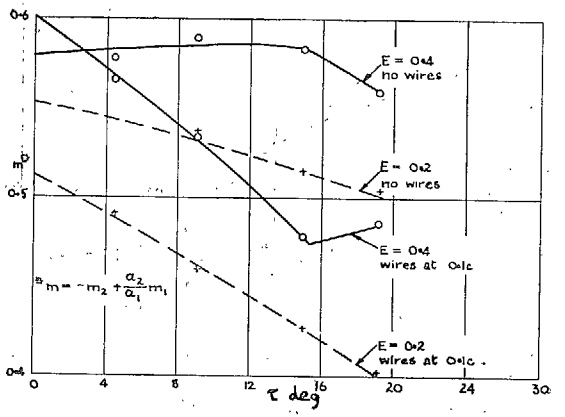

FIG. 59. Effect of trailing-edge angle on m.

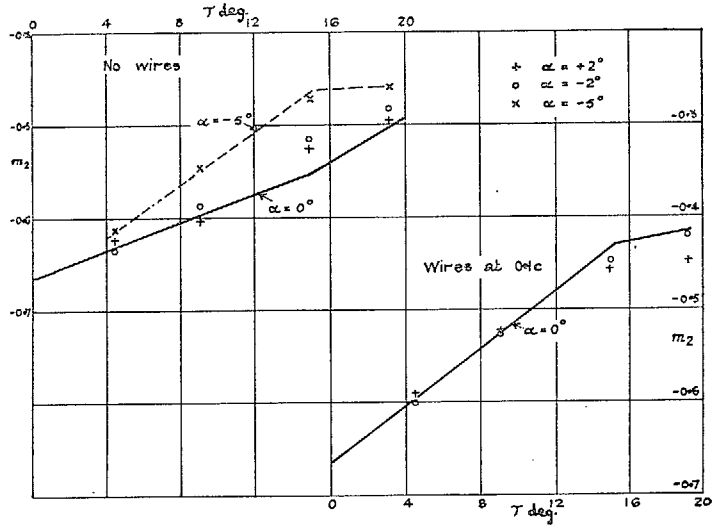

FIG. 60. Effect of incidence on m_2. $E = 0{\cdot}4$.

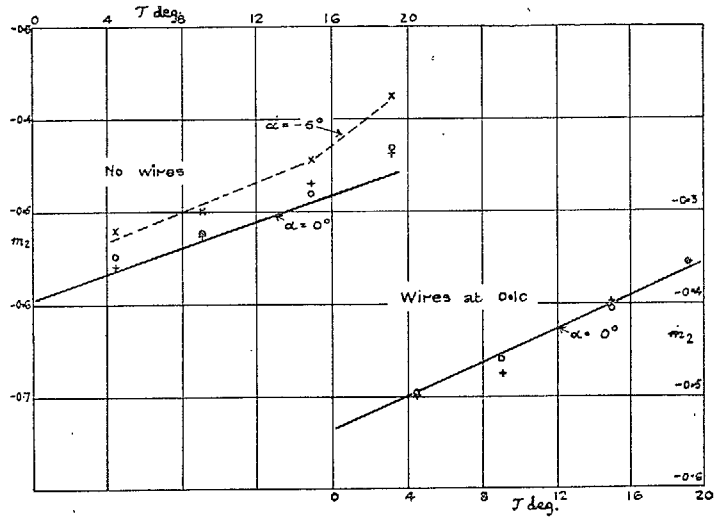

FIG. 61. Effect of incidence on m_2. $E = 0{\cdot}2$.

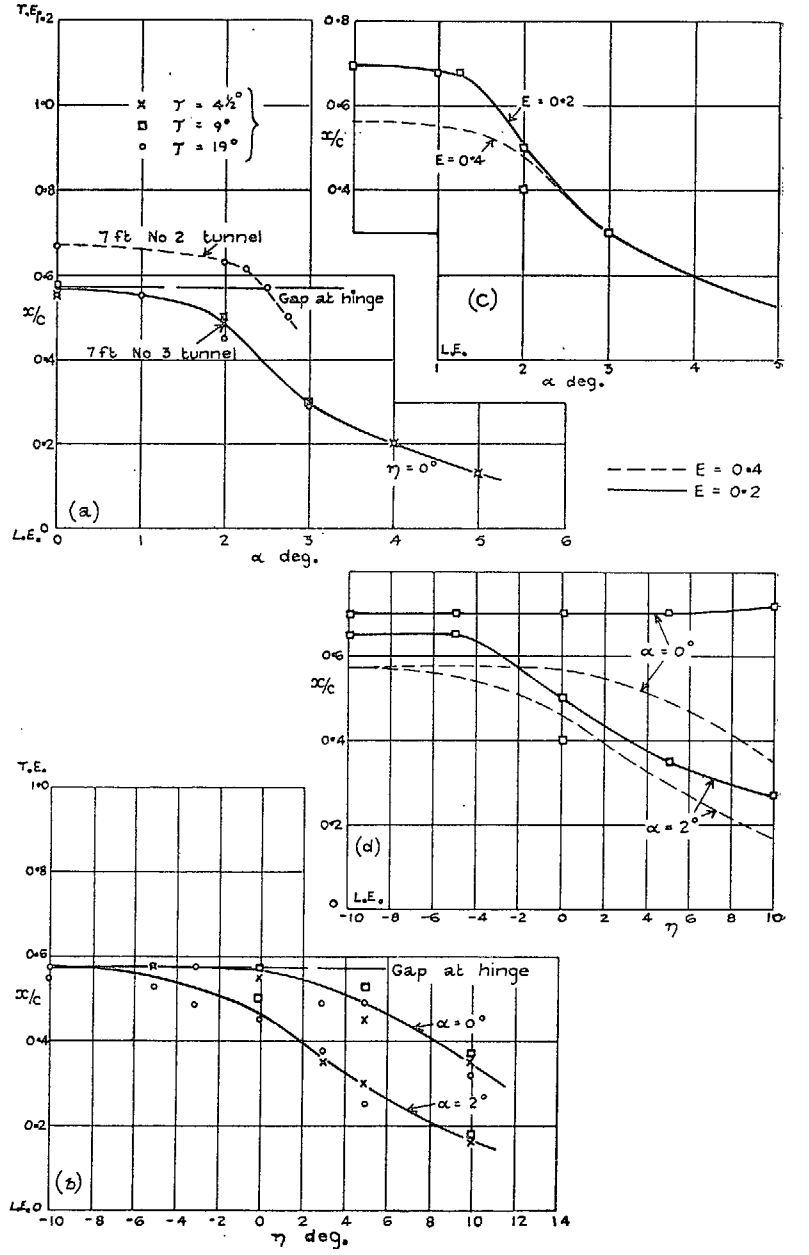

FIG. 62. Measurement of transition. 1541 section. $E = 0{\cdot}4$. Effect of control chord on transition.

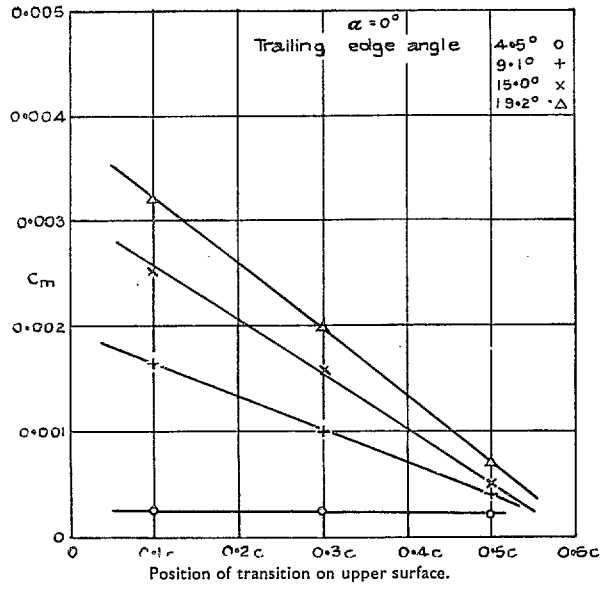

FIG. 63. Effect of transition on C_m.

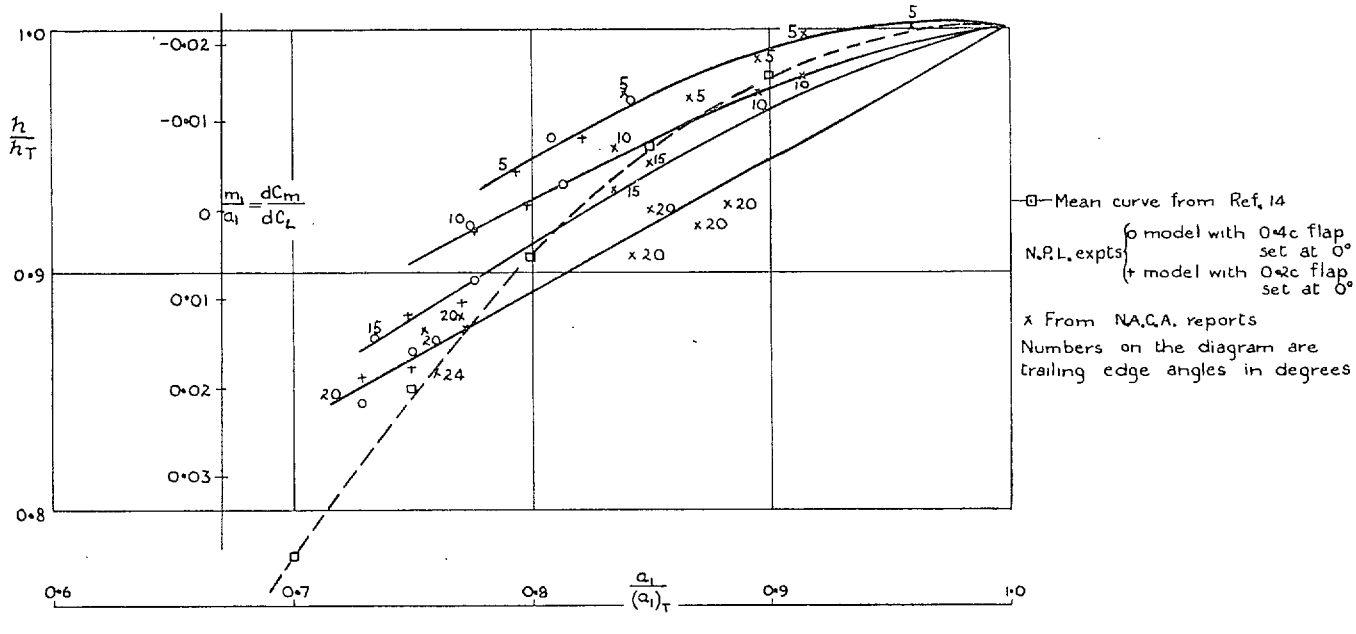

FIG. 64. Aerodynamic centre.

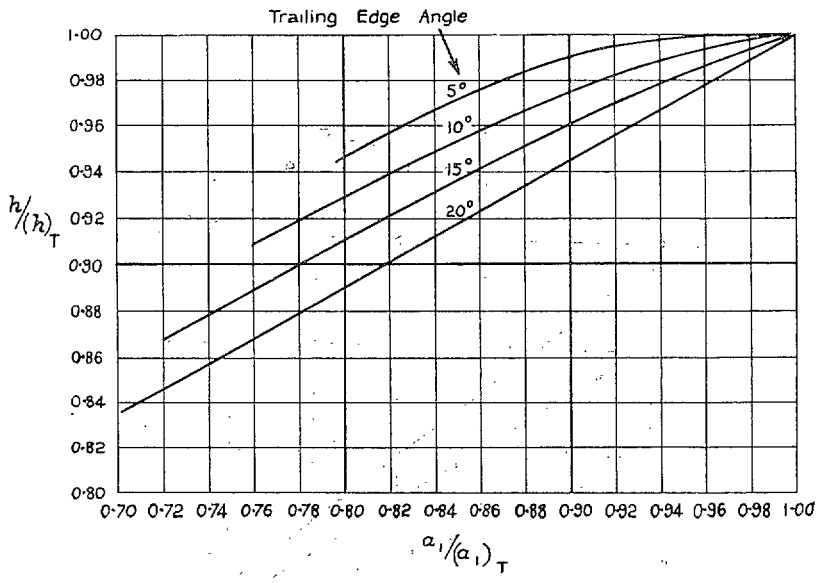

FIG. 65. Estimation of aerodynamic centre.

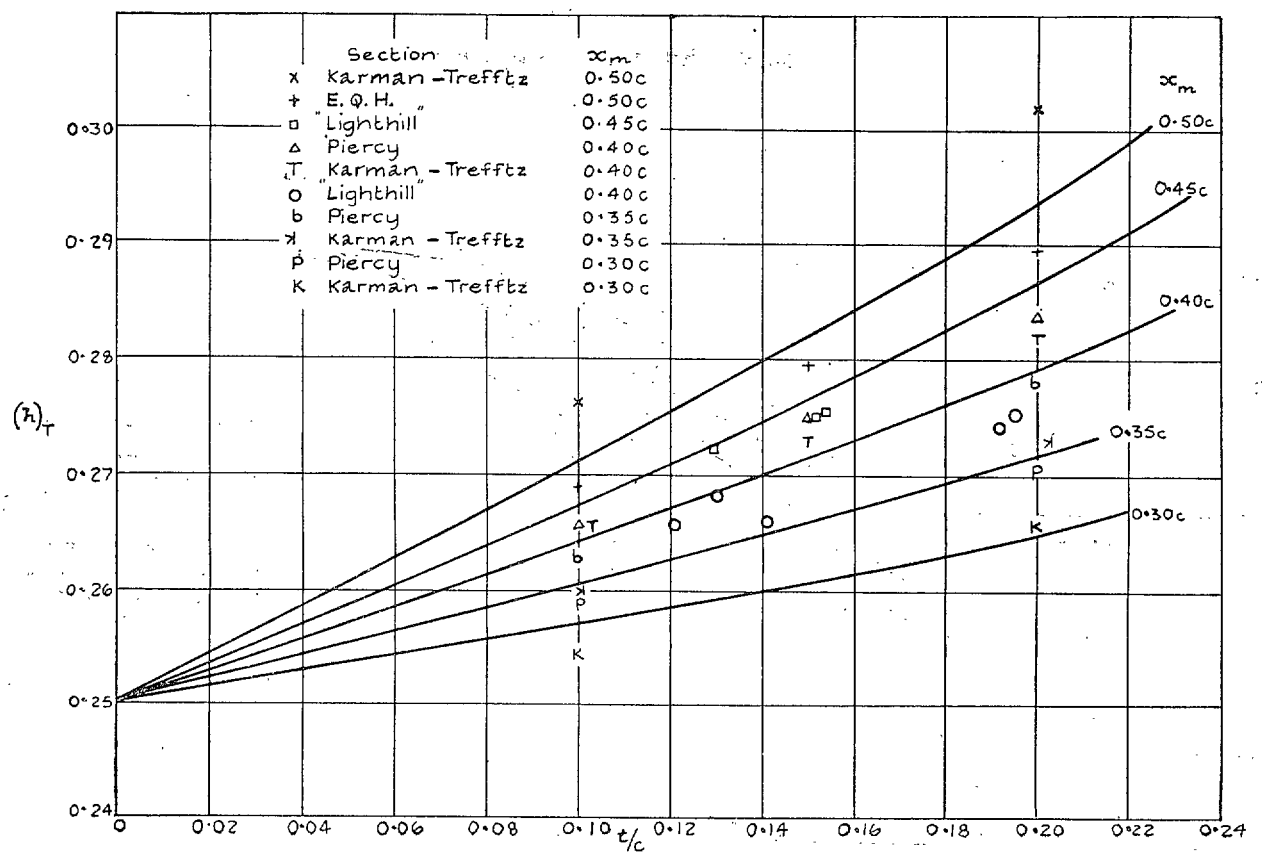

FIG. 66.

J4289 Wt.1/680 K9 5/55 D&Co. 34/263

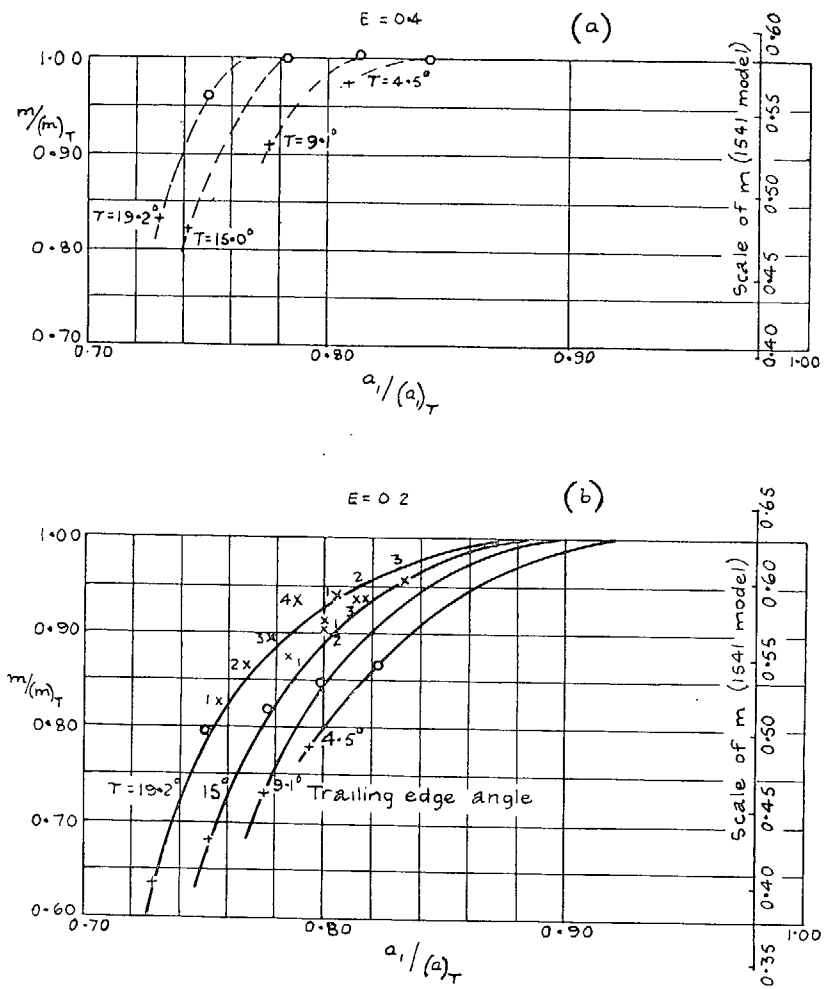

FIG. 67. Pitching-moment coefficient charts for m.

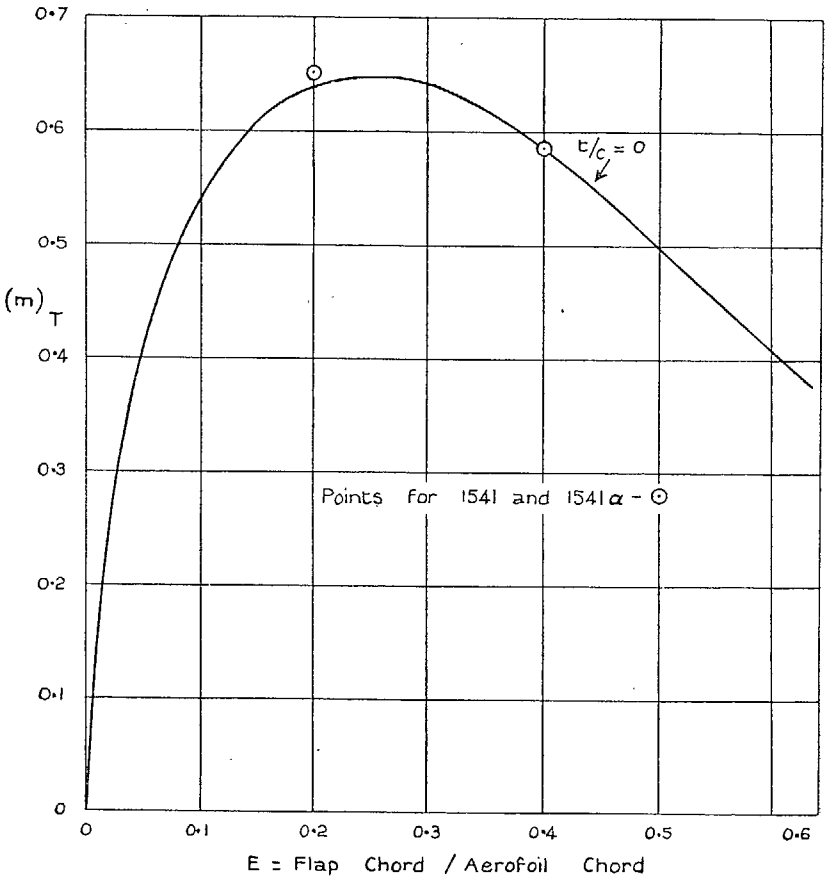

FIG. 68. Theoretical values of m.

PRINTED IN GREAT BRITAIN

Publications of the Aeronautical Research Council

ANNUAL TECHNICAL REPORTS OF THE AERONAUTICAL RESEARCH COUNCIL (BOUND VOLUMES)

1936 Vol. I. Aerodynamics General, Performance, Airscrews, Flutter and Spinning. 40*s.* (41*s.* 1*d*).

Vol. II. Stability and Control, Structures, Seaplanes, Engines, etc. 50*s.* (51*s.* 1*d.*)

1937 Vol. I. Aerodynamics General, Performance, Airscrews, Flutter and Spinning. 40*s.* (41*s.* 1*d.*)

Vol. II. Stability and Control, Structures, Seaplanes, Engines, etc. 60*s.* (61*s.* 1*d.*)

1938 Vol. I. Aerodynamics General, Performance, Airscrews. 50*s.* (51*s.* 1*d.*)

Vol. II. Stability and Control, Flutter, Structures, Seaplanes, Wind Tunnels, Materials. 30*s.* (31*s.* 1*d.*)

1939 Vol. I. Aerodynamics General, Performance, Airscrews, Engines. 50*s.* (51*s.* 1*d.*)

Vol. II. Stability and Control, Flutter and Vibration, Instruments, Structures, Seaplanes, etc. 63*s.* (64*s.* 2*d.*)

1940 Aero and Hydrodynamics, Aerofoils, Airscrews, Engines, Flutter, Icing, Stability and Control, Structures, and a miscellaneous section. 50*s.* (51*s.* 1*d.*)

1941 Aero and Hydrodynamics, Aerofoils, Airscrews, Engines, Flutter, Stability and Control, Structures. 63*s.* (64*s.* 2*d.*)

1942 Vol. I. Aero and Hydrodynamics, Aerofoils, Airscrews, Engines. 75*s.* (76*s.* 3*d.*)

Vol. II. Noise, Parachutes, Stability and Control, Structures, Vibration, Wind Tunnels. 47*s.* 6*d.* (48*s.* 7*d.*)

1943 Vol. I. Aerodynamics, Aerofoils, Airscrews, 80*s.* (81*s.* 4*d.*)

Vol. II. Engines, Flutter, Materials, Parachutes, Performance, Stability and Control, Structures. 90*s.* (91*s.* 6*d.*)

1944 Vol. I. Aero and Hydrodynamics, Aerofoils, Aircraft, Airscrews, Controls. 84*s.* (85*s.* 8*d.*)

Vol. II. Flutter and Vibration, Materials, Miscellaneous, Navigation, Parachutes, Performance, Plates, and Panels, Stability, Structures, Test Equipment, Wind Tunnels. 84*s.* (85*s.* 8*d.*)

ANNUAL REPORTS OF THE AERONAUTICAL RESEARCH COUNCIL—

1933–34	1*s.* 6*d.* (1*s.* 8*d.*)	1937	2*s.* (2*s.* 2*d.*)
1934–35	1*s.* 6*d.* (1*s.* 8*d.*)	1938	1*s.* 6*d.* (1*s.* 8*d.*)
April 1, 1935 to Dec. 31, 1936.	4*s.* (4*s.* 4*d.*)	1939–48	3*s.* (3*s.* 2*d.*)

INDEX TO ALL REPORTS AND MEMORANDA PUBLISHED IN THE ANNUAL TECHNICAL REPORTS, AND SEPARATELY—

April, 1950 – – – – – R. & M. No. 2600. 2*s.* 6*d.* (2*s.* 7½*d.*)

AUTHOR INDEX TO ALL REPORTS AND MEMORANDA OF THE AERONAUTICAL RESEARCH COUNCIL—

1909–1949 – – – – – R. & M. No. 2570. 15*s.* (15*s.* 3*d.*)

INDEXES TO THE TECHNICAL REPORTS OF THE AERONAUTICAL RESEARCH COUNCIL—

December 1, 1936 — June 30, 1939.	R. & M. No. 1850.	1*s.* 3*d.* (1*s.* 4½*d.*)
July 1, 1939 — June 30, 1945.	R. & M. No. 1950.	1*s.* (1*s.* 1½*d.*)
July 1, 1945 — June 30, 1946.	R. & M. No. 2050.	1*s.* (1*s.* 1½*d.*)
July 1, 1946 — December 31, 1946.	R. & M. No. 2150.	1*s.* 3*d.* (1*s.* 4½*d.*)
January 1, 1947 — June 30, 1947.	R. & M. No. 2250.	1*s.* 3*d.* (1*s.* 4½*d.*)
July, 1951 – – – –	R. & M. No. 2350.	1*s.* 9*d.* (1*s.* 10½*d.*)

Prices in brackets include postage.

Obtainable from

HER MAJESTY'S STATIONERY OFFICE

York House, Kingsway, London W.C.2 ; 423 Oxford Street, London W.1 (Post Orders : P.O. Box No. 569, London S.E.1) ; 13A Castle Street, Edinburgh 2 ; 39 King Street, Manchester 2 ; 2 Edmund Street, Birmingham 3 ; 109 St. Mary Street, Cardiff ; Tower Lane, Bristol 1 ; 80 Chichester Street, Belfast OR THROUGH ANY BOOKSELLER

S.O. Code No. 23-2730